Post-urgonian cephalopods (Lower Aptian) from the Massif de la Clape (Aude, France)

Philippe Fauré[1,*], Camille Frau[2], Dominique Téodori[3], Émile Hourqueig[4]

Manuscrit reçu le 9 mai 2026 ; accepté dans sa forme révisée le 6 juillet 2026 ; disponible en ligne 25 juillet 2026.

Abstract. The present paper provides a revised lithostratigraphic framework for the Lower Cretaceous succession of the Clape Massif (Aude, southern France) and a detailed account of the cephalopod fauna (ammonoids and nautiloids) from two condensed horizons at the transition between the Estagnol Formation and the Ramade Marls Formation, here referred to as the "Niveau de Saint-Martin" and the "Niveau de Vires". The cephalopod assemblage from the "Niveau de Saint-Martin" is rare and generally poorly preserved, allowing only tentative identification of ammonites that may indicate either the *Deshayesites forbesi* Zone or/to the lower *Deshayesites deshayesi* Zone. In contrast, the "Niveau de Vires" yields a diverse and well-preserved assemblage, including the nautiloids *Cymatoceras neocomiense* and *Anglonautilus praeundulatus*. The ammonoid fauna comprises *Deshayesites grandis* (Deshayesitidae), *Cheloniceras crassum* (Douvilleiceratidae), *Procolombiceras* sp. (Acanthohoplitidae), *Toxoceratoides rochi* (Acrioceratidae), *Macroscaphites* sp. cf. *striatisulcatus* (Macroscaphitidae), *Ammonitoceras* aff. *lahuseni*, and *Delanoyites* gen. nov., represented by species A and B (Ancyloceratidae). The latter genus is herein introduced to replace *Lithancylus*, considered a *nomen nudum*. This cephalopod assemblage shows strong affinities with that recorded at the maximum flooding surface of the Scaphites Beds Member (Lower Greensand Group, UK), which is precisely dated to the upper part of the *Deshayesites grandis* Subzone (upper *D. deshayesi* Zone, Lower Aptian).

Keywords: Fossil cephalopods, Aptian, Massif de la Clape, Aude, France.

Céphalopodes post-urgoniens (Aptien inferieur) du massif de la Clape (Aude, France)

Résumé : Le présent article propose une révision de la lithostratigraphie de la succession du Crétacé inférieur du massif de la Clape (Aude, sud de la France) et une description détaillée de la faune de céphalopodes (ammonites et nautiles) provenant de deux horizons condensés à la transition entre la Formation de l'Estagnol et la Formation des Marnes de Ramade, désignés ici comme les "Niveau de Saint-Martin" et "Niveau de Vires". La faune de céphalopodes du "Niveau de Saint-Martin" est rare et généralement mal conservée, permettant seulement l'identification approximative d'ammonites pouvant indiquer soit la Zone à *Deshayesites forbesi*, et/soit la partie inférieure de la Zone à *Deshayesites deshayesi*. En revanche, le "Niveau de Vires" fournit un assemblage diversifié et bien conservé, incluant les nautiles *Cymatoceras neocomiense* et *Anglonautilus praeundulatus*. La faune d'ammonites comprend *Deshayesites grandis* (Deshayesitidae), *Cheloniceras crassum* (Douvilleiceratidae), *Procolombiceras* sp. (Acanthohoplitidae), *Toxoceratoides rochi* (Acrioceratidae), *Macroscaphites* sp. cf. *striatisulcatus* (Macroscaphitidae), *Ammonitoceras* aff. *lahuseni* et *Delanoyites* gen. nov., représenté par les espèces A et B (Ancyloceratidae). Ce dernier genre est introduit ici pour remplacer *Lithancylus*, considéré comme un *nomen nudum*. Cet assemblage de céphalopodes montre de fortes affinités avec celui enregistré au niveau de la surface de maximum transgression du Scaphites Beds Member (Lower Greensand Group, Royaume-Uni), daté précisément de la partie supérieure de la Sous-zone à *Deshayesites grandis* (partie supérieure de la Zone à *Deshayesites deshayesi*, Aptien inférieur).

Mots-clés : Céphalopodes fossiles, Aptien, Massif de la Clape, Aude, France.

[1] Philippe Fauré: 3 quai Duquesne, F-11430, Gruissan; Muséum d'Histoire naturelle de Toulouse, 35 allées Jules Guesde, F-31000, Toulouse, philipfaure@gmail.com [*]Corresponding author.

[2] Camille Frau: Palaeo-Expertise, 8 Rue du Moulin, F-65350 Cabanac, France; ICUB Fellowships for Young Researchers, University of Bucharest, Romania, camille_frau@hotmail.fr

[3] Dominique Téodori: 8 impasse de San Marino, F-31140 Pechbonnieu, France, domiteo@free.fr

[4] Émile Hourqueig: 129 rue du général Guerin, F-85000 La Roche-sur-Yon, e.hourqueig@gmail.com

1. Introduction

Situated in the coastal region of Languedoc, within the Aude department, the Clape Massif holds a pivotal position at the intersection of the easternmost folds of the Pyrenean orogenic system and the Languedocian Arc, placing it structurally in an intermediate zone between the Pyrenean and Provençal orogens (**Fig. 1, 2**). This location positions the Clape Massif as a transitional area between two contrasting palaeogeographical domains. On one side, it borders the Basse Provence chains, and on the other, the southern Pyrenees, both of which host well-developed, ammonite-rich marine successions of Aptian age. These regions are part of a larger palaeogeographical realm known as the Pyrenean-Provençal Gulf (**Fig. 2**) (Canérot, 2008) or the South Provence Basin (Masse *et al*., 2000). Within the Basse Provence, particularly the region around Cassis-Roquefort-la-Bédoule, lies the depositional center of the South Provence Basin. This area serves as the unit-stratotype for the lower Aptian, which is formally recognized as the *Bédoulien* Substage (Toucas, 1888). In contrast, the Pyrenees were characterised by a sub-meridional axial basin that developed within the extensional zone between the Iberian and Eurasian plates, with the most continuous marine successions preserved in the Organyà Basin of Upper Catalonia (Peybernès, 1976; Bernaus, 2000; Moreno-Bedmar, 2010) (**Fig. 2**).

Beyond these two principal regions, Aptian faunas remain poorly studied. Ammonites are scarce and often poorly preserved, sedimentary successions are frequently disrupted by tectonic activity, and the biostratigraphic data provided by the so-called "*Marnes à Deshayesites*" of the Pyrenees are unreliable. The Clape Massif, however, presents a notable exception. Its exceptionally well-exposed outcrops and favourable conditions for observation have long made it an important fossiliferous area, with its rich Aptian faunas documented by various French authors (d'Archiac, 1859; Cairol, 1872; Léenhard, 1887; Doncieux, 1903, 1921). Yet despite this historical interest, the precise age of these Aptian deposits has remained uncertain, and no systematic *in situ* sampling of ammonite successions had previously been undertaken.

The condensed levels described here, with their distinctive cephalopod fauna, where identified during a biostratigraphic revision of the Lower Cretaceous succession in the Clape Massif conducted by one of us (PF)(**Fig. 3**). The present papers aims to clarify the lithostratigraphy of the Lower Cretaceous succession of the Clape Massif (Aude, southern France), and provides a detailed description of the cephalopod fauna (ammonoids and nautiloids) from two condensed horizons at the contact between the Estagnol Formation and Ramade Marls Formation, herein termed to as the "Niveau de Saint-Martin" (NSM) and "Niveau de Vires" (NV). These levels yield two distinct cephalopod assemblages indicative of the (?) *Deshayesites forbesis* to *Deshayesites deshayesi* Zone, a biozone that is rarely well-developed in southwestern Europe. In a similar sedimentological context associated with maximum flooding surface deposition, this assemblage shows strong affinities to that of the Scaphites Beds Member of the Lower Greensand Group (UK), which is of the same age (upper *Deshayesi* Zone, lower Aptian).

2. Geological setting

The Clape Massif rises to the east of Narbonne, between the Narbonnais coastal lagoon plain and the shoreline of the Gulf of Lion (**Fig. 1**). This massif also encompasses the Île Saint-Martin, the Roc de Conilhac, and several rocky outcrops surrounding Gruissan. Although it is separated from the Corbières Massif by the Oligo-Miocene-filled collapse basin of Narbonne-Sigean, the Clape Massif is unequivocally part of the external zone of the Eastern Corbières Nappe, which is detached along the Triassic décollement (**Fig. 1**). It represents the easternmost Pyrenean outlier of this thrust sheet, marking the transition towards the folded system that, through the Languedocian Arc, once linked the two segments of the larger Pyrenean-Provençal orogenic belt (Dercourt *et. al.*, 2000).

2. 1. Geological background

Building upon the pioneering work of Léenhard (1887), the stratigraphy of the Clape Massif is traditionally divided into five main lithological formations. At the core of this sequence lies the fossil-rich marl unit, the "*Marnes inférieures*," which is sandwiched between two prominent cliff-forming bars of Urgonian-type rudist-bearing limestones. The lower, more massive bar, known as the "*Calcaires inférieurs*", forms vast causses, covered by a characteristic semi-arid Mediterranean vegetation. Above it, the thinner bar refers to the "*Calcaires moyens*" and creates a striking, easily identifiable rock unit within the landscape of the Clape Massif. This trilogy is followed by a thick and complex stratigraphic succession—the "*Marnes et calcaires supérieurs*"—which alternates between orbitolinid-bearing marls, sandy limestones, and rudist-bearing limestones. These layers stretch across the lower synclinal zones and the collapsed southeastern compartment of the massif. The entire series is capped by red and green sandstones, often attributed to the Albian by various authors. At both its western and eastern margins, the Cretaceous substratum of the Clape Massif is overlain by Neogene lacustrine deposits (Oligo-Miocene) and marine formations (Middle Miocene), completing the geological framework of the Clape Massif.

Despite its apparent simplicity, this stratigraphic scheme was only accepted after extensive debates across generations of geologists. D'Archiac (1859), followed by Hébert (1867) and Cairol (1872), rejected the existence of two superimposed Urgonian-type limestone formations in the Clape Massif, arguing that their apparent positioning was a result of faulting. According to their interpretation, the "Aptian fossiliferous marls" of the Clape Massif, which they dated to the "Neocomian," would rest directly

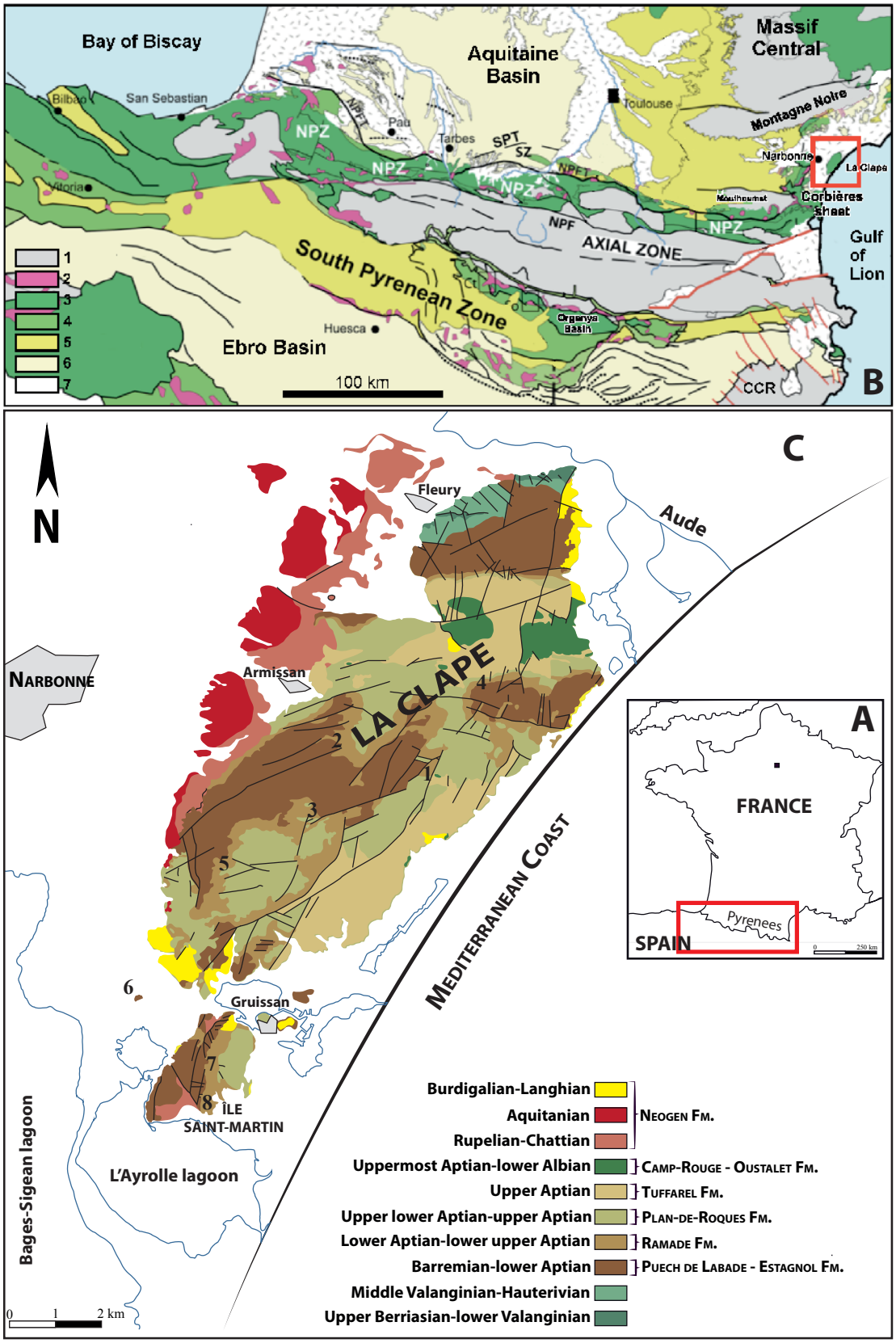

Fig. 1 - A. Location of the Pyrenees; **B.** Simplified geological map of the Pyrenees. NPZ: Nord-Pyrenean Zone; NPFZ: Nord-Pyrenean Frontal Thrust; SZ: Sous-Pyrenean Zone; SPT: Sous-Pyrenean Thrust; CCR: Costal Catalan Ranges. 1. Paleozoic basement; 2. Upper Triassic; 3. Jurassic to Lower Cretaceous; 4. Upper Cretaceous; 5. Paleocene; Eocene-Oligocene; 6. Miocene; 7. Quaternary. **C.** Geological map of the massif de la Clape and of the Île Saint-Martin. Localities cited in the text: **1.** Vires-Parets d'en Sales; **2.** Ramade; **3.** Pech Redon; **4.** Les Rompudes; **5.** Figuères; **6.** Roc de Conilhac; **7.** L'Estagnol; **8.** Saint-Martin-le-Bas.

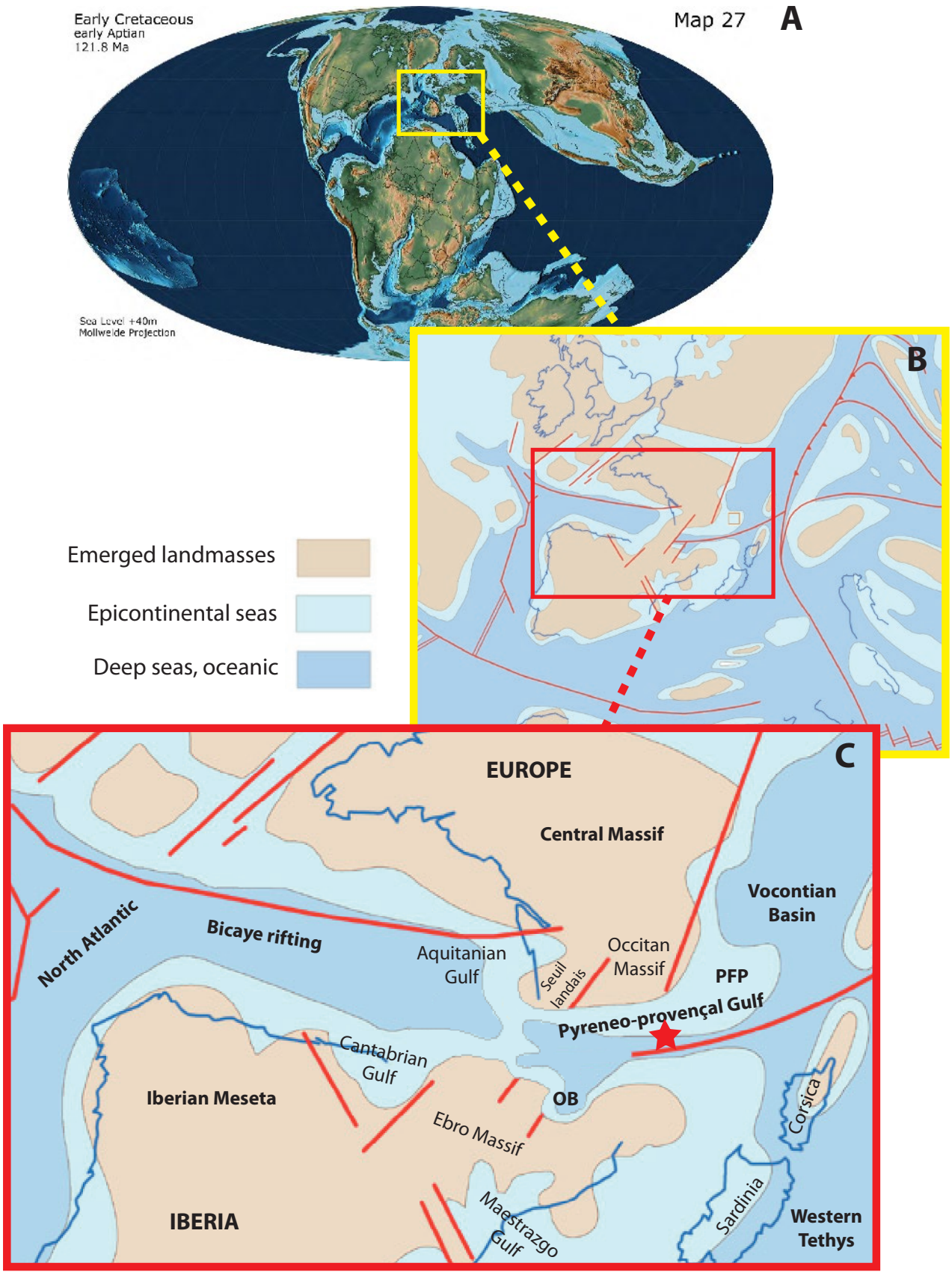

Fig. 2 - Paleogeographical framework for the Lower Aptian on the scale of the globe (**A**), of the western Tethys (**B**) and of South Europa (**C**). Red star: Location of the studied area. OB: Organya Basin; PFP: Provence platform (modified from Canerot, 2008).

upon the Jurassic and would be capped by a single bar of "Caprotina Limestone". It was only through the work of Coquand (1868), Magnan (1872), and, more crucially, Léenhard (1887) and Doncieux (1903, 1921), that the stratigraphic superposition of several rudist-bearing limestone formations was definitively proven. Two main cliffed bars of Urgonian-type rudist-bearing limestones clearly frame the fossiliferous formation actually known as the "*Marnes inférieures*" of the Clape Massif, whose Aptian age is now firmly established. The search for hydrocarbons along the Languedoc margin, coupled with the first micropaleontological studies, facilitated the recognition of the Berriasian–Barremian within the "*Calcaires inférieurs*" of the Clape Massif (Gottis, 1957; Dufaure, 1964). Beginning in the 1970s, the concurrent works of Peybernès (1971, 1973, 1976) and Jaffrézo (1971, 1980) substantially enhanced our understanding of the Lower Cretaceous of the Clape Massif. While these two distinct schools of thought emerged, each differing on various points, their lithostratigraphic results ultimately converged, with only minor discrepancies.

2.2. Lithostratigraphie

2.2.1 - The first four formations are only exposed in the lowest compartment of the Clape Massif (**Fig. 1**). Recognized by Peybernès (1973, 1976) and Jaffrézo (1980), to whom the reader is referred for a more detailed description, these formations are shallow-marine carbonate deposits that span from the Berriasian to the Hauterivian (**Fig. 3**):

- Trocholines and dasycladaceae-bearing Limestones Formation (Peybernès, 1976) (30 m, Upper, non-terminal, Berriasian);

- Red Limestones Formation (Peybernès, 1976) (30 m, Upper Berriasian to Lower Valanginian);

- Pfenderines-bearing Limestones Formation (Peybernès, 1976) (30 m, Middle to Upper Valanginian);

- Yellow bryozoan-bearing Limestones Formation (Peybernès, 1976) (40-50 m, Hauterivian).

2.2.2 - Pech de Labade Limestones Formation (Peybernès, 1976) (approximately 200 m) **(Fig. 3, 4):**

Whitish, compact limestones of shallow-marine platform carbonates, rich in algae and microfauna (*Paleodictyoconus* gr. *cuvillieri-barremianus* biozone, Peybernès, 1976). These limestones are characterized by an abundance of rudists, among which Masse (1995) identifies at the top: *Horiopleura* aff. *dumortieri*, *Pachytraga paradoxa*, *Offneria interrupta*, *Toucasia* sp., and *Praecaprina* sp. In comparison with the adjacent Languedoc and Provence record, these caprinid-bearing limestones date from the latest Barremian (Frau *et al.,* 2018, 2020a; Masse *et al.,* 2020). This formation is overlain by a prominent planar sedimentary discontinuity (**Fig. 4A ; Fig. 5A**).

2.2.3 - Estagnol Limestones Formation (10 m) (Fig. 3, 4, 5A):

The Estagnol Limestones Formation consists of dull grey, silty, and marly limestones, arranged in irregular, undulating beds. Their bedding planes are often densely populated with orbitolinids, particularly *Palorbitolina lenticularis*, which led Peybernès (1976) and Jaffrézo (1980) to assign this unit to the "Basal Barremian-Bedoulian transition".

At the top of the formation a brachiopods biostrom is here termed as "*Niveau de Figuières"* (NF) (**Fig. 4**). It includes *Sellithyris sella, S. essertensis* and *Psilothyris chloris*. The formation is overlain by a condensed horizon, the "*Niveau de Saint-Martin"* (NSM) (**Fig. 4A**). This rubefied and karstified horizon followed by a sharp erosional surface, contains a few solitary corals and molluscs, including, ammonites wich are more frequent in the Île Saint-Martin (**Fig. 5B**) and Roc de Conilhac (**Fig. 5C**), with ?*Cheloniceras* sp., *Deshayesites* sp., *Ammonitoceras* sp. and *Macroscaphites* sp. cf. *striatisulcatus* (d'Orbigny), suggesting either part of the *Deshayesites forbesi* Zone and/or the lower *Deshayesites deshayesi* Zone.

2.2.4 - Ramade Marl Formation (Peybernès, 1976) **(Fig. 3, 4):**

The Ramade Marl Formation consists of an approximately 80 m thick succession of marls, interbedded with clayey limestone beds and horizons of carbonate nodules. Its soft deposits blanket the valleys, most of which are planted with vineyards nestled between two cliffed Urgonian limestone bars. These features shape the distinctive cuesta reliefs that make the Clape Massif so remarkable.

At the base of the formation, the "*Niveau de Vires"* (NV) is recognized as a condensed horizon, infilling in the irregularities of the surface atop the Estagnol Limestones Formation. This level is particularly fossiliferous, yielding an abundant and diverse basinal marine fauna. The cephalopods it has yielded are described in the present study.

2.2.4.1. The "*Niveau de Vires"* (Fig. 3, 4B): It is a decimetric-thick condensed bioclastic limestone bed, reworked, ferruginous, and highly organogenic, topped by a hardground (**Fig. 5D**). This condensation horizon had remained unknown to geologists until now. Among the fossils found out of context in the Clape Massif, Peybernès (1976) did mention a few ammonites from the *Deshayesites deshayesi* Zone, most likely from this level, including "*Deshayesites involutus* var. *hythensis* and *Cheloniceras cornueli"* (identified by Collignon). Meanwhile, Jaffrézo (1980) reported "*Deshayesites deshayesi* (d'Orbigny), *D.* cf. *multicostatum* Swin., *D. involutus* Spath, *D.* cf. *wilthshirei* Casey, and *Cheloniceras crassum* Spath" (identified by Busnardo).

At Parets d'en Sales (level 1) near Narbonne-Plage, the fauna is particularly rich and diverse (**Fig. 4B**). Among

the collected and identified specimens in this work are the nautiloids *Cymatoceras neocomiense* (d'Orbigny) and *Anglonautilus praeundulatus* Lehman *et al.*, along with a diverse assemblage of ammonites, including *Deshayesites grandis* Spath (Deshayesitidae), *Cheloniceras crassum* Spath (Douvilleiceratidae), *Procolombiceras* sp. (Acanthohoplitidae), *Delanoyites* nov. gen. nov. sp. A, *Delanoyites* nov. gen. nov. sp. B, *Ammonitoceras* aff. *lahuseni* (Sinzow) (Ancyloceratidae), *Toxoceratoides rochi* Casey (Acrioceratidae), *Macroscaphites* sp. cf. *striatisulcatus* (d'Orbigny) (Macroscaphitidae), *Pseudohaploceras matheroni* (d'Orbigny) and *Pseudohaploceras* sp. (Desmoceratidae). The biophase also includes numerous bivalves, such as *Plicatula placunea*, *Aetostreon latissimum*, *Sphaera corrugata*, *Panopea attenuata*, *P. prevostii*, *Gervillaria sowerbyana*, *G. anceps*, as well as gastropods, including *Natica clapensis*, echinoids like *Pliotoxaster collegnoi* and *Pseudodiadema malbosi*, and brachiopods such as *Sellithyris* gr. *sella*, *S. upwarensis*, and *Burrirhynchia miliani*.

The lateral extent of the ammonite-rich condensation horizon is limited to less than a hundred meters, but a few isolated ammonite discoveries within the Clape Massif indicate its presence in few other localities: Ramade (Narbonne), with *Deshayesites grandis*; Pech-Redon, northeast of Gueites (level 1) (Narbonne), with *D. grandis* and *Ancyloceras* sp.; Les Rompudes (level 2) (Fleury), with *Cheloniceras* gr. *crassum* and *Macroscaphites* sp. It reappears at Roc de Conilhac (levels 3), where it is clearly preserved in the irregularities of the erosional surface of the "*Niveau de Saint-Martin"*, and where it still contains *Deshayesites* gr. *grandis*.

Age: The ammonite assemblage contains allows us to confirm its **early Aptian age, Deshayesi Zone, Grandis Subzone** (see chap. 4).

None of the previous authors has described the transitional facies between the "Niveau de Vires" and the overlying Ramade Marls Formation. In the field, the onset of terrigenous marly sedimentation appears to occur abruptly, directly above the top hardground of the "Niveau de Vires", with no observable transitional interval (**Fig. 6B, D**). Within the Ramade Formation, we have distinguished the following units, in a synthetic manner, from bottom to top:

2.2.4.2. Parets d'en Sales Marls Member (20 m) (Fig. 3, 4B). Two distinct units:
- Fine, homogeneous grey marls (6.5 m) intercalated with some carbonate nodular beds. At the base, limonite nodules often correspond to pyritized small-sized fossils, including ammonites *Dufrenoyia furcata*, *Deshayesites* sp. (juveniles), *Aconeceras nisus*, *Cheloniceras crassum,* and *C.* cf. *meyendorffi*, miniaturized brachiopods (*Psilothyris* sp.), bivalves (*Plicatula placunea*, *Nucula* sp.), belemnites (*Neohibolites semicanaliculatus*, *Duvalia dilatata*), and undetermined pentacrines (**Fig. D, E**).

- Fine beige marls intercalated with argillaceous carbonate nodular beds (13.5 m). *Dufrenoyia furcata* is present, along with *Cheloniceras crassum, C. meyendorffi*, *Procolombiceras* sp., juvenile *Ammonitoceras* sp., and a diverse macrofauna (*Pliotoxaster collegnoi*, *Sellithyris* gr. *sella*, *Psilothyris chloris*, numerous bivalves and gastropods) that is currently under description.
The unit is capped by a bioclastic marly limestone bed, which is itself topped by a ferruginous hardground.

Age: The ammonites *Dufrenoyia furcata*, *Cheloniceras* gr. *meyendorffi*, and *Procolombiceras* sp., all belong to the ***Furcata* Zone, *Furcata* Subzone**.

2.2.4.3. Combe Longue Marls and Marly limestones Member (approximately 20 m) (Fig. 3, 4B): A succession of sequences with irregular thickness (ranging from 0.5 to 3 m), typically starting with a thick layer of beige marls intercalated with carbonate nodule bands, followed by nodular marly limestones containing a particularly rich biophase. This member, widely exposed across the La Clape Massif (Combe Longue, Ramade, Capitoul, Les Monges, Les Colombiers, Les Exals, etc.), represents the main fossiliferous horizon of the study area. Its rich faunal assemblages were extensively documented by d'Archiac (1859), Reynès (1861), Cairol (1872), and Doncieux (1903, 1921). However, no comprehensive inventory exists of the remarkable diversity of brachiopods, echinoderms, bivalves, and gastropods it contains (Guibbert & Fauré 2019).

Age: The ammonites *Dufrenoyia furcata*, *D. praedufrenoyi*, *Aconeceras nisus*, and *Cheloniceras meyendorffi* all belong to the ***Furcata* Zone**, ***Furcata* Subzone**. Notably, Peybernès (1971, 1976) and Jaffrézo (1980) assigned a similar age to this member (= Bowerbanki Zone in their framework) but also suggested that its uppermost levels encompassed the lower/upper Aptian transition (interpreted as the "*Nisus-Martinoides* Zone of the Lower Gargasian"). However, this interpretation is refuted below.

2.2.4.4. Saint-Martin Marls and Marl-Limestones Member (44 m) (Fig. 3) : This unit, rarely exposed in the Clape Massif due to the scree debris from the overlying Urgonian cliff, is outcropping on the Île Saint-Martin as a series of about ten shallowing-up sequences, with thicknesses ranging from one meter to several meters. These sequences consist of organogenic marl-limestone with very nodular bedding, brown silty marl, and a single bed of red, bioturbated, silty marly limestone, capped by a more or less distinctive hardground. The top of the member is characterized by a thick horizon containing the orbitolinids *Mesorbitolina parva* and *M. lotzei*.

Age: The ammonites *Dufrenoyia dufrenoyi* and *Cheloniceras meyendorffi* are found throughout the entire thickness of the member, corresponding to the ***Furcata* Zone, *Dufrenoyi* Subzone**.

Thus, contrary to the dating commonly accepted by previous authors (Peybernès, 1971, 1976, 2012; Jaffrézo, 1980), who attributed the upper part of the Ramade

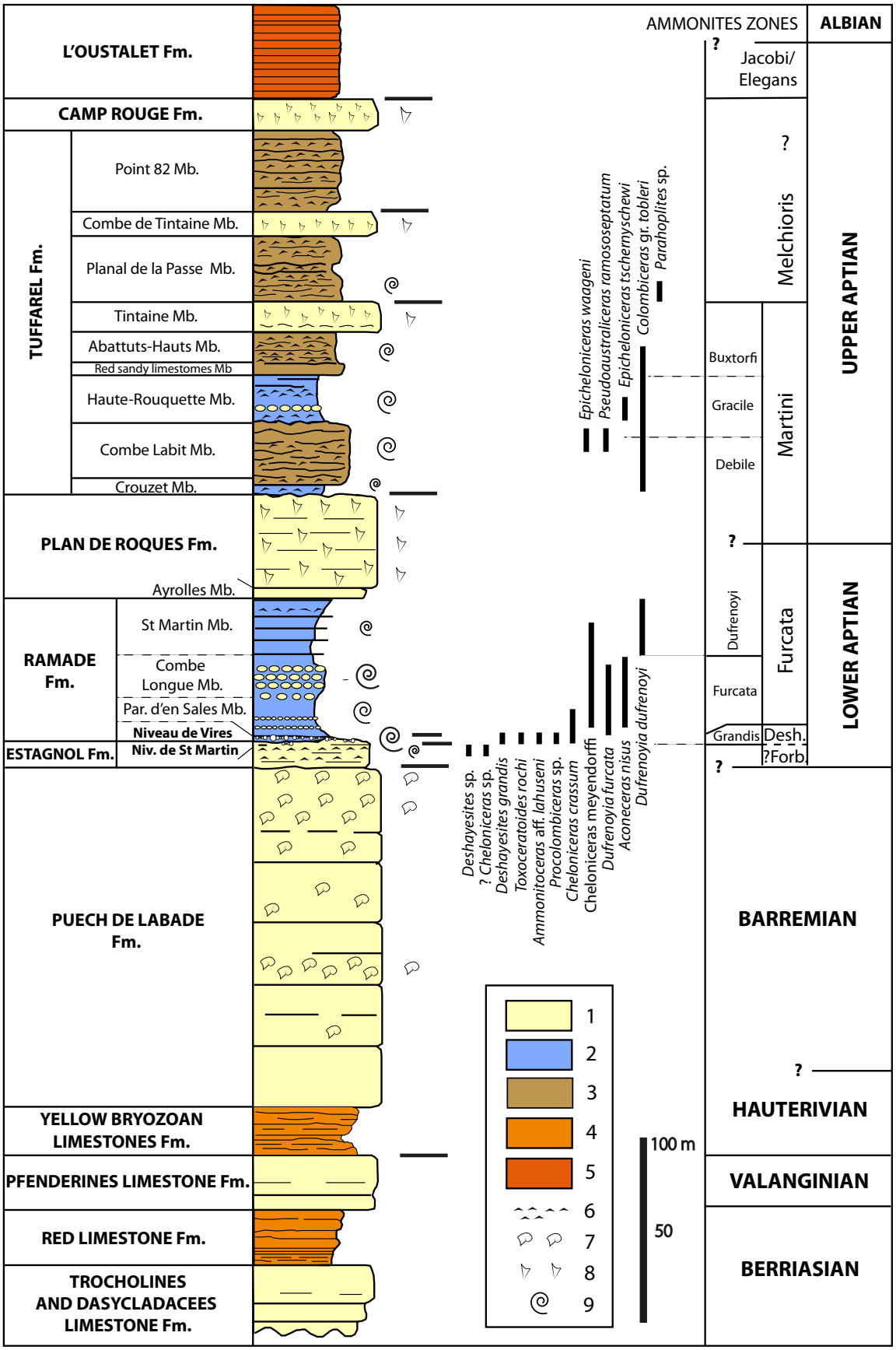

Fig. 3 - Lithostratigraphic synthetic setting of the Lower Cretaceous (Barremian to Albian) of the Clape Massif. Main ammonites and chronostratigraphic 1. Limestone; 2. Marls; 3. Bioclastic limestone; 4. Sandy and bioclastic limestone; 5. Red sandstone; 6. orbitolinids; 7. Requieniidae; 8. Polyconitidae; 9. Ammonites

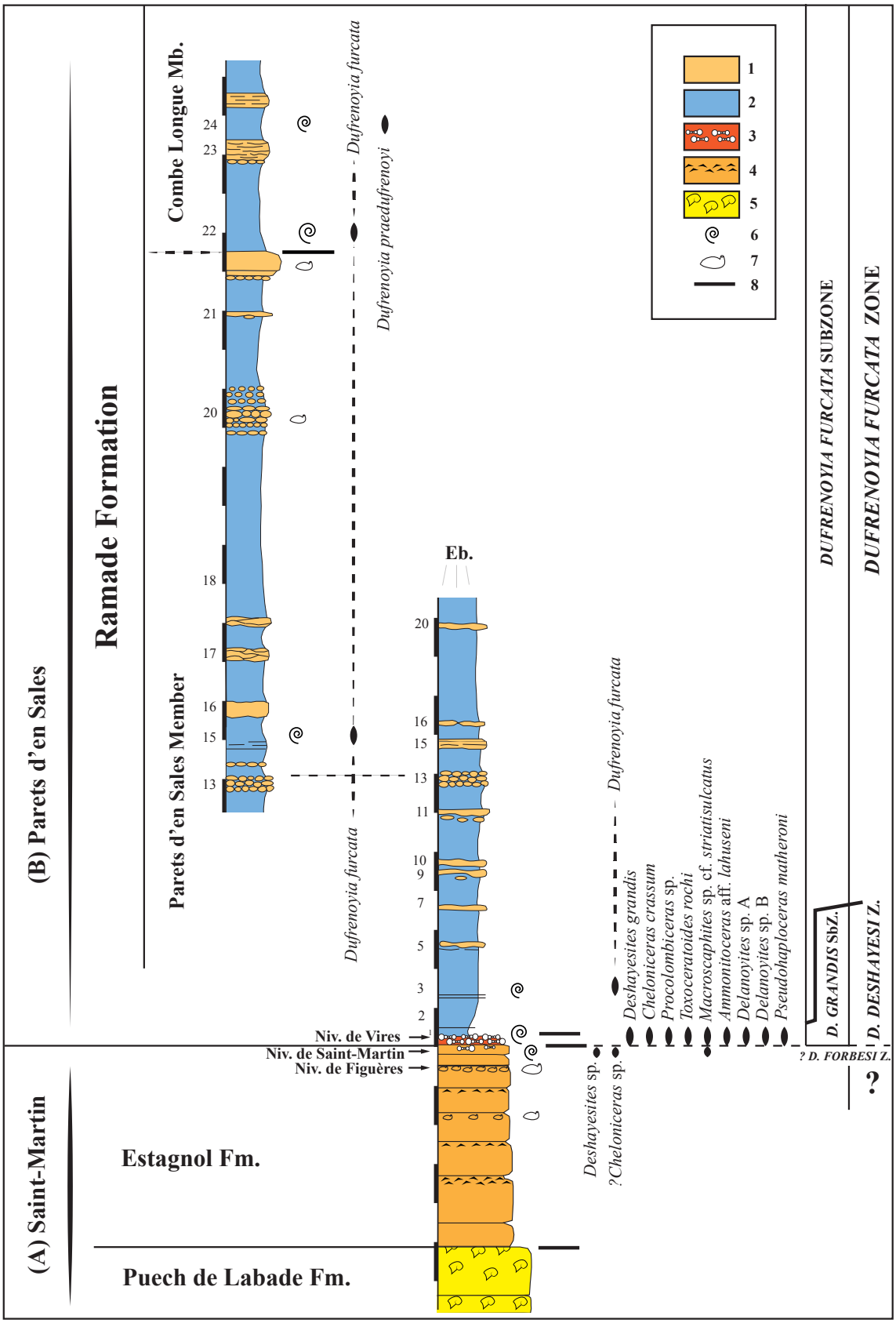

Fig. 4 - Litho-log of Saint-Martin-le-Bas outcrop (A) (topmost of Puech de Labade Fm. and Estagnol Fm.) and litho-log of the Paret d'en Sales outcrop (**B)** (Ramade Fm., lev. 1 to 24, Parets d'en Sales and lower Combe Longue Mb.). Distribution of the collected ammonites and correlation with the aptian biozonation. 1. Marly limestone; 2. Marls; 3. NV, condensed bioclastic limestone with Ammonites; 4. Limestone with orbitolinids; 5. Limestone with Requieniid, 6. Ammonites; 7. Brachiopods; 8. Erosional surface.

Formation to the early Late Aptian, its faunas correspond only to the Furcata Zone, representing the upper part of the lower Aptian (Szives *et al.,* 2024).

Below, we will not describe in detail the overlying Lower Cretaceous formations, as the description of their lithology and fossil content will be the subject of futures publications. The following can be distinguished:

2.2.5 - Plan de Roques Limestone Formation (Peybernès, 1976) (55 m) (Fig. 3):

It is a cliff-forming formation of compact, whitish Urgonian-type limestones, corresponding to the "*Calcaires moyens*" of Doncieux (1903). Its imposing cliffs rise above the marls of the Ramade Formation, shaping the picturesque landscapes of the La Clape Massif. The orbitolinid *Mesorbitolina parva* is the dominant microfossil. Masse (1995) identified several rudists, including *Toucasia* sp., *Horiopleura lamberti* (Munier-Chalmas), *Polyconites cf. verneuili* Bayle, *Eoradiolites plicatus* (Conrad), and *Agriopleura? dardeni*. The top of the Plan de Roques Limestone Formation is marked by a distinct erosive surface, previously overlooked in past studies.

Age: Despite its rich fauna, the age of this formation remains imprecise, having been assigned to the "Upper Gargasian" by Peybernès and the "Lower Gargasian" by Jaffrézo. However, as it is intercalated between the marls of the Ramade Formation—dated to the Furcata Zone (Furcata and Dufrenoyi subzones)—and the Tuffarel Formation, whose lower levels correspond to the *Epicheloniceras martini* Zone *pro parte*, it occupies a position at the transition between the lower and upper Aptian according to the Standard Mediterranean Ammonite Zonation (Szives *et al.,* 2024).

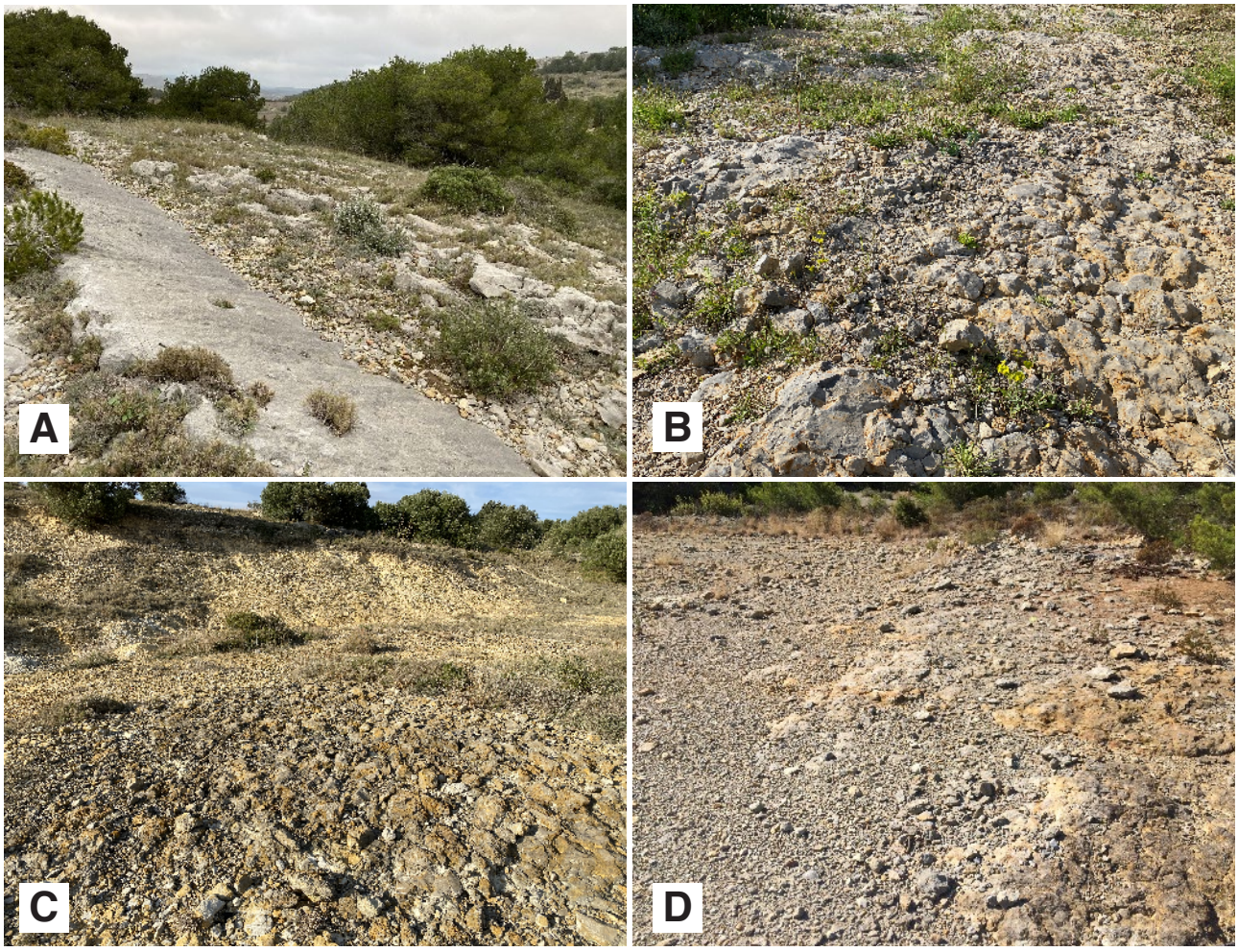

Fig. 5A-D: A. The discontinuity between the massive rudists limestones of the Puech de Labade Fm. and the orbitolinid limestones of the Estagnol Fm. is materialized by a flat surface (L'Estagnol, Gruissan); **B.** The "*Niveau de Saint-Martin"* at the top of the Estagnol Fm. Erosional surface of red limestones with ?*Cheloniceras* sp. (Saint-Martin, Gruissan); **C.** Erosional condensed ferruginous surface of the "*Niveau de Saint-Martin"* (Roc de Conilhac, Gruissan). The condensed marly limestones with *Deshayesites grandis* of the "*Niveau de Vires"* are preserved in the irregularities of the erosional; **D.** The "*Niveau de Vires"* at the base of the Ramade Fm. whose marls are visible in the background. Condensed marly limestones with ammonites (Vires, Narbonne).

2.2.6 - Tuffarel Marls and Limestones Formation (Peybernès, 1976) (200 m) (Fig. 3):

Within this clayey-carbonate complex, lithofacies alternate between marls, clayey limestones with the orbitolinid *Mesorbitolina texana*, calcareous sandstones, and several rudist-bearing limestone bars containing *Polyconites verneuili*, *Horiopleura lamberti*, among others. None of the previous authors (Cairol, 1872; Léenhardt, 1887; Doncieux, 1903; Peybernès, 1976; Jaffrezo, 1980) has established a detailed lithological succession, much like the geological map of Narbonne, which does not recognize any subdivisions (Lespinasse *et al.,* 1982). However, it has been possible to distinguish nine lithostratigraphic members that can be correlated across the La Clape Massif, and their description is currently in progress. All past studies have highlighted the strong faunal similarity between the Ramade and Tuffarel formations. While the bivalve and echinoderm assemblages remain nearly identical, a significant turnover is observed among the brachiopods and ammonites, all of which belong to the upper Aptian. The following newly identified subdivisions, listed from bottom to top, refine the stratigraphic framework (**Fig. 3**):

- Crouzet Member: *Martini* Zone, *Debile* Subzone, with *Colombiceras* gr. *tobleri*.

- Combe Labit Member: *Martini* Zone, *Debile* Subzone, with *Colombiceras* gr. *tobleri*, *C.* gr. *crassicostatus*, *Epicheloniceras waageni*, *Pseudoaustraliceras ramososeptatum*.

- Haute Rouquette Member: *Martini* Zone, *Gracile* Subzone, with *Epicheloniceras tschernyschewi*, *Colombiceras tobleri*, and *Colombiceras* sp.

- Red sandy limestones Member

- Abattuts-Hauts Member: *Martini* Zone, *Buxtorfi* Subzone likely, with *Colombiceras* gr. *tobleri*.

- Tintaine Member: Limestones with Polyconidae rudists.

- Planal de la Passe Member: *Melchioris* Zone, with *Parahoplites* sp.

- Combe de Tintaine Member: Limestones with Polyconidae rudists.

- Point 82 Member.

2.2.7 - Camp Rouge Formation (37 m) (**Fig. 3**)**:**

This massive carbonate formation is composed of various types of limestones, including Polyconidae rudists-bearing limestones, orbitolinid-bearing limestones, and lumachelle limestones with oysters. The formation is truncated by a hardground surface encrusted with oyster shells and corals. Its latest Aptian age is confirmed by the presence of numerous brachiopods from the genera *Cyrtothyris*, *Cyclothyris*, *Psilothyris*, *Gemmarcula*, among others.

2.2.8 - The Oustalet Sandstone Formation (more than one hundred meters) (**Fig. 3**)**:**

This formation consists of a monotonous accumulation of ferruginous or glauconitic sandstones, sometimes hard and quartzitic, sometimes softer, intercalated with red, sandy, and micaceous marls. The presence of *Hypacanthoplites elegans* (Fritel) (Magnan collection, Muséum d'Histoire Naturelle de Toulouse) confirms that at least the lower levels belong to the uppermost Aptian, *Jacobi* Zone of Reboulet *et al.* (2018) or *Elegans* Zone of Szives *et al.* (2024).

3. Palaeontological study (by Camille Frau)

Unless otherwise mentioned, the studied material is deposited in the Fauré, Frau, Téodori and Hourqueig collection at the Muséum d'Histoire Naturelle de Toulouse. Acronym repositories indicate:

MNHN: Muséum National d'Histoire Naturelle, Paris, France.

FSL: Faculté des Sciences de Lyon (Université Claude Bernard - Lyon-I), Lyon, France.

UJF-ID: Université Joseph Fourier, Institut Dolomieu, Grenoble, France.

BGSM: British Geological Survey and Mines, Nottingham, UK.

OUM: Oxford University Museum of Natural History, Oxford, UK.

GSUB: Geowissenschaftliche Sammlung of the University of Bremen, Germany.

A palaeobiological study is conducted on the representatives of the Deshayesitidae and Douvilleiceratidae thanks to collection of sufficient sample populations from the NSM and NV. We follow the measurements of Bersac *et al.* (2012) and Bersac & Bert (2015, 2018) for which the reader is referred. In this study, Python (Python Software Foundation, 2024) was used for data analysis and scripting through the assistance of the ChatGPT-4 model for natural language processing tasks. The studied measurements, given in millimetres, are as follows:

- For the Deshayesitidae (see Bersac *et al.* 2012, Bersac & Bert, 2015): D: shell diameter; Wh: whorl height; Ww: whorl width; U: umbilical diameter; R1: total number of ribs on the last half whorl; R2: number of primary ribs on the last half whorl; SSB: end diameter of the smooth siphonal band. Note that the duration of the SSB is used as one of the main criteria to be used for taxonomy of *Deshayesites*.

- For the Douvilleiceratidae (see Bersac & Bert, 2018): D: shell diameter; Wh: whorl height; Ww: whorl width; U: umbilical diameter; R: total number of ventral ribs on the last half whorl preserved; HT: number of heterotuberculated ribs (i.e. bituberculated ribs with a larger lateral tubercle) on the last half whorl; IT: number of isotuberculated ribs (i.e. bituberculated ribs with umbilical and lateral tubercles of equal strength) on the last half whorl; MTU: number of ribs with one single tubercle (umbilical) on the last half whorl; IN: number of inermous ribs on the last half whorl; STC: end diameter of the *Cheloniceras* stage (taken at the

last heterotuberculated rib of the shell); STP: end diameter of the *Prochelonicera*s stage (taken at the last isotuberculated rib of the shell).

- In addition to Deshayesitidae and Douvilleiceratidae, the Ancyloceratidae *Ammonitoceras* representatives are prevalent in the NV. Due to the deformations and fragmentary state of available materials, no statistical analysis was conducted. Measurements were limited to shell diameter (Ds) for criocone forms, and for ancylocone forms, spire diameter (Dsp), whorl height at the flexus (Whf), and total shell length (Ls) as given in Bersac & Bert (2022).

The synonymy lists for the identified species are restricted to the type specimens and those cited in key works that provide a comprehensive synonymy, to which readers are referred [*cum. syn.*].

Order Nautilida Agassiz, 1847
Superfamily Nautilaceae De Blainville, 1825
Family Nautilidae De Blainville, 1825
Genus *Cymatoceras* Hyatt, 1884

Type species: *Nautilus pseudoelegans* d'Orbigny, 1840; by original designation.

Cymatoceras neocomiense (d'Orbigny, 1840)

Pl. 1, Fig. 1-2; Pl. 2, Fig. 1-2

1840. *Nautilus neocomiensis* sp. nov. d'Orbigny, p. 74, pl. 11, fig. 1-3.
2006. *Cymatoceras neocomiense* (d'Orbigny) – Tintant & Gauthier *in* Gauthier *et al.,* p. 20, pl. 2, fig. 3 (= lectotype), 4.
2012. *Cymatoceras neocomiense* (d'Orbigny) – Delanoy *et al.,* p. 163, pl. 6, fig. 1a-c, 2; pl. 7, fig. 2a-b; pl. 8, fig. 3a-b; pl. 10, fig. 2a-b; pl. 12, fig. 2a-b; pl. 13, fig. 1, 3a-b [*cum. syn*.].

Type: The lectotype designated by Tintant & Gauthier *in* Gauthier *et al.* (2006) is specimen MNHN-F.R04249 (d'Orbigny collection) from the Barremian of Escragnolles, southeast France.

Material: Narbonne, Parets d'en Sales, lev. 1, 2 ex.: NV1 (Pl. 1, Fig. 1-2); NV3 (Pl. 2, Fig. 1-2).

Dimensions: in mm.

Specimens	D	U	Wh	Ww
NV1	107.1	13.0	57.5	c.61.8
NV3	c.125	-	c.72	c.83

Description:

Medium-sized nautiloid characterised by a nautiliconic, globular involute coiling with closed umbilicus, rounded umbilical margin, venter, and flanks. The whorl section is subcircular, wider than high, whose maximum whorl width occurs at the dorsal third. The adult shell ornamentation consists of dense, flat-topped, and broad flexuous ribs which describe a convex curve on the upper flanks and end in a large ventral, adorally convex sinus. Ribs are weakened at mid-flank. The suture line is composed of moderately low ventral saddle, followed by a wide, shallow lateral lobe that continues in the umbilical shoulder as a narrow and low umbilical saddle.

Discussion:

The reader is referred to Delanoy *et al.* (2012) for a detailed description of that species and a comparison with other *Cymatoceras* species.

Distribution: According to Delanoy *et al.* (2012) and subsequent studies, the species is widespread in the Mediterranean and Caucasian Tethys, with undoubted records from Spain, France, Switzerland, Germany, Czech Republic, Bulgaria, Turkmenistan, the Caucasus, Crimea, and Algeria, where it ranges through Hauterivian to Barremian deposits.

Family Cenoceratidae Tintant & Kabamba, 1983
Genus *Anglonautilus* Spath, 1927

Type species: *Nautilus undulatus* Sowerby, 1813; by original designation.

Anglonautilus praeundulatus Lehmann, Maisch, Baudouin, Salfinger-Maisch, 2017

Pl. 1, Fig. 3-4

2017. *Anglonautilus praeundulatus* Lehmann *et al.,* p. 69, fig. 2.
2021. *Anglonautilus praeundulatus* Lehmann *et al.* – Baudouin *et al*., p. 12, Pl. I, fig. 1.a-b; Pl. II, fig. 1.a-b; Pl. III, fig. 1.a-c; Pl. IV, figs. 1.a-b, 2; Pl. V, figs. 1, 2.a-b; Pl. VI, fig. 1 [*cum. syn*.].

Type: The holotype by monotypy is specimen GSUB C7505 designated by Lehmann *et al.* (2017) from the Lower Aptian of the Forcall Formation of Castellote, northeast Spain.

Material: Narbonne, Parets d'en Sales, lev. 1, 1 ex.: NV2 (Pl. 1, Fig. 3-4).

Dimensions: in mm.

Specimen	D	U	Wh	Ww
NV2	113.2	12.7	69.8	-

Description:

Medium-sized nautiloid characterised by a nautiliconic, involute coiling with moderately small, deep umbilicus, rounded to steep umbilical margin, slightly rounded flanks and venter. The whorl section is subrectangular and slightly compressed and becomes quadrate as growth increases. The

ornamentation is smooth on the inner whorls and consists of large, well-rounded transverse undulations in the last part of the phragmocone. Beside the ventral undulation, the ornamentation reverts to smooth through the early part of the body chamber. The suture line is slightly sinusoidal and composed of a wide, shallow ventral saddle, wide, deep lateral lobe with a convex curvature at mid flank and a shallow umbilical saddle

Discussion:

Based on the ventral transverse undulations on the phragmocone, the specimen is identified as belonging to the genus *Anglonautilus*. It is specifically assigned to *Anglonautilus praeundulatus* due to its compressed whorl section, open umbilicus, flattened ventral undulations, and distinct lateral lobes. For a comprehensive description of *Anglonautilus praeundulatus* and a comparison with other species within the genus, including the type species, readers are referred to Lehmann *et al.* (2017) and Baudouin *et al.* (2021).

Distribution: According to Baudouin *et al.* (2021), the species is only recorded in eastern Spain and southeastern France, ranging through the Lower Hauterivian (*Nodosoplicatum* Zone) to the lower Aptian (*Deshayesi* Zone).

Super-order Ammonoida Haeckel, 1866
Order Ammonitida Haeckel, 1866
Superfamily Deshayesitoidea Stoyanow, 1949
Family Deshayesitidae Stoyanow, 1949
Genus *Deshayesites* Stoyanow, 1949

Type species: *Ammonites deshayesi* d'Orbigny, 1841; by original designation.

***Deshayesites* sp.**

Pl. 3, Fig. 7-8

Material: Narbonne, La Ramade, "Niveau de Saint-Martin", 1 ex.: NSM5 (Pl. 3, Fig. 7-8).

Dimensions: in mm.

Specimen	D	U	Wh	Ww
NSM5	47	-	16	10

Description:

The specimen at our disposal corresponds to a body-chamber fragment of a small deshayesitid ammonite, with an estimated diameter not exceeding a few centimetres. Its whorl section is compressed and sub-oval, with a rounded venter. The ribbing consists of alternating strong, widely spaced, slightly flexuous primary ribs, showing a faint retrocurvature at the umbilical margin, and short secondary ribs originating high on the flank. All ribs cross the siphonal area without losing relief, forming a slightly projecting chevron at the end of the whorl.

Discussion:

Due to its state of preservation, a precise identification of the specimen is not possible, particularly as the morphology of the ventral area in the inner whorls is missing. Nevertheless, the general morphology and ribbing recall certain deshayesitid forms typically observed in pre-upper *Deshayesites deshayesi* Zone (Casey, 1962), although this cannot be confirmed with certainty.

Distribution: We tentatively assign this specimen to an age range spanning the *Deshayesites forbesi* Zone and/or the lower *Deshayesites deshayesi* Zone, without the possibility of firm confirmation.

***Deshayesites grandis* Spath, 1930**

Pl. 4, Fig. 1-19; Pl. 5, Fig. 1-17; Pl. 6, Fig. 1-16; Pl. 7, Fig. 1-6; Pl. 8, Fig. 1-5; Pl. 9, Fig. 1-4; Pl. 10, Fig. 1-5; Pl. 11, Fig. 1-3; Pl. 12, Fig. 1

1930. *Deshayesites grandis* sp. nov. Spath, pl. XVII, fig. 2a, b.
2012. *Deshayesites grandis* Spath – Bersac, Bert & Matrion, p. 251 [*cum*. *syn*.].

Type: The holotype designated by Casey (1963, p. 308) is specimen BGSM.Geol.Soc.Col.2300 (F.W. Simms coll.) from the *Scaphites* Beds Member (Group V) of Atherfield, Isle of Wight, southern UK. It was first illustrated by Spath (1930, pl. XVII, fig. 2a, b).

Material: Narbonne, Parets d'en Sales, lev. 1:
- 47 figured ex.: NV4-13, NV22 (Pl. 4, Fig. 1-19); NV14-21, NV50 (Pl. 5, Fig. 1-17); NV23-30 (Pl. 6, Fig. 1-16); NV31-35 (Pl. 7, Fig. 1-6); NV36-38 (Pl. 8, Fig. 1-5); NV39-41 (Pl. 9, Fig. 1-4); NV42-45 (Pl. 10, Fig. 1-5); NV46-47, NV49 (Pl. 11, Fig. 1-3; NV48 (Pl. 12, Fig. 1).
- 12 non figured ex.: NV104-111; NV117-120.

Dimensions: See **Tabl.2 in adnex.**

Description:

The studied material includes typical *Deshayesites* with very small to very large diameters ranging from 24 mm to 274 mm. The studied sample exhibits a clear bimodal distribution in adult diameter frequency, with smaller individuals clustered around 40–100 mm, while the larger specimens are concentrated in the 200–250 mm range (**Fig. 6A**). This result conforms with the size-related sexual dimorphism documented in British *Deshayesites* by Bersac & Bert (2012, 2015) or the southern French *Deshayesites* by Frau & Delanoy (2022). Here we consider the specimens of very small to moderate size, up to 115 mm with an average diameter of approximately 55.6 mm, as the putative microconchs. These microconchs represent almost 62% of the studied material. The putative macroconchs reach larger sizes, with an average diameter of approximately 205 mm and a maximum diameter of

274 mm. The bivariate diagrams for the growth of the shell's dimensional parameters (U, Wh, and Nb ribs as functions of D) show homogeneous scatter around the mean curve in all cases, with R^2 values greater than 0.75–0,9 (**Fig. 6B**). This indicates that the growth of these parameters is broadly isometric and harmonic, which attests to the overall homogeneity of the studied material. The relationship between whorl width and diameter is more problematic to assess due to the limited number of available measurements and the potential distortion caused by fossil preservation. Nevertheless, the putative microconchs exhibit an extremely discoidal shape ($0.21 \leq Ww/D \leq 0.33$; average ~ 0.27), are weakly compressed ($0.52 \leq Ww/Wh \leq 0.81$; average ~ 0.62), and have very evolute coiling ($0.35 \leq U/Wh \leq 1.06$; average ~ 0.63). They mainly embrace discocone to subdiscone shapes, with rare occurrences of virgacone shapes ($0.18 \leq Uw/D \leq 0.31$; average ~ 0.27), according to the terminology of Klug *et al.* (2015a) (**Fig. 6C**). On the other hand, the putative macroconchs are of larger average size, yet they share similarities with the microconchs in being extremely discoidal ($0.15 \leq Ww/D \leq 0.32$; average ~ 0.21), weakly compressed ($0.42 \leq Ww/Wh \leq 1$; average ~ 0.58), and very evolute in their coiling ($0.32 \leq U/Wh \leq 0.97$; average ~ 0.73). In terms of conch shapes, the macroconchs exhibit belocone to virgacone shell shape ($0.18 \leq Uw/D \leq 0.32$; average ~ 0.26) (**Fig. 6C**).

Based on the ontogenetic sequences of *Deshayesites* redefined by Bersac and Bert (2012, 2015), our material lacks observations of the post-embryonic stages due to its incompleteness. Consequently, we are unable to determine the presence or absence of the globular Stage A or the Kossmatella-related Stage B of these authors. The first observation of ribbing typically begins with Stage C of Bersac & Bert (2012, 2015) in the best-preserved microconch individuals. This stage is characterized by dense, flexuous, thin ribs, which later show more or less regular alternation between primary and secondary ribs. The secondary ribs are usually denser and emerge at various heights on the flanks (specimens Pl. 4, Fig. 8-9 (NV9), Pl. 5, Fig. 1 (NV14), Fig. 12 (NV19), Pl. 6, Fig. 13-14 (NV30)). This quickly transitions in Stage D of Bersac & Bert (2012, 2015), characterized by thicker, more spaced, and less flexuous ribbing with a relatively regular alternation between primary and secondary ribs, often showing slight peri-umbilical retrocurvature (specimens Pl. 4, Fig. 2-4 (NV15) and (Pl. 6, Fig. 11-12 (NV28)). This stage persists until the end of the adult whorl. When fully formed, the body chamber occupies approximately half of the last whorl. In large macroconchs, a subsequent Stage E as defined by Bersac & Bert (2012, 2015) develops on the adult whorls, featuring straight, spaced simple and thick ribs that terminate in a simple and sinuous peristome with a discrete collared aperture as observed in specimens non fig and Pl. 11, Fig. 1 (NV46)).

The correlation between the parameters U/D, Wh/D, Ww/Wh, R1 and R2—potential indicators of variability linked to Westermann's first law—was calculated using Pearson's correlation coefficient, which evaluates the strength and direction of the linear relationship between two variables. The results are presented in **Fig. 6D**. We found a moderate to strong negative correlation between U/D and Wh/D, and between Wh/D *versus* Ww/Wh, while U/D *versus* Ww/Wh is moderately positively correlated. In contrast, R1 and R2 show only weak positive or negative correlation with other morphological parameters. Consequently, this can be interpreted as a strong correlation between degree of involution and aspect of the whorl section, while the ribbing density is not have a strong degree of variation. In practice, it can be recognised in the putative microconchs a continuous chain ranging from an evolute morphotype with robust ornamentation, resembling *Deshayesites vectensis* (Spath, 1930) from a typological point of view (specimen Pl. 6, Fig. 6-8 (NV26) and Pl. 5, Fig. 1 (NV14)) to an involute morphotype with slender ornamentation resembling *Deshayesites grandis* var. *grandis* (Spath, 1930) and *Deshayesites grandis* var. *lacertosus* (Casey, 1964) (for exemple specimen Pl. 6, Fig. 4-5 (NV25)). Such polymorphism partly fit with the variability of type 1, as defined by Bersac & Bert (2012, 2015), in the genus *Deshayesites*, resulting from Westermann's First Law of Covariation, which encompasses poles of extreme morphologies. This law also influences the respective duration of Stage C "with thin ribbing" and Stage D "with strong ribbing," as previously noted by Bersac *et al.* (2012). In putative macroconchs, a similar continuous spectrum is recognized, but it is more complex, progressing from an evolute morphotype with unattenuated ornamentation (specimen Pl. 1, Fig. 1 (NV46)) to an involute morphotype with attenuated ornamentation on the phragmocone (specimen Pl. 10, Fig. 1-2 (NV42)), and occasionally an involute morphotype with unattenuated ornamentation (specimen Pl. 11, Fig. 1 (NV46)). The criterion of secondary attenuation of ribbing in macroconchs is observed, aligning with the variability of type 2 as defined by Bersac & Bert (2012, 2015). In contrast, putative microconchs do not exhibit secondary attenuation of ornamentation either in the phragmocone or in the body chamber. Instead, a regression of the latter adult whorl often occurs, with an undifferentiated peristome (specimen Pl. 6, Fig. 11-12 (NV28)).

The aspect of the whorl shape in the material at our disposal, both in micro- and macroconchs, is challenging to observe according to the criteria established by Bersac & Bert (2012, 2015). In the best-preserved putative microconchs, it can only be confirmed that a smooth siphonal band is present at approximately D ~ 20 mm (specimens Pl. 6, Fig. 6-8 (NV26) and Pl. 5, Fig. 8-9 (NV16)). This is followed by a subtabulate ventral area without rib attenuation up to D ~ 20 mm, and finally transitions to a rounded venter up to the peristome, with ribs crossing the siphonal area without losing their relief. Broadly speaking, these are the criteria adopted for the palaeospecies *Deshayesites grandis* (Casey, 1964) as defined by Bersac & Bert (2012, 2015). In two other microconchs, the ventral area is distinctly flattened, with a smooth siphonal band still present up to approximately D ~ 27 mm, and rib branches almost forming

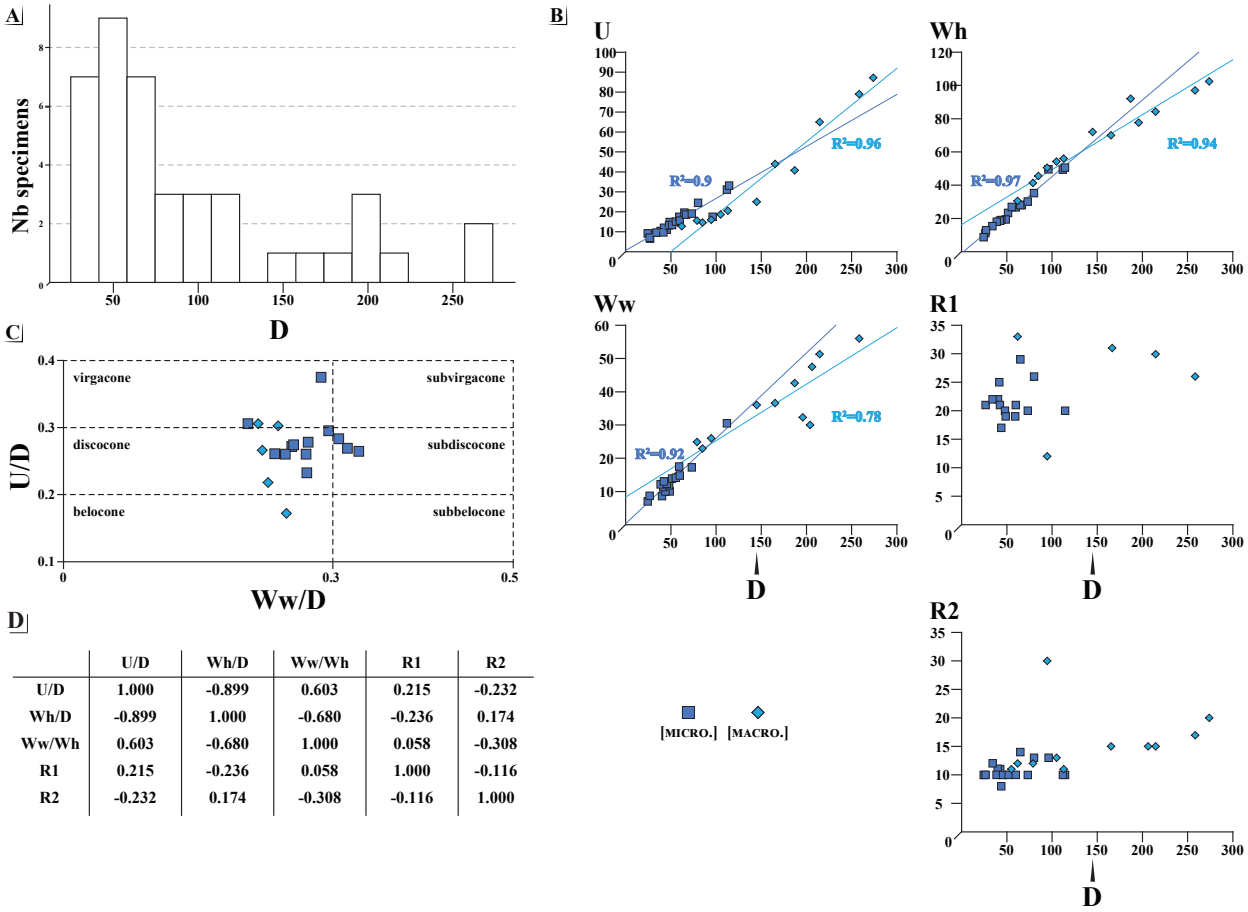

D

	U/D	Wh/D	Ww/Wh	R1	R2
U/D	1.000	-0.899	0.603	0.215	-0.232
Wh/D	-0.899	1.000	-0.680	-0.236	0.174
Ww/Wh	0.603	-0.680	1.000	0.058	-0.308
R1	0.215	-0.236	0.058	1.000	-0.116
R2	-0.232	0.174	-0.308	-0.116	1.000

Fig. 6 - Palaeobiological study of the Deshayesitidae *Deshayesites grandis* Spath, 1930, with representation of putative antidimorphs. **A**: Asymmetric bimodal distribution of adult diameter frequencies; **B**: Bivariate diagrams showing the growth of shell parameters (U, Wh, and number of ribs) as a function of D; **C**: Relationships between the U/D and Ww/U ratios, describing conch shapes ranging mainly from discocone to subdiscone morphologies; **D**: Pearson correlation coefficients between U/D, Wh/D, Ww/Wh, and the numbers of ribs R1 and R2.

latero-ventral tubercles (specimen Pl. 4, Fig. 3-4 (NV4)). This typologically corresponds with the understanding of basal representatives of the genus *Dufrenoyia* as redefined by Bersac & Bert (2012).

The suture lines are of *Deshayesites*-type but no so well preserved for further description.

Discussion:

The studied *Deshayesites* from the NV consist of well-preserved microconchs and macroconchs, displaying the characteristic high degree of polymorphism previously documented by Bersac *et al.* (2012). Many individuals correspond to Casey's typological taxa *Deshayesites grandis grandis* Spath, 1930, *Deshayesites grandis lacertosus* Casey, 1964, *Deshayesites vectensis* Spath, 1930, *Deshayesites geniculatus* Casey, 1964, and *Deshayesites wiltshirei* Casey, 1964; all originally from the *Scaphites* Bed Member of the Atherfield Clay series, Isle of Wight, southern UK. These typological taxa are now grouped under the palaeospecies *Deshayesites grandis* by Bersac & Bert (2012, 2015). Although based on limited observations the SSB ending value of the material from the NV confirms the assignment to *Deshayesites grandis*. However, rare individuals develop a *Dufrenoyia*-like tabulate juvenile venter with almost latero-ventral tubercles, and a SSB extending beyond 27 mm (specimen Pl. 4, Fig. 3-4 (NV4)). Those individuals surpass the taxonomic limits of the palaeospecies *Deshayesites grandis* as defined by Bersac & Bert (2012, 2015). The question arises whether these peculiar *Dufrenoyia*-like individuals from the NV could represent the most basal forms of *Dufrenoyia*, or if they correspond to extreme morphologies of the palaeospecies *Deshayesites grandis*. Initially, it could be argued that the NV represents a condensed horizon, containing polyzonal populations around the boundary between the *Deshayesites deshayesi* Zone and the *Dufrenoyia furcata* Zone, and that the peculiar specimens at our disposal illustrate basal relatives of *Dufrenoyia*. However, the NV is regionally capped by marls of the *Dufrenoyia furcata* Zone, where *Dufrenoyia* specimens with pyritic nuclei exhibit SSB ending values characteristic of the palaeospecies *Dufrenoyia furcata* as defined by Bersac *et al.* (2012). Therefore, investigating the broader spectrum of the palaeospecies *Deshayesites grandis* appears to be a compelling hypothesis for future

research. However, definitive conclusions cannot be drawn from the NV material due to its condensed nature.

Distribution:

According to its current definition, the species is known with certainty from the southern United Kingdom, Germany, France, and Spain, and possibly from Bulgaria, within the *Deshayesi* Zone, where it defines a nominative subzone in its upper part.

Superfamily Douvilleicerataceae
Parona & Bonarelli, 1897
Family Douvilleiceratidae Parona & Bonarelli, 1897
Genus *Cheloniceras* Hyatt, 1903

Type species: *Ammonites cornuelianus* d'Orbigny, 1841; see opinion 428 of the I.C.Z.N.

?*Cheloniceras* sp.

Pl. 3, Fig. 1-4

Material: Gruissan, Saint-Martin, "Niveau de Saint-Martin", 4 ex.: NSM1 (Pl. 3, Fig. 1-2); NMS2 (Pl. 3, Fig. 3-4); NSM6; NSM7.

Dimensions: See **Tabl 1**.

Description:

The two specimens at our disposal correspond to large-sized outer whorls of pachyconic douvilleiceratid ammonites. They develop a more or less depressed subquadrate section with a broad convex venter. In specimen Pl. 3, Fig. 1-2 (NSM1), the ribbing in the last preserved whorl consists of bituberculate primary ribs with equally sized umbilical and lateral tubercles. These correspond to the isotuberculated ribbed stage referred to as the *Prochelonicera* stage by Bersac & Bert (2018). Additionally, one to three atuberculate intercalary ribs may occur between the primary ribs, occasionally connecting indistinctly to the main ribs. The ribbing progressively transitions to rather uniform, rigid, straight inermous ribs crossing the venter, characteristic of the Adult stage (sensu Bersac & Bert, 2018). The peristomes are not preserved in either specimen.

Discussion:

Based on the morphology and ribbing of their outer whorls, these specimens undoubtedly belong to early Aptian douvilleiceratids. However, the absence of inner whorls makes it difficult to assign them confidently to either *Prochelonicera* or *Cheloniceras* as currently defined (Bersac & Bert, 2018, and references therein), since both genera share very similar adult growth ontogeny stages (*Prochelonicera* and Adult stages), also observed in specimens from the NSM. We tentatively classify these specimens within ?*Cheloniceras*, based on the general ribbing pattern and the relatively less evolute coiling, which better matches the current understanding of *Cheloniceras*.

Distribution: We tentatively assign this specimen to an age range spanning the *Deshayesites forbesi* Zone and/or the lower *Deshayesites deshayesi* Zone, without the possibility of firm confirmation.

***Cheloniceras crassum* Spath, 1930**

Pl. 13, Fig. 1-20; Pl. 14, Fig. 1-8; Pl. 15, Fig. 1-8; Pl. 16, Fig. 1-4; Pl. 17, Fig. 1-4; Pl. 18, Fig. 1-8; Pl. 19, Fig. 1

1930 *Cheloniceras crassum* Spath, p. 449, pl. XV, fig. 6.
1961 *Cheloniceras* (*Cheloniceras*) *crassum* Spath – Casey, p. 208, pl. XXXIV, fig. 2, pl. XXV, fig. 4a-b (= Spath, 1930, pl. XV, fig. 6); text-fig. 64, 65, 66a-e [*cum*. *syn*.].

Type: The holotype is specimen MUM.L11605/A (Dixon coll.) from the Hythe Beds, Kent southeast UK. It was properly re-illustrated by Spath (1930, pl. XXV, fig. 4a-b).

Material: Narbonne, Parets d'en Sales, lev. 1 :
- 29 figured ex.: NV51-60 (Pl. 13, Fig. 1-20), NV61-64 (Pl. 14, Fig. 1-8), NV65-68 (Pl. 15, Fig. 1-8), NV69-70 (Pl. 16, Fig. 1-4), NV71-72 (Pl. 17, Fig. 1-4), NV73-78 (Pl. 18, Fig. 1-8), NV79 (Pl. 19, Fig. 1).
- 5 non figured ex.: NV112-116.

Dimensions: See **Tabl.3 in adnex.**

Description:

The specimens under our examination comprise a large collection of pachyconic douvilleiceratid ammonites, encompassing a wide size range from very small to very large, with diameters varying from 23 mm to 211 mm (**Fig. 7A**). These specimens exhibit a discoidal morphology (Ww/D ~ 0.52), are slightly depressed (Ww/Wh ~ 1.39), and display highly evolute coiling (U/Wh ~ 0.94). This morphology aligns with the paragicone to subvirgacone shell shapes as described by Klug *et al.* (2015a) (**Fig. 7B**). The body chamber of these ammonites typically occupies approximately half of the adult whorl.
The analysis of the ontogenetic sequences confirms the

Specimens	D	U	Wh	Ww	R	HT	R1	R2	MTU	IN	STC	STP
NSM1	225	85	75	-	19	3			12			
NMS2	165	64	56	-	20							

Tabl. 1 - Dimensions in mm of the material assigned to Douvilleiceratidae ?*Cheloniceras* sp. See text for acronyms.

assignment of this sample to *Cheloniceras*, following the criteria established by Bersac & Bert (2018). The first observation of ribbing typically begins with the post-embryonic Stage Royerianum, as observed in specimen Pl. 13, Fig. 5-6 (NV53); however, the precise diameter at which this stage finishes cannot be accurately determined from the material at our disposal. This stage is characterized by a reniform whorl section, a crateriform umbilicus, and spaced, flat-topped ribs adorned with spiny tubercles. These tubercles are separated by smooth interspaces, or sometimes include a variable number of faintly simple intercalary ribs and periodic constrictions.

Following the Royerianum Stage, the ontogenetic sequence transitions into the Stage *Cheloniceras sensu* Bersac & Bert (2018). This stage is distinguished by a more or less depressed subquadrate whorl section with a convex venter. Ribbing during this stage develops into primary, Y-shaped heterotuberculate ribs, which usually bear elongated or rounded peri-umbilical tubercles and prominent upper lateral tubercles situated at the points of rib bifurcation (e.g., specimens Pl. 15, Fig. 1-2 (NV65) and Pl. 15, Fig. 5-6 (NV67) for exemple) the best illustrations of this stage. These lateral tubercles are often inflated and pinched opposite to the axis of coiling but generally maintain rounded bases on molds. The two branches of the primary ribs cross the venter with noticeable thickening, where the forward branch is typically stronger than the backward one. Occasionally, a slightly thickened shoulder appears on the latero-ventral margin of the ventral branches. Constrictions following primary ribs, similar to those seen in the Royerianum Stage, may also be present in the *Cheloniceras* Stage (e.g., specimen Pl. 15, Fig. 3-4 (NV66) and also Pl. 18, Fig. 8 (NV78)). Additionally, atuberculate intercalary ribs—typically one or two—can occur between the main ribs or connect at the points of furcation, forming indistinct trifurcate primary ribs. This stage concludes at an average diameter of 74.61 mm in the studied sample, with a modal value of 60 mm.

As growth progresses, the succeeding Stage *Procheloniceras* emerges, generally occupying the adult whorl. This stage is marked by a more rounded but still depressed subquadrate whorl section. The ribbing consists of primary bituberculate ribs with umbilical and upper lateral tubercles of approximately equal size, typically with a single branch crossing the venter (e.g., specimens Pl. 18, Fig. 1 (NV73)). These are identified as isotuberculate ribs by Bersac & Bert (2018). Atuberculate intercalary ribs, usually one and occasionally two, may appear between the primary ribs, with variable lengths—the backward rib generally being the longer of the two. Our data on this stage is limited, but it typically ends at an average diameter of 111 mm, with no distinct modal value calculated.

In the best-preserved specimens, the sequence culminates in the Adult Stage as defined by Bersac & Bert (2018). This stage is characterized by a compressed subquadrate whorl section, with ribbing becoming more uniform. It primarily consists of single or bifurcate ribs of equal size, with bifurcation occurring at peri-umbilical tubercles or bullae, and sporadic intercalary ribs (e.g., specimens Pl. 16, Fig. 3-4 (NV70)). All ribs pass straight or slightly prorsiradiate over the flank and venter, generally thickening at the peri-ventral shoulders; in some instances, there is a slight concavity of the ribs over the venter. The length of this stage varies and is sometimes absent, depending on the specimen.

A statistic analysis has been conducted on a selection of the best preserved specimens, with values summarised in **Tabl. 2**. The results of the bivariate analyses for the variables D, U, Wh, STC and STP are well-described by an isometric function, indicating homogeneity within the studied sample (**Fig. 7C**). This is not the case for whorl width (Ww), which is affected by a limited number of measurements and more distortions from fossil preservation. The overall distribution of diameters in the sample is bimodal, with smaller individuals clustered around 50-100 mm, while the larger specimens are concentrated in the 125-175 mm range (**Fig. 7A**). The mean diameter (93 mm) and median (84,4 mm) of diameters are relatively close, yet the high standard deviation indicates substantial variability in the diameters. The Shapiro-Wilk test, which was employed to assess normality, yielded a p-value of 0.176757. Since this p-value exceeds the 0.05 threshold, we do not reject the null hypothesis, suggesting that the data is normally distributed. However, the distribution remains fairly dispersed around the mean. Among the specimens with diameters below the mean, several—including Pl. 13, Fig. 19-20 (NV60), and notably Pl. 13, Fig. 17-18 (NV58), which is the best-preserved—exhibit a sudden regression, and subsequent tightening of the whorl cross-section as it approaches the aperture. Additionally, the ribbing becomes rursiradiate, with the peristome marked by two final elevated ribs that converge at the umbilical seam, followed by a brief smooth apertural margin partly visible in the left side. The combination of small size relative to the overall paleopopulation, modifications in adult coiling, and a differentiated peristome are the primary criteria for identifying mature microconchs, as outlined by Klug *et al.* (2015b). Based on these characteristics, we hypothesize that the specimens in question represent putative microconchs. In contrast, some of the larger, well-preserved individuals exhibit a slight egression of the adult whorl, a feature that could suggest their identification as putative macroconchs. However, the lack of a complete peristome in these specimens prevents definitive confirmation, and the approximation of the sutures cannot be fully assessed due to the limitations in fossil preservation.

Nevertheless, the variation in the duration of the STC stage—the only stage that allows a comprehensive analysis within our sample—further supports the hypothesis of morpho-dimensional sexual dimorphism within the population. The duration of the STC stage is significant, ranging from 25 mm to 130.7 mm. We explored the probability of a normal distribution of STC variables and analyzed their histograms (**Fig. 7D**). The STC sum distribution exhibits clear signs of bimodality, with two peaks occurring in the 60-80 mm and 120-140 mm

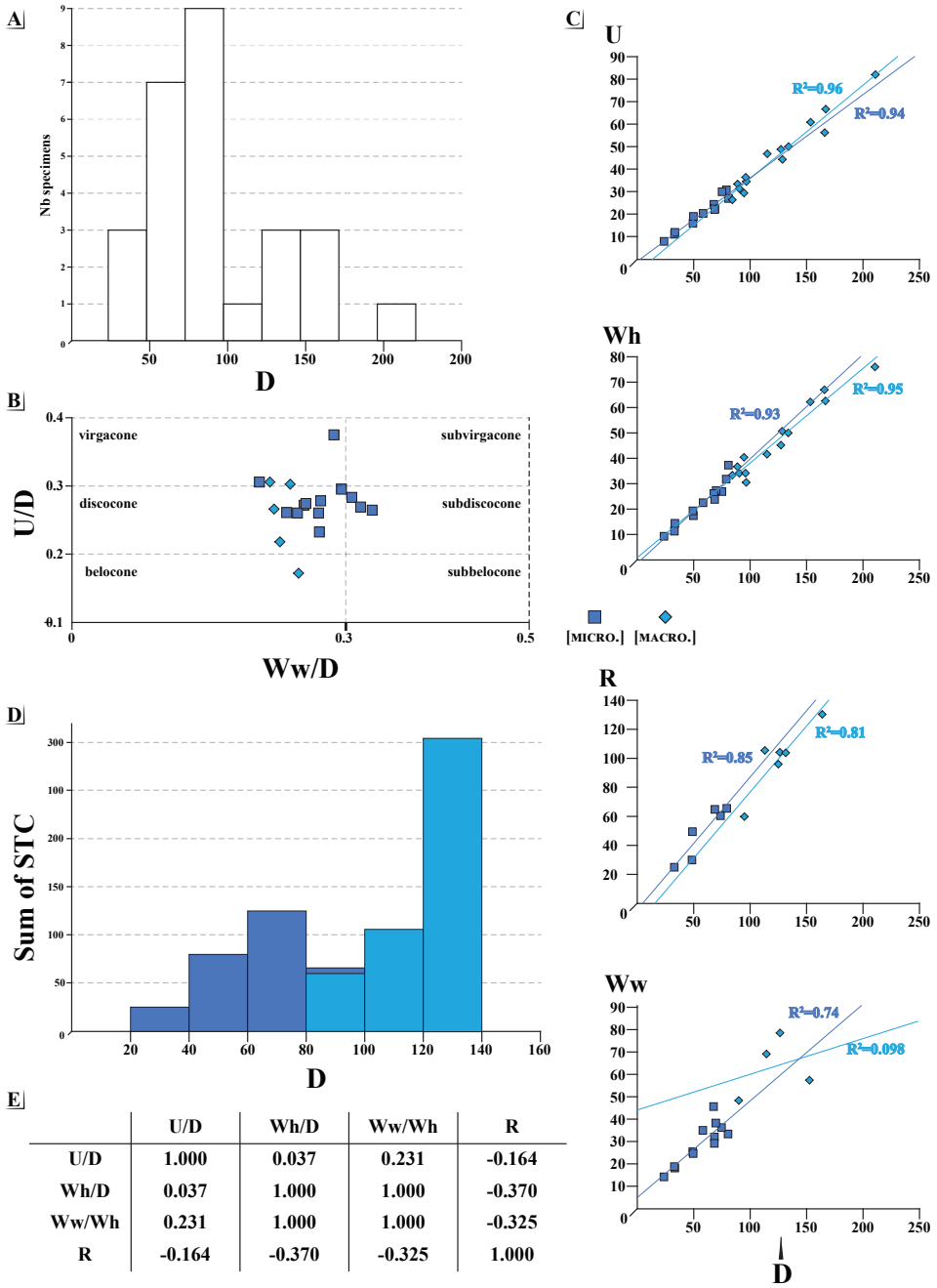

E

	U/D	Wh/D	Ww/Wh	R
U/D	1.000	0.037	0.231	-0.164
Wh/D	0.037	1.000	1.000	-0.370
Ww/Wh	0.231	1.000	1.000	-0.325
R	-0.164	-0.370	-0.325	1.000

Fig. 7 - Palaeobiological study of the Douvilleiceratidae *Cheloniceras crassum* Spath, 1930, with representation of putative antidimorphs. **A**: Asymmetric bimodal distribution of adult diameter frequencies; **B**: Relationships between the U/D and Ww/U ratios, describing conch shapes ranging mainly from paragicone to subvirgacone morphologies; **C**: Bivariate diagrams showing the growth of shell parameters (U, Wh, Ww, and number of ribs, R) as a function of D; **D**: Histograms of STC variable distributions showing asymmetric bimodality; **E**: Pearson correlation coefficients between U/D, Wh/D, Ww/Wh, and R.

intervals. This suggests the presence of two predominant groups within the dataset, centered around these ranges. In this context, our identification of anti-dimorphs strongly correlates with the bimodal distribution of STC values. The putative microconchs form a cluster with generally lower STC values, while the putative macroconchs form a cluster with higher STC values.

The correlation between the parameters U/D, Wh/D, Ww/Wh, and R—potential indicators of variability linked to Westermann's first law—was calculated using Pearson's correlation coefficient. The results are presented in **Fig. 7E**. We found a weak to moderate correlation between U/D and Ww/Wh, while Wh/D and Ww/Wh exhibit a very strong correlation. In contrast, R shows a moderate negative correlation with both Wh/D and Ww/Wh, and a weak negative correlation with U/D. Consequently, there is no strong correlation between all parameters except for Wh/D and Ww/Wh, which are highly correlated, as expected due to their direct relationship.

Finally, the question of asymmetry within the Douvilleiceratidae, as highlighted by Bersac & Bert (2018), does not appear to be a significant factor in our studied sample. Although many specimens exhibit corrosion on one side that hampers precise observation, we note only two examples (approximately 4% of the population) displaying asymmetry. Specimen Pl. 17, Fig. 1-2 (NV71) shows a single heterotuberculate rib on the left side that transitions to an isotuberculate rib by the end of the STC stage, while specimen Pl. 16, Fig. 3-4 (NV70) features primary atuberculate ribs on the right side that become intercalatory on the left during the adult stage. Additionally, one specimen displays a clear pathology on its body chamber, characterized by a ribbing vertex in a latero-ventral position (specimen Pl. 18, Fig. 5 (NV76)).

Discussion:

The *Cheloniceras* specimens from the NV are notably well-preserved, possibly dimorphic, with no strong covariation of morphological pattern, and exhibit a low degree of asymmetry. They display characteristics consistent with *Cheloniceras crassum* var. *crassum* and *Cheloniceras crassum* var. *impar*, whose best record is from bed 15 of the *Scaphites* Bed Member of the Atherfield Clay series, Isle of Wight, southern UK (Casey, 1962), but with published occurrences through the *Deshayesites deshayesi* Zone and *Dufrenoyia furcata* Zone in the western Tethys (see complete synonymy in Klein & Bogdanova, 2013). The morphological criteria and ontogenetic trajectory of the studied material align closely with the understanding of *Cheloniceras crassum* as proposed by Bersac & Bert (2018). This alignment is based on the distinctive long *Cheloniceras* stage characterized by prominent heterotuberculated Y-shaped ribs, which concludes in an average diameter of 74.61 mm. Additionally, the dating of *Cheloniceras crassum*, frequently reported from the *Deshayesites grandis* Subzone, corresponds well with the age of the NV herein identified.

Biometric analysis of the studied sample provides the first evidence of morpho-dimensional sexual dimorphism within *Cheloniceras crassum*. Specifically, smaller microconchs display a shorter *Cheloniceras* stage and a regressed adult whorl, while larger macroconchs exhibit a longer *Cheloniceras* stage accompanied by slight egression of the adult whorl. The peristome is distinct in the putative microconchs but remains uncharacterised in the putative macroconchs. These findings are particularly noteworthy, as such morpho-dimensional dimorphism has not yet been demonstrated in the *Cheloniceras cornuelianum* (the type species of *Cheloniceras*), as noted by Bersac & Bert (2018). It has only been suggested in other Douvilleiceratidae, such as in the genus *Douvilleiceras* (see Courville & Lebrun, 2010), and in the Roloboceratinae genera *Roloboceras* and *Megatyloceras* (see Delanoy *et al.,* 2022; Frau & Bulot, 2023), which are derivatives of the Douvilleiceratidae.

Distribution: According to its current definition, the species is known with certainty from the southern United Kingdom, France, and Spain, and doubfully from Bulgaria and Colombia, within the *Deshayesi* Zone and/or the *Furcata* Zone.

Superfamily Acantohoplitoidea Stoyanow, 1949
Family Acanthohoplitidae Stoyanow, 1949
Genus *Procolombiceras* Sharikadze, 1979

Type species: *Procolombiceras aptus* Sharikadze, 1979; by original designation.

***Procolombiceras* sp.**

Pl. 20, Fig. 1-3

Material: Narbonne, Parets d'en Sales, lev. 1, 1 ex.: NV80 (Pl. 20, Fig. 1-3).

Dimensions: in mm.

Specimen	D	U	Wh	Ww
NV80	34.9	12,8	13.6	13,3

Description:

Specimen NV80 is a small-sized, nearly complete but slightly deformed acanthohoplitid ammonite with a discoidal, weakly compressed, and highly evolute coiling, illustrating a subvirgacone conch shape in the sense of Klug *et al.* (2015a). The ornamentation of the early whorls is worn, with only a Crassicostatum stage *sensu* Frau *et al.* (2020a) presents in the adult whorl. It bears thickened primary ribs that initially bifurcate but then become mostly simple, separated by a variable number, one to three, of secondary ribs on the flank. The point of furcation of the primary ribs is low, at the umbilical margin, or higher on the flank, and shows thickening at their base. All ribs are flat-topped or cuneiform on the venter. No ventral furrow is observed along the adult whorl, but the venter remains rather flattened throughout the preserved whorl.

Discussion:

Based on its general coiling and ornaments, our specimen best matches the little-known genus *Procolombiceras*, primarily documented from the *Dufrenoyia furcata* Zone of Georgia (Sharikadze, 1979). As currently understood, *Procolombiceras*, which includes *Procolombiceras antiquus* Sharikadze, 1979, and the type species *Procolombiceras aptus* Sharikadze, 1979, represents the most primitive Acanthohoplitidae. If our specimen's identification is correct, it extends the known age of the genus to the *Deshayesites grandis* Subzone *auctorum*. The validity of *Procolombiceras* remains under debate (Frau *et al.,* 2021), and further material will be necessary to elucidate its relationship with supposed descendants belonging to the genus *Colombiceras* Spath, 1923.

Distribution:

The genus *Procolombiceras* was previously known with certainty only from the *Furcata* Zone of the southern

Caucasus (Sharikadze, 1979). With this work, we provide the first documented occurrence of the genus in southern France to our current knowledge.

Superfamily Ancyloceratoidea Gill, 1871
Family Ancyloceratidae Gill, 1871

Genus *Delanoyites* gen. nov.
(= *Lithancylus* Casey, 1961 *nomen nudum*;
type species: *Hamites grandis* Sowerby, 1828)

Derivation of the name: Named in honor of Gérard Delanoy, formerly of the University of Nice-Sophia-Antipolis, France, for his outstanding contributions to Cretaceous ammonoid palaeontology over the past four decades

Type species: The type species here designated is *Lithancylus renatae* Pictet, Delanoy, Baudouin & Boselli, 2009 from the lower Aptian of Pierrelatte, southern France.

Diagnosis:

Large- to very large-sized hamuliniform ancyloceratids with a long, straight to slightly curved proversum and U-shaped retroversum. Early whorls remain unknown, and presence of a residual spire cannot be upheld. Phragmocone usually ends in the upper proversum. Sub-circular to elliptical whorl section, occasionally exhibiting a flattened venter and sometimes developing hexagonal at rib cross section. Phragmocone ends at various heigh in the upper proversum. Ornamentation generally begins with uniform ribbing on the dorsum, and regular, atuberculate prorsiradiate ribs crossing the venter with or without attenuation. As growth increases, ornamentation changes toward regular or irregular alternation of trituberculate primary ribs and variable number of atuberculate secondary ribs. Tubercles disposed on the peri-ventral, lateral and latero-dorsal positions; they appearance can be either simultaneous, progressive or delayed during ontogeny. Ribs can be lopped on the tubercles on the flank and/or venter. Primary ribs strengthen in the upper proversum, with generally three enlarged tubercles with more or less complex system of associated secondary ribs. primary ribs typically continue onto the flexus and/or retroversum, remaining trituberculate or thickened, spaced, and occasionally rectiradiate. They pass over the venter with slight marginal tubercles, then become cretiform without tubercles, while secondary ribs decrease or disappear, except sometimes on the dorsum. Peristome not precisely known but usually marked by two joined ribs from a dorsal bullae. Complex quadrilobate suture featuring a diagnostic enlarged trifid umbilical lobe divided into three smaller lobes with horizontally oriented upper digits, closely approaching those of the lateral lobes' ventral and dorsal digits.

Specific content:

Besides its type species, *Delanoyites* gen. nov. is composed of *Toxoceratoides godeti* Thieuloy, 1990 from southeast France, as well as *Lithancylus glebi* Mikhailova & Baraboshkin, 2001, *L. bifurcatus* Delanoy *et al,* 2017, *L. igori* Mikhailova & Baraboshkin, 2001 and *L. russiensis* Mikhailova & Baraboshkin, 2001 from southwest Russia. Pending the revision of their type material and the collection of new specimens, *L. tirolensis* Casey, 1961, *L. pushevensis* Nikolov & Parashkevanov, 1995, *L. fustis* Casey, 1961 and *L. tirolensiformis* Casey, 1961 are doubtfully included in the new genus.

Remark:

The genus *Lithancylus* was recently revised by Pictet *et al.* (2009); however, they did not revise its type species, *Lithancylus grandis*. The holotype of *Lithancylus grandis*, specimen OUM.K.00188 from the Lower Greensand of Smeeth, Kent, UK, is described as a worn fragment of an ancyloceratid proversum. According to Klein *et al.* (2007), this holotype lacks sufficient diagnostic features to establish a valid typification of the genus *Lithancylus*. Additionally, no topotype of *Lithancylus grandis* has been collected yet, and the taxonomic relationship between the holotype and other specimens from the Lower Greensand described and illustrated by Casey (1961, 1980) remains uncertain (Delanoy *et al.,* 2017). As a result, *Lithancylus grandis* should be considered a *nomen dubium* in the sense of the ICZN (Vermelen, 2006 ; Klein *et al.,* 2007). Therefore, we propose *Delanoyites* gen. nov. as a valid substitute name. *Delanoyites* gen. nov. is distinguished from all other ancyloceratid genera by the large-sized hamuliniform coiling of its members, with a reduced or absent inner spire (Mikhailova & Baraboshkin, 2001; Pictet *et al.,* 2009). This genus includes taxa previously classified under *Lithancylus* by Mikhailova & Baraboshkin (2001), later revised by Pictet *et al.* (2009).

***Delanoyites* gen. nov. sp. A**

Pl. 20, Fig. 4-7; Pl. 21, Fig. 1-4

Material: Narbonne, Parets d'en Sales, lev. 1, 5 ex.: NV81 (Pl. 20, Fig. 4-5), NV82 (Pl. 20, Fig. 6-7), NV89 (Pl. 21, Fig.1-2), NV90 (Pl. 21, Fig. 3), NV91 (Pl. 21, Fig. 4).

Description:

We have several fragmented specimens available that depict a moderate-sized hamuliniform ancyloceratid. Specimen Pl. 21, Fig. 4 (NV91) specifically can be assigned to the genus *Delanoyites* gen. nov. It consists of a fragment of the *proversum* and incomplete *flexus*, with the *proversum* being long and straight, and the end of the phragmocone located in its upper part. The *flexus* appears to be of a U-shaped type. The ornamentation on the middle *proversum* is made of strong, distinctly prorsiradiate ribs with thickening at the latero-ventral margin, and then attenuated passing over the venter. Later, irregularly disposed trituberculate thickened ribs appear, with tubercles positioned peri-dorsally, laterally, and latero-ventrally. An atuberculate branch originates from the lateral tubercles,

and the rib continues uninterrupted over the venter. These trituberculate ribs strengthen in the upper *proversum*, while secondary ribs diminish, leaving smooth interrib spaces or occasionally a residual single atuberculate secondary rib starting high on the flank. We unite specimens Pl. 21, Fig. 4-5 (NV81), Pl. 21, Fig. 6-7 (NV82), Pl. 21, Fig. 1-2 (NV89) and Pl. 21, Fig. 3 (NV90) under *Delanoyites* sp. A, as they represent incomplete fragments of lower and middle proversums. These specimens exhibit dense, atuberculate prorsiradiate ribbing with an attenuated siphonal band, similar to those observed in the middle *proversum* of specimen Pl. 21, Fig. 4 (NV91). Specimen Pl. 20, Fig. 6-7 (NV82) is somewhat distinct from these specimens. As a fragment of the lower *proversum*, it stands out due to the presence of two enlarged trituberculate primary ribs amidst the dense, atuberculate prorsiradiate ribbing observed in the others.

Discussion:

The specimens from the NV show closest affinities with the type species *Delanoyites* gen. nov. *renatae*, characterized by its general coiling, long stage with dense, prorsiradiate atuberculate ribs on the proversum, and the rapid appearance of trituberculate ribbed stages with decreasing secondary ribs on the flexus. However, the type material of *Delanoyites* gen. nov. *renatae* appear notably larger than the individuals from the NV, and they are from an older age (i.e., *Deshayesites forbesi* Zone). Better-preserved material is needed for further comparison. *Delanoyites* gen. nov. *godeti* (Thieuloy, 1990), another species from southern France, differs from the NV specimens by its larger size and the early appearance of trituberculate ribbed stages lower in the proversum (Pictet *et al.,* 2009). Pending the discovery of better-preserved specimens, we are keeping the nomenclature open.

Distribution: The material at our disposal has the closest affinities with French relatives of the genus *Delanoyites*.

Delanoyites gen. nov. sp. B

Pl. 22, Fig. 4-9

Material: Narbonne, Parets d'en Sales, lev. 1, 3 ex.: NV94 (Pl. 22, Fig. 4-5), NV95 (Pl. 22, Fig. 6-7), NV96 (Pl. 22, Fig. 8-9).

Description:

Specimens Pl. 22, Fig. 4-5 (NV94) and Fig. 6-7 (NV95) are two moderate-sized fragments of slightly arcuate *proversum* that align with our diagnosis of *Delanoyites*. The body chamber begins in the upper *proversum*. The whorl section is sub-oval throughout the *proversum* with a flattened venter. The ornamentation is first composed of an alternation of slightly prorsiradiate, trituberculate primary ribs and atuberculate, dense, single secondary ribs. The peri-ventral tubercles of the primary ribs are rounded and enlarged compared to the others. As growth increases, the primary ribs strengthen and become more spaced. The three tubercles are enlarged, and the ribs can be lopped between the two lateral and/or the two peri-ventral ones. Secondary ribs still occur but they are less numerous. They cross the venter with a slight weakening.

Discussion:

Some features of the material we have match with the Russian species *Delanoyites glebi* (Mikhailova & Baraboshkin, 2001), such as moderate size, flattened venter on the *proversum*, and the rapid appearance of a complex trituberculate ribbed stage on the lower *proversum* extending upward into the upper proversum. However, the absence of *flexus* and *retroversum* in the NV material limits further comparison.

Distribution: The material at our disposal has the closest affinities with Russian relatives of the genus *Delanoyites*.

Genus *Ammonitoceras* Dumas, 1876

Type species: *Ammonitoceras ucetiae* Dumas, 1876, by original designation.

Ammonitoceras sp.

Pl. 3, Fig. 5

Material: Gruissan, Saint-Martin, "Niveau de Saint-Martin", 1 ex.: NSM3 (Pl. 3, Fig. 5).

Description:

The specimen at our disposal corresponds to a small portion of a whorl. It is characterized by a depressed oval whorl section, wider than high, with flat flanks and a large, slightly convex venter. The ribbing consists of thick, spaced simple ribs bearing large, smooth lateroventral tubercles positioned high on the flank, from which each rib bifurcates to cross the venter. Due to the state of preservation, the presence or absence of peri-siphonal tubercles cannot be confirmed.

Discussion:

Due to its preservation, precise identification of the specimen is not possible. Nevertheless, its general morphology and ribbing recall certain forms of early Aptian *Ammonitoceras*, although this assignment cannot be confirmed with certainty.

Distribution: We tentatively assign this specimen to an age range spanning the *Deshayesites forbesi* Zone and/or the lower *Deshayesites deshayesi* Zone, without the possibility of firm confirmation.

Ammonitoceras aff. *lahuseni* (Sinzow, 1906)

Pl. 23, Fig. 1-4; Pl. 24, Fig. 1-3; Pl. 25, Fig. 1; Pl. 26, Fig. 1; Pl. 27, Fig. 1

aff. 1906 *Crioceras Lahuseni* sp. nov. Sinzow, p. 192, pl. V, fig. 3a-c.

aff. 2022 *Ammonitoceras lahuseni* (Sinzow) – Bersac & Bert, p. 11, Figs. 8R-D1, 9, 10, 11 [*cum*. *syn*.].

Type: The specimen figured by Sinzow (1906, pl. V, fig. 3a-c) from the Mangyschlak Peninsula, western Kazakhstan, is taken as the reference specimen. However, it was deposited in the CNIG Museum collections and is possibly lost to date (Bersac & Bert, 2022). Clarification of the type specimen is urgently needed for nomenclatural stability.

Material: Narbonne, Parets d'en Sales, lev. 1.
- 7 figured ex. : NV97-98 (Pl. 23, Fig. 1-4), NV 99-100 (Pl. 24, Fig. 1-3), NV101 (Pl. 25, Fig. 1), NV102 (Pl. 26, Fig. 1), NV103 (Pl. 27, Fig. 1).
- 3 ex. non figured : NV121-123.

Dimensions: in mm.

For criocone

Specimens	Ds	Dsp	
NV101	327	208	
NV103	460	220	
NV121	300	210	

For ancylocone

Specimens	Ls	Dsp	Whf
NV99	393	2014	104
NV102	306	172	85
NV122	260	-	58

Description:

Our study material consists of very large-sized criocone and ancylocone *Ammonitoceras* individuals. This coiling pattern seemingly confirms the size-related sexual dimorphism observed in the palaeopopulation of the genus *Ammonitoceras*, as reported by Bersac & Bert (2022). The average shell diameter for both putative anti-dimorphs reaches approximately Ds/Ls ~ 350 mm, but criocone macroconchs tend to be larger with significant adult size variation. Those criocone macroconchs display coiling with inner whorls in contact (specimen Pl. 25, Fig. 1 (NV101)) or exhibit a slight spiral hiatus that increases in the latter adult whorl (specimen Pl. 27, Fig. 1 (NV103)). The putative ancylocone microconchs feature a large spire, comprising nearly 55% of the shell's total length. Their *proversum* is slightly curved, while the *flexus* is open, with an average whorl height at the *flexus* of approximately 94.5 mm, concluding with a long *retroversum* that may come into contact with the spire (specimen Pl. 24, Fig. 1 (NV99)). The whorl section in both anti-dimorphs is circular to oval, with ribs exhibiting a hexagonal cross-section in the adult. In criocone macroconchs, the adult body chamber occupies the two third of the last whorls while it starts at the proximal third of the *proversum* in the ancylocone microconchs.

Based on the ontogenetic sequences of *Ammonitoceras* redefined by Bersac & Bert (2022), our material only includes observations of the Trituberculate juvenile stage in specimen Pl. 24, Fig. 2-3 (NV100), making it difficult to ascertain if it truly matches the large individuals, given it consists to an incomplete juvenile whorl fragment. In this specimen, the Trituberculate stage is characterized by a depressed sub-oval whorl section. It bears straight primary ribs with umbilical, upper lateral, and latero-ventral rounded tubercles, separated by one or two atuberculate secondary ribs. These secondary ribs originate high on the flank and are mostly expressed on the venter.

The first observable ribbing typically begins with the *Ammonitoceras* stage as defined by Bersac & Bert (2022) in larger specimens. This stage is characterized by a circular to oval whorl section that is wider than it is high. The ribbing becomes denser and thicker compared to juvenile whorls. Lateral tubercles are situated in the outer third of the flanks and are generally stronger than the umbilical ones. Towards the end of this stage, this pattern reverses, with the lateral tubercles diminishing as the shell continues to grow. Secondary ribs vary, mostly numbering one to three, originating at different heights on the flank and often connecting at their base to the lateral tubercles. All ribs appear to equally traverse the venter, sometimes with or without ventral attenuation over the siphonal area, forming discrete peri-siphonal bulges. The end diameter of the *Ammonitoceras* stage is observed at Dsp of 171 mm in specimen Pl. 24, Fig. 1 (NV99) and Dsp of 193 mm in specimen Pl. 25, Fig. 1 (NV101). This is also confirmed in the incomplete spires of specimens Pl. 23, Fig. 1-2 (NV97) and Fig. 3-4 (NV98), which still exhibit an *Ammonitoceras* stage at Dsp of 175 mm. These observations suggest that the end diameter of the *Ammonitoceras* stage is around 180 mm in specimens from the NV. Finally, the *Ammonitoceras* stage transitions into a Late trituberculate stage, as described by Bersac & Bert (2022), in most specimens at our disposal. However, specimen Pl. 23, Fig. 1-2 (NV97) appear to exhibit an intermediate Slender stage in between, characterized by dense, atuberculate ribbing. The Late *Ammonitoceras* stage resembles juvenile features except that rib relief consistently features tubercles. Finally, near the aperture, a Gerontic stage emerges, characterized by spaced, sharp, and subatuberculate ribs without intercalary ribs (specimens Pl. 26, Fig. 1 (NV102), Pl. 25, Fig. 1 (NV101), Pl. 27, Fig. 1 (NV103)). In both putative anti-dimorphs, the adult peristome is not preserved.

The septal suture is observable but it is too poorly preserved to study its aspect.

Discussion:

Through their stratigraphic range in the lower Aptian *pro parte* of southern France and the UK, it is suggested that the genus *Ammonitoceras* includes large-sized criocone and ancylocone representatives, which may form anti-dimorphic pairs (Bersac & Bert, 2022). Early representatives from the *Deshayesites forbesi* Zone *auctorum* remain poorly known in the literature, although an excellent sample collection from southeast France is awaiting detailed publication (Pictet, 2011). The genus has a broader record during the upper lower Aptian, featuring

species such as *Ammonitoceras ucetiae* Dumas, 1876 from the lower part of the *Deshayesites deshayesi* Zone, followed by *Ammonitoceras* sp. in the upper part of the *Deshayesites deshayesi* Zone, and *Ammonitoceras lahuseni* (Sinzow, 1906) in the *Dufrenoyia furcata* Zone (Bersac & Bert, 2022). According to Bersac & Bert (2022), *Ammonitoceras ucetiae* is notably characterized by the end diameter of the *Ammonitoceras* stage occurring at approximately 130 mm on average, while *Ammonitoceras lahuseni* exhibits an end diameter of about 180 mm. By contrast, the end diameter of *Ammonitoceras* sp. remains poorly constrained, as only fragmentary spires and tripartite specimens with the *Ammonitoceras* stage are known from the *Deshayesites grandis* Subzone of both the UK and southern France. Based on their age, the *Ammonitoceras* population from the NV matches *Ammonitoceras* sp., as they occur in the condensed deposits of the *Deshayesites grandis* Subzone. Here, the end diameter of the *Ammonitoceras* stage in specimens from the NV is found to be approximately 180 mm on average. This matches with the species *Ammonitoceras lahuseni* as defined by Bersac & Bert (2022). However, the SE French population of the latter species is apparently characterised by a much larger size in average for both putative anti-dimorphs, while the spire of the putative microconch is smaller representing 41.76% of the length of the shell (Bersac & Bert, 2022). A diagnostic criteria of the species *Ammonitoceras lahuseni* is the presence of a Monoatuberculate stage *sensu* Bersac & Bert (2022) in the juveniles of that species. However, this criteria cannot be determined in the material from the NV due to incompletess of the early whorls. Regarding the latter stages, the material from the NV match with the ontogeny of *Ammonitoceras lahuseni*, similarly exhibiting a wide range of variability regarding the duration of the sub-adult and adult stages as noted before by Bersac & Bert (2022). The *Ammonitoceras* from the NV may either belong to a basal population of *Ammonitoceras lahuseni* or more likely a very closely allied population pending confirmation of the presence of the Monoatuberculate stage. This material is therefore therein assigned to *Ammonitoceras* aff. *lahuseni* pending more material to be collected from the Clape Massif.

Distribution: According to Bersac & Bert (2022), *Ammonitoceras lahuseni* is confidently identified from southeastern France and western Kazakhstan, within beds assigned to the Furcata Zone, Furcata Subzone. Based on the available material, we document a slightly older occurrence for closely allied relatives of this species collected from the Clape Massif.

Family Acrioceratidae Vermeulen, 2004

Genus *Toxoceratoides* Spath, 1924

Type species: *Toxoceras royerianus* d'Orbigny, 1842, by subsequent designation of Casey (1961, p. 77-78

***Toxoceratoides rochi* Casey, 1961**

Pl. 22, Fig. 1-3

Type: The lectotype designated by Frau *et al*. (2017a, p. 338) is specimen UJF-ID.78 (Roch coll.) illustrated by Roch (1927, pl. 1, fig. 4) from the lower Aptian of Cassis, southern France.

Material: Narbonne, Parets d'en Sales, lev. 1, 2 ex.: NV92 (Pl. 22, Fig. 1), NV93 (Pl. 22, Fig. 2-3).

Description:

Specimen Pl. 22, Fig. 1 (NV92) represents a medium-sized toxoceratid hook, including the upper part of the proversum, the flexus, and the entire retroversum, but lacking the peristome. The whorl cross section seems to be suboval with flattened flanks on the proversum. The latter exhibits worn but dominant stout primary trituberculate ribs with one or two secondary ribs, corresponding to stage *ii* of Bulot *et al.* (2018). The primary trituberculate ribs terminate as prominent flattened tubercles. On the retroversum, the ribs become simple and spaced, with fine ribbing at the dorsal margin, illustrating stage *iii* of Bulot *et al*. (2018), and bear the typical "rochi ribs" as understood by Bersac & Bert (2021).

Discussion:

Although incomplete, the morphology and ontogenetic sequence of the specimen we have match well with the species *Toxoceratoides rochi* as revised by Frau *et al*. (2017a) and Bersac & Bert (2021). For a detailed comparison with other *Toxoceratoides* species, the reader is referred to these publications. *Toxoceratoides rochi* is best represented during the *Dufrenoyia furcata* Zone of the Mediterranean Tethys, but older individuals found in the underlying *Deshayesites grandis* Subzone *auctorum* are presumed to have derived from *Toxoceratoides royerianus* (d'Orbigny, 1842), according to Bersac & Bert (2021).

Distribution: According to Frau *et al*. (2017a), the species is distributed across the Mediterranean-Caucasian Tethys, occurring in the *Furcata* and *Deshayesi* Zones in regions such as southeast France, southern United Kingdom, Spain, Romania, the Caucasus, and Egypt.

Super-family Ptychoceratoidea Gill, 1871

Family Macroscaphitidae Hyatt, 1900

Genre *Macroscaphites* Meek, 1876

emend. Delanoy *et al.* (2008)

Type species: *Scaphites yvani* Puzos, 1832; by subsequent designation of Roman (1938, p. 380).

***Macroscaphites* sp. cf. *striatisulcatus* (d'Orbigny, 1841)**

Pl. 3, Fig. 6; Pl. 22, Fig. 14, 15

cf. 1841 *Ammonites striatisulcatus* d'Orbigny, p. 153, pl. 49, fig. 4, 5, 6, 7.

cf. 2015 *Macroscaphites striatisulcatus* (d'Orbigny) –

Frau, Delanoy & Hourquieg, p. 46, pl. 1, fig. 4, 5, 6a-b, 7a-b, 8a-b, 9a-b; pl. 2, fig. 1a-b, 2a-b, 3a-b, 4a-b, 5a-b, 6a-b, 7a-b [*cum. syn.*].

Type: The neotype designated by Busnardo *in* Gauthier *et al.* (2006, p. 55, pl. 23, fig. 5a-b) is specimen FSL-EM.55-10 (École des Mines coll.) from the Lower Aptian of Hyèges, southeast France.

Material: Gruissan, Saint-Martin, "Niveau de Saint-Martin", 1 ex.: NSM4 (Pl. 3, Fig. 6); Narbonne, Parets d'en Sales, lev. 1. 2 ex.: NV85 (Pl. 20, Fig. 14), NV87 (Pl. 20, Fig. 15).

Description:

Poorly preserved, small-sized evolute spire with a dense, uniform, simple, sharp ribs and rare constrictions.

Discussion:

The three specimens we have correspond to the imprint of spires of a small-sized microconch of *Macroscaphites*. Their poor state of preservation limits further comparison with contemporaneous taxa, such as *M. striatisulcatus* recently revised by Frau *et al.* (2015), but the small size and ornamental features of our material likely align with that species.

Distribution: According to Frau *et al.* (2015), the species is distributed across the Mediterranean-Caucasian Tethys, occurring in the lower Aptian of regions such as southeast France, Spain, Bosnia and Herzegovina, Bulgaria, Slovakia, Romania, and the Caucasus. Its presence in Germany and Canada remains uncertain, but the distribution across these regions confirms widespread faunal dispersal.

Superfamily Desmoceratacеae Zittel, 1895
Family Desmoceratidae Zittel, 1895
Genus *Pseudohaploceras* Hyatt, 1900

Type species: *Ammonites liptoviensis* Zeuschner, 1856; by original designation.

***Pseudohaploceras matheroni* (d'Orbigny, 1841)**

Pl. 20, Fig. 8-13

Material: Narbonne, Parets d'en Sales, lev. 1, 3 ex.: NV83 (Pl. 20, Fig. 8-9), NV84 (Pl. 20, Fig. 10-11), NV85 (Pl. 20, Fig. 12-13).

Description:

The best-preserved specimens NV83 and NV84 are a medium-sized desmoceratid phragmocone, with inner whorls that are deformed. It exhibits an involute coiling with a sub-rounded whorl section, wider than high on the last preserved whorl, and slightly rounded flanks and venter. The umbilical wall is steep and slightly incurved with a rounded margin. The ornamentation, although somewhat erased, conforms to that of *Pseudohaploceras*, characterized by distinctive constrictions bordered by enlarged ribs, and a variable number of intercalatory ribs, sometimes fasciculate.

Discussion:

The reader is referred to Baudouin *et al.* (2012) for a detailed discussion and comparison with other *Pseudohaploceras* species.

Distribution: According to its current definition, the species is distributed across the entire Tethys, occurring in the lower Aptian of regions as wide as northern and western Europe, northeastern and southern Africa, and the Caucasus.

***Pseudohaploceras* sp.**

Pl. 20, Fig. 16

Matériel: Narbonne, Parets d'en Sales, lev. 1, 1 ex : NV88 (Pl. 20, Fig. 16).

Description:

As with other desmoceratid forms from the Clape Massif, the specimen at hand conforms to the diagnosis of *Pseudohaploceras*. However, it differs in exhibiting a more inflated shell and a stronger ornamentation than other *Pseudohaploceras* forms from the NV. It bears five weakly expressed constrictions, bordered by strongly enlarged primary ribs, and three to four simple intercalatory ribs, which may be fasciculate or closely approximated to the anterior or posterior primary ribs.

Discussion:

We distinguish this form from typical *P. matheroni* based on its more inflated shell and stronger ribbing. In the absence of a comprehensive population study of *P. matheroni* in the current literature, it is difficult to assess whether this specimen represents an end-member within the variability of that species or a distinct taxon. Moreover, the limited material—restricted to a single, incomplete specimen—precludes further detailed comparison.

4. Sedimentary context and biostratigraphic implications

In the Clape Massif, the Estagnol Limestones Formation, of uncertain latest Barremian to earliest Aptian age, is terminated by the "Niveau de Saint-Martin" (NSM), a rubefied and karstified horizon with a sharp erosional top surface. Locally, the NSM contains poorly preserved early Aptian ammonites. Due to their preservation, precise identification is not possible, but we recognize the following taxa: ?*Cheloniceras* sp., *Deshayesites* sp., *Ammonitoceras* sp., and *Macroscaphites* sp. cf. *striatisulcatus* (d'Orbigny), suggesting deposition during the upper part of the

Deshayesites forbesi Zone and/or the lower *Deshayesites deshayesi* Zone.

The irregular top surface of the Estagnol Limestones Formation is regionally overlain by the Ramade Marls Formation, marking the onset of a major regional transgressive event, recorded from the French Pyrenees (Peybernès, 1976; Masse, 1995) to Provence (Frau *et al.,* 2017b, 2020b). In some localities, the Estagnol Limestones are capped by the "Niveau de Vires" (NV), a cephalopod-rich, condensed horizon at the base of the Ramade Marls Formation. The ammonoid assemblage in the NV is diverse, dominated by *Deshayesites grandis*, *Cheloniceras crassum*, and *Ammonitoceras* aff. *lahuseni*, with other taxa represented by only a few specimens. A similar pattern is observed in the nautiloids. The cephalopod assemblage of the NV closely resembles, and in many respects matches, that of bed 15 in the Scaphites Beds Member of the Atherfield Clay Formation, Isle of Wight, UK. For comparison, a compilation of taxa from bed 15 is provided based on Casey *et al.* (1998) (**Fig. 8**). Bed 15 similarly represents a cephalopod-rich horizon, marking the top of the *Deshayesites grandis* Subzone, corresponding to the upper part of the *Deshayesites deshayesi* Zone *auctorum* (Casey *et al.,* 1998). Ruffell & Wach (1991) interpreted bed 15 as a maximum flooding surface associated with fossil condensation. As in the NV, this bed is overlain by deposits assigned to the *Dufrenoyia furcata* Zone, analogous to the Ramade Marls in the Clape Massif.

It is worth noting that the interval around the *Deshayesites deshayesi*/*Dufrenoyia furcata* zonal boundary is often characterized by a condensation event, sometimes leading to hiatus development. This phenomenon is observed in various settings across southern (Frau *et al.,* 2017b; Frau & Bulot, 2023) and southeastern France (Picourel beds *in* Pictet *et al*., 2015), the French and Swiss Jura (base of Mortier beds *in* Pictet *et al.,* 2016), central Switzerland (Plaine Morte bed *in* Linder *et al.,* 2006; Föllmi & Gainon, 2008), northwest Germany (Green band *in* Lehmann *et al.,* 2012; Frau, 2020), and northeastern Spain (Moreno-Bedmar *et al.,* 2010). This sedimentary context accounts for the evolutionary jump observed at this level between *Deshayesites* and *Dufrenoyia* representatives. Both genera are phyletically linked but can be differentiated based on their juvenile venter morphology. In one, the venter transitions from a subtabulate form to a tabulate venter bordered by latero-ventral tubercles, sometimes accompanied by a smooth siphonal band (Bersac & Bert, 2012, 2015 for a review). However, examination of the Deshayesitidae paleopopulation from the "*Niveau de Vires"* suggests that the taxonomic differentiation between late *Deshayesites* and early *Dufrenoyia* is challenging due to the high polymorphism of the juvenile whorls of *Deshayesites grandis*, which may exceed the current definitions of the two genera.

According to Pictet *et al.* (2015) and Moreno-Bedmar *et al.* (2007), the condensation or hiatus event at the boundary between the *Deshayesites deshayesi* and *Dufrenoyia furcata* zones is not reflected in the standard eustatic charts of Hardenbol *et al.* (1998) or Haq (2014). However, some researchers consider this event a sub-event within the Ap2 or Ap3 sequences. Regardless of its classification, this event complicates the precise definition and correlation of the base of the *Dufrenoyia furcata* Zone, which seems to be diachronous across different locations (Frau, 2020). As Frau (2020) also pointed out, published carbon isotope signals suggest a variable base for the *Dufrenoyia furcata* Zone within the C7 isotope segment, supporting this diachrony. Further research in well-developed basin successions is crucial to refine the first appearance of early *Dufrenoyia*, clarify the taxonomy of its initial representatives, and better define the boundary between the *Deshayesites deshayesi* and *Dufrenoyia furcata* zones. The sedimentary succession of the South Provence Basin, which contains the unit-stratotype of the Lower Aptian at Cassis–Roquefort-la-Bédoule, is undoubtedly key to initiating a resolution of this issue.

Conclusion

The present study provides a refined lithostratigraphic framework for the Lower Cretaceous succession of the Clape Massif, highlighting two condensed horizons — the "Niveau de Saint-Martin" (NSM) and the "Niveau de Vires" (NV)—at the transition between the Estagnol Limestones Formation and the Ramade Marls Formation. The NSM, although yielding a sparse and poorly preserved ammonite fauna, allows tentative assignment to the upper *Deshayesites forbesi* Zone and/or the lower *Deshayesites deshayesi* Zone. In contrast, the NV contains a diverse and well-preserved cephalopod assemblage, including both ammonoids and nautiloids, which confirms deposition in the upper *Deshayesites deshayesi* Zone (Grandis Subzone). The taxonomic composition of this assemblage, including the newly proposed genus *Delanoyites*, demonstrates strong palaeobiogeographic affinities with coeval condensed horizons such as bed 15 of the Scaphites Beds Member (Atherfield Clay Formation, UK), supporting a broader pattern of early Aptian marine faunal distribution across western Europe. Overall, the study emphasizes the importance of the Clape Massif as a key reference area for the Lower Cretaceous of southwestern Europe. The integration of detailed cephalopod taxonomy with lithostratigraphy not only clarifies the age and depositional context of these successions but also provides a framework for future palaeobiogeographic and stratigraphic studies in the region.

Fig. 8 - Atherfield section Casey *et al.*, 1998

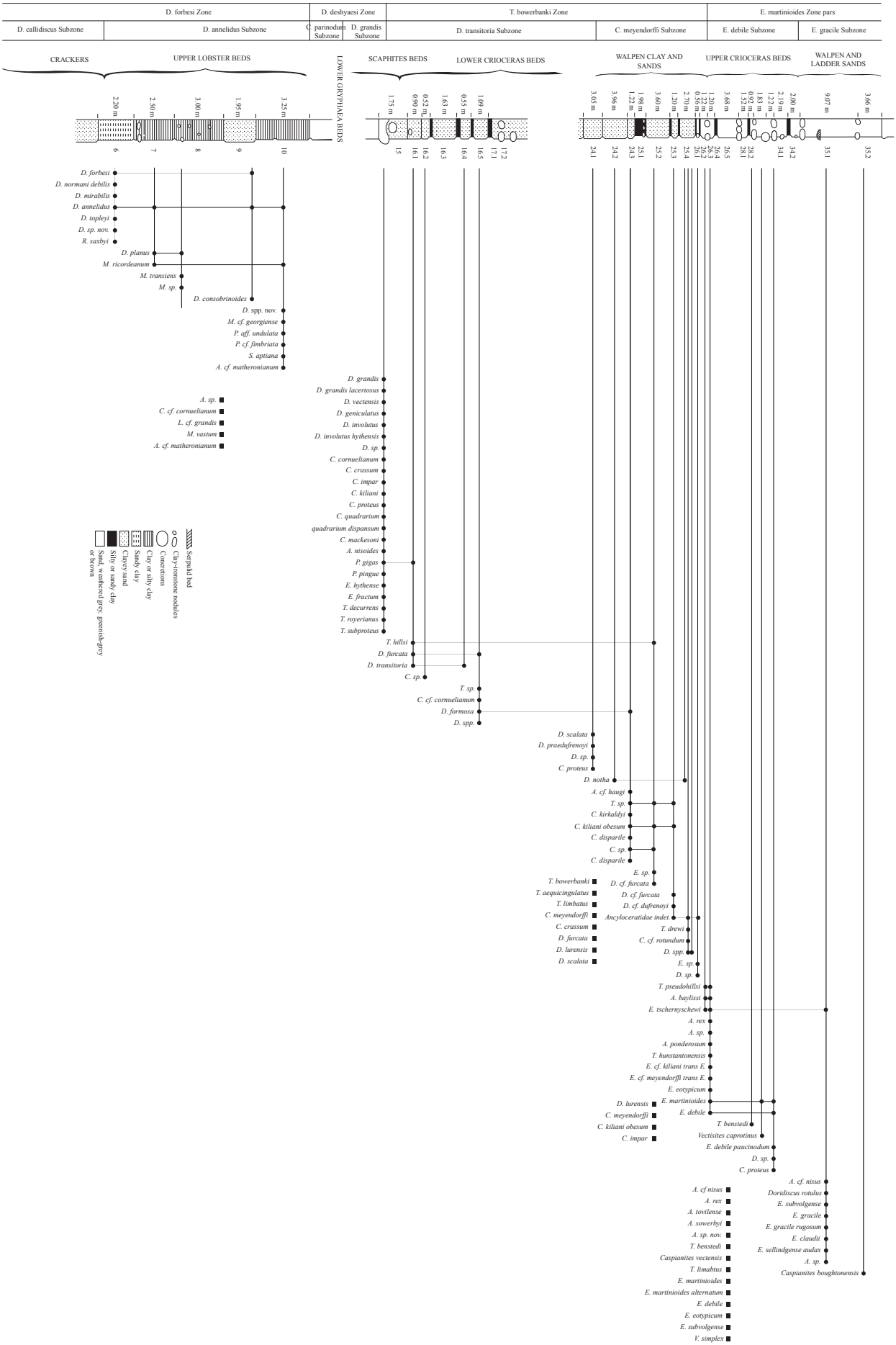
D. forbesi Zone
D. deshyaesi Zone
T. bowerbanki Zone
E. martinioides Zone pars
D. callidiscus Subzone
D. annelidus Subzone
C. parinodum Subzone
D. grandis Subzone
D. transitoria Subzone
C. meyendorffi Subzone
E. debile Subzone
E. gracile Subzone
CRACKERS
UPPER LOBSTER BEDS
LOWER GRYPHAEA BEDS
SCAPHITES BEDS
LOWER CRIOCERAS BEDS
WALPEN CLAY AND SANDS
UPPER CRIOCERAS BEDS
WALPEN AND LADDER SANDS
D. forbesi
D. normani debilis
D. mirabilis
D. annelidus
D. topleyi
D. sp. nov.
R. saxbyi
D. planus
M. ricordeanum
M. transiens
M. sp.
D. consobrinoides
D. spp. nov.
M. cf. georgiense
P. aff. undulata
P. cf. fimbriata
S. aptiana
A. cf. matheronianum
A. sp.
C. cf. cornuelianum
L. cf. grandis
M. vastum
A. cf. matheronianum
D. grandis
D. grandis lacertosus
D. vectensis
D. geniculatus
D. involutus
D. involutus hythensis
D. sp.
C. cornuelianum
C. crassum
C. impar
C. kiliani
C. proteus
C. quadrarium
quadrarium dispansum
C. mackesoni
A. nisoides
P. gigas
P. pingue
E. hythense
E. fractum
T. decurrens
T. royerianus
T. subproteus
T. hillsi
D. furcata
D. transitoria
C. sp.
T. sp.
C. cf. cornuelianum
D. formosa
D. spp.
D. scalata
D. praedufrenoyi
D. sp.
C. proteus
D. notha
A. cf. haugi
T. sp.
C. kirkaldyi
C. kiliani obesum
C. disparile
C. sp.
C. disparile
E. sp.
T. bowerbanki
D. cf. furcata
T. aequicingulatus
D. cf. furcata
T. limbatus
D. cf. dufrenoyi
C. meyendorffi
Ancyloceratidae indet
C. crassum
T. drewi
D. furcata
C. cf. rotundum
D. lurensis
D. spp.
D. scalata
E. sp.
D. sp.
T. pseudohillsi
A. baylissi
E. tschernyschewi
A. rex
A. sp.
A. ponderosum
T. hunstantonensis
E. cf. kiliani trans E.
E. cf. meyendorffi trans E.
E. eotypicum
D. lurensis
E. martinioides
C. meyendorffi
E. debile
C. kiliani obesum
T. benstedi
C. impar
Vectisites caprotinus
E. debile paucinodum
D. sp.
C. proteus
A. cf. nisus
Doridiscus rotulus
E. subvolgense
E. gracile
E. gracile rugosum
E. claudii
E. sellindgense audax
A. sp.
Caspianites boughtonensis
A. cf nisus
A. rex
A. tovilense
A. sowerbyi
A. sp. nov.
T. benstedi
Caspianites vectensis
T. limabtus
E. martinioides
E. martinioides alternatum
E. debile
E. eotypicum
E. subvolgense
V. simplex
Silty or sandy clay
Clayey sand
Sandy clay
Clay or silty clay
Concretions
Clay-ironstone nodules
Serpulid bed
Sand, washbored grey, greenish-grey or brown

Acknowledgements: Many thanks to Annie and Jean-Baptiste Marion, who kindly granted us access to the outcrops on their property in Saint-Martin-le-Bas. A big thank you to all my friends at the GGN (Narbonne Geology Group), and especially to Michel Ricard, who enabled us to study numerous samples. Completion of the palaeontological study by CF was made possible through financial support from the ICUB Fellowships for Young Researchers (registration number 12942), provided by the University of Bucharest Research Institute, Romania. We would like to thank Gérard Delanoy for proofreading the manuscript and for his advice, which helped to improve it.

References

Agassiz, L. (1846). *Nomenclator zoologicus: continens nomina systematica generum animalium tam viventium quam fossilium, secundum ordinem alphabeticum disposita, etymologia et familiis, ad quas pertinent, in singulis classibus*. Fascicule I-XII, Soloduri (Jent & Gassmann).

Archiac, A. d' (1859). Les Corbières. Études géologiques d'une partie des départements de l'Aude et des Pyrénées-Orientales. *Mémoire de la Société géologique de France*, 2e, VI, 2 : 27-446.

Baudouin, C., Delanoy, G., Boselli, P., Bert, D. & Boselli, M. (2012). Les faunes d'ammonites de la sous-zone à *Sarasini* (Barrémien supérieur) dans les Baronnies (Drôme, France*). Revue de Paléobiologie*, 31(2) : 601-677.

Baudouin, C., Delanoy, G., Lehmann, J., Frau, C., Gonnet, R. & Vermeulen, J. (2021). The Cretaceous nautiloid genus *Anglonautilus* SPATH, 1927, in France. *Carnets de Geologie*, 21(12): 235-263.

Bernaus, J.-M. (2000). L'Urgonien du Bassin d'Organyà (NE de l'Espagne). Micropaléontologie, sédimentologie et stratigraphie séquentielle. *Géologie Alpine*, mém. HS, 33. 138 p.

Bersac, S. & Bert, D. (2015). Two ammonite species under the same name: Revision of *Deshayesites deshayesi* (d'Orbigny, 1841) based on topotype material (Lower Aptian, Lower Cretaceous, Northeast of France). *Annales de Paléontologie*, 101, 4: 265-294.

Bersac, S. & Bert, D. (2018). Revision of the lower Aptian (Lower Cretaceous) ammonite species *Cheloniceras cornuelianum* (d'Orbigny, 1841). *Annales de Paléontologie*, 104, 1: 45-70.

Bersac, S. & Bert, D. (2021). The ammonites of the Les Ferres Aptian Basin (Lower Cretaceous, Southeast of France): the genus *Toxoceratoides* (Ancyloceratina, Helicancylidae). *Cretaceous Research*, 118, 104661.

Bersac, S. & Bert, D. (2022). The heteromorph ammonite genus *Ammonitoceras* Dumas, 1876 (Ancyloceratidae) in the lower Aptian (Lower Cretaceous) of the Les Ferres Aptian Basin (southeastern France). *Annales de Paléontologie*, 108, 3, p. 102570.

Bersac, S., Bert, D. & Matrion, B. (2012). Revision of the index-species *Deshayesites deshayesi* (Ammonoidea, Lower Aptian, Lower Cretaceous): Taxonomic and biostratigraphic consequences. In First meeting of the Research Group for Paleobiology and Biostratigraphy of the Ammonites. *Boletin del Instituto de Fisiografia y Geologia*, Rosario, 82: 31-33.

Blainville, H. M. D. (1825). Manuel de malacologie et de conchyliologie (Vol. 2). Levrault.

Bulot, L. G., Frau, C., & Pictet, A. (2018). Revision of *Toxoceratoides royeri* (d'Orbigny, 1842) and its bearing on the systematics of the Aptian Acrioceratidae Vermeulen, 2004 (Ammonoidea, Ancyloceratina, Ancyloceratoidea*). Cretaceous Research*: 88: 187-196.

Cairol, F. (1872). Recherche sur le Terrain crétacé inférieur de la Clape et des Corbières. *Annales des Sciences géologiques*, 3. 177 p.

Canérot, J. (2008). Les Pyrénées. Histoire géologique. Atlantica-BRGM éditions. 516 p.

Casey, R. (1961). The stratigraphical palaeontology of the Lower Greensand. *Palaeontology*, 3(4): 487-621.

Casey, R. 1962. A monograph of the Ammonoidea of the Lower Greensand, part IV. *Palaeontographical Society*: 217-288.

Casey, R. (1963). A monograph of the Ammonoidea of the Lower Greensand, part V. *Palaeontographical Society*: 289-398.

Casey, R. (1964). A monograph of the Ammonoidea of the Lower Greensand, part VI. *Palaeontographical Society*: 399-546.

Casey, R., 1980. A monograph of the Ammonoidea of the Lower Greensand, part IX. *Palaeontographical Society*: 633-660.

Casey, R., Bayliss, H. M. & Simpson, M. I. (1998).

PLANCHE 1

Fig. 1-2: ***Cymatoceras neocomiense*** (d'Orbigny, 1840). Deshayesi Zone, Grandis Subzone, Narbonne, Parets d'en Sales, lev. 1, "Niveau de Vires", Ramade Fm. (NV1).

Fig. 3-4: ***Anglonautilus praeundulatus*** Lehmann, Maisch, Baudouin, Salfinger-Maisch, 2017. Deshayesi Zone, Grandis Subzone, Narbonne, Parets d'en Sales, lev. 1, "Niveau de Vires", Ramade Fm. (NV2).

All the specimens are belonging to the Philippe Fauré, Camille Frau, Dominique Téodori and Emile Hourqueig collection; Photographies by Philippe Fauré. All specimens are coated with ammonium chloride prior to photography.
Without other indication, the specimens are full sized and the scale bar is 10 mm.

PLANCHE 1

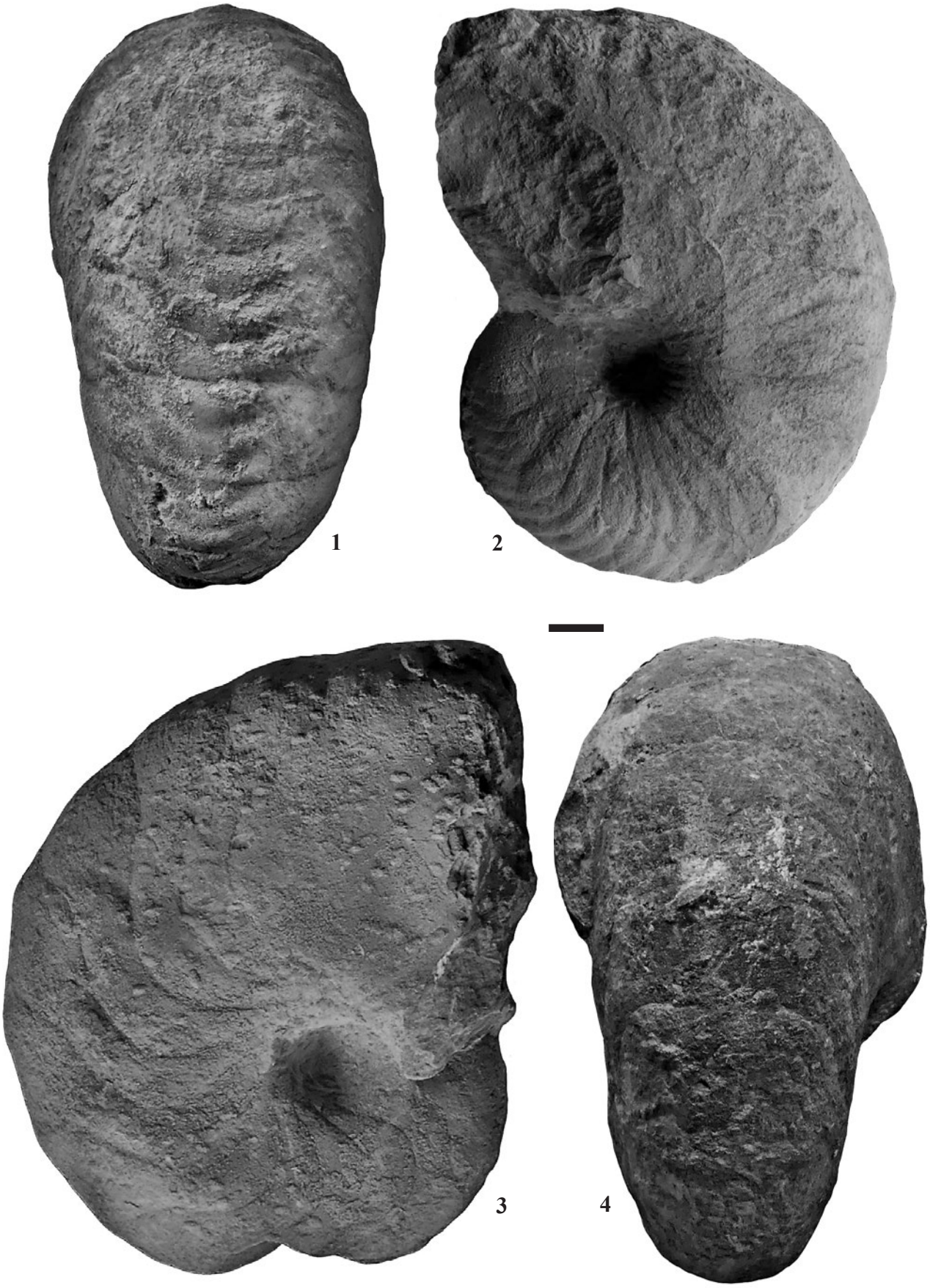

Observations on the lithostratigraphy and ammonite succession of the Aptian (Lower Cretaceous) Lower Greensand of Chale Bay, Isle of Wight, UK. *Cretaceous Research*, 19(3-4) : 511-535.

Coquand, H. (1868). Note sur la formation crétacée de la montagne de la Clape, près Narbonne (Aude). *Bulletin de la Société géologique de France*, 2, XXVI : 187-214.

Courville, P., & Lebrun, P. (2010). L'Albien (Crétacé) de la région de Troyes (Aube) et ses ammonites : Hoplitidae et Douvilleiceratidae. *Fossiles*, 4 : 4-30.

Delanoy, G., Baudouin, C., Gonnet, R., & Bert, D. (2008). Sur les faunes d'ammonites (Crétacé inférieur) du niveau glauconieux de la carrière des Trois-Vernes, près de Crest (Drôme, Sud-est de la France). *Annales du Muséum d'Histoire Naturelle de Nice*, 23 : 11-65.

Delanoy, G., Baudouin, C., Gonnet, R., Conte, G. & Frau, C., (2012). Sur la présence des genres *Heminautilus* Spath, 1927 et *Eucymatoceras* Spath, 1927 (Nautilida, Nautilaceae) dans le Barrémien inférieur du Gard (sud-est de la France). *Annales du Muséum d'Histoire naturelle de Nice*: 155-195.

Delanoy, G., Baudouin, C., Pictet, A., Delattre, P., Pénagé, E., (2017). Ancyloceratidae (Ammonoidea, Ancyloceratoidea) nouveaux ou peu connus de l'Aptien inférieur des Alpes-Maritimes (Sud-Est de la France). *Annales du Muséum d'Histoire Naturelle de Nice*: 35-90.

Delanoy, G., Baudouin, C., Pictet, A., Moreno-Bedmar, J., Frau, C., & Matrion, B. (2022). The genera *Roloboceras* Casey, 1954, and *Megatyloceras* Humphrey, 1949 (Ammonoidea, Ancyloceratina, Douvilleiceratidae), from the Lower Aptian of Ardèche (SE France). Taxonomic and biostratigraphic implications. *Carnets de Géologie/Notebooks on Geology*, 22(2): 7-109.

Delanoy, G., Baudouin, C., Pictet, A., Delattre, P., & Penagé, E. (2018). Ancyloceratidae (Ammonoidea, Ancyloceratoidea) nouveaux ou peu connus de l'Aptien inférieur des Alpes-Maritimes (Sud-Est de la France). *Annales du Muséum d'Histoire Naturelle de Nice,* 32 : 35-90.

Dercourt, J., Gaetani M., Vrielynck B, Barrier E., Biju-Duval B, Brunet M.-F., Cadet J.-P., Crasquin S. & Sanduescu M. Atlas Peri-Téthy. Paleogeographical maps. *CCGM/CGMW,* Paris, 24 maps and explanatoy notes : I-XX : 1-269.

Doncieux, L. (1903). Monographie géologique et paléontologique des Corbières orientales. *Annales de l'Université de Lyon*, nouvelle série, I, 11. 377 p.

Doncieux, L. (1921). Environs de Narbonne. Corbières septentrionales (Aude) et Minervois (Hérault). *Réunion extraordinaire de la Société géologique de France* du 28 septembre au 5 octobre 1913. 90 p.

Dufaure, Ph. (1967). Stratigraphie du Crétacé inférieur et du Jurassique dans le forage de la Clape 1. *Comptes-rendus de l'Académie des Science*, Paris, 258 : 266-268.

Dumas, E. (1876). *Statistique géologique, minéralogique, métallurgique et paléontologique du Département du Gard. Deuxième partie, constitution géologique* (p. 1-422). Paris: Imprimerie Bertrand; Nîmes: Imprimerie Peyrot-Tinel et Cie; Alais: Imprimerie Brugueirolle et Cie.

Föllmi, K. B., & Gainon, F. (2008). Demise of the northern Tethyan Urgonian carbonate platform and subsequent transition towards pelagic conditions: the sedimentary record of the Col de la Plaine Morte area, central Switzerland. *Sedimentary Geology*, 205(3-4): 142-159.

Frau, C. (2020). Stable carbon-isotope chemostratigraphy versus ammonite biostratigraphy: Data from around the Barremian/Aptian boundary (Lower Cretaceous). *Strata*, 2, 56: 1-31.

Frau, C., & Bulot, L. G. (2023). An account of the lower Aptian ammonites of the Niveau Goguel (= OAE 1a) in the Vocontian Basin, SE France. *Cretaceous Research*, 149, 105556.

Frau, C., Bulot, L.G., Delanoy, G., (2017a). New and poorly known Aptian Acrioceratidae (Ancyloceratoidea, Ammonoidea) from Cassis-Roquefort-la-Bédoule (Bouches-du-Rhône, France). *Neues Jahrbuch für Geologie und Paläontologie* 283/3 : 335-346.

Frau, C. & Delanoy, G., (2022). Taxonomic notes on some Barremian-Aptian cephalopods from the Station de Cassis section and surrounding sites, Bouches-du-Rhône, southern France. *Strata*, 2, 58: 1-45.

Frau, C., Delanoy, G., & Hourquieg, E. (2015). Le genre *Macroscaphites* Meek, 1876 (Ammonoidea) dans l'Aptien inférieur de Cassis-La Bédoule (Bouches-du-Rhône, France). Proposition d'un nouveau schéma zonal pour la série stratotypique. *Revue de Paléobiologie*, 34: 45-57.

Frau, C., Pictet, A., Caïssa, M., (2020b). The affinities between the Lower Cretaceous Ammonoidea *Ammonites crassicostatus* d'Orbigny, 1841 and *Ammonites gargasensis* d'Orbigny, 1841. *Paleontología Mexicana*, 9 : 53-72.

Frau, C., Pictet, A., Spangenberg, J., Masse, J.-P., Tendil, A.J.B.T., Lanteaume, C., (2017b). New insights on the age of the post-Urgonian marly cover of the Apt region (Vaucluse, SE France) and its implications on the demise of the North Provence carbonate platform. *Sedimentary Geology,* 359: 44-61.

Frau, C., Tendil, A.J.-B., Pohl, A., Lanteaume, C., (2020a). Revising the timing and causes of the Urgonian rudistid-platform demise in the Mediterranean Tethys. *Global and Planetary Change,* 187: 103-124.

PLANCHE 2

Fig. 1: ***Cymatoceras neocomiense*** (d'Orbigny, 1840). Deshayesi Zone, Grandis Subzone, Narbonne, Parets d'en Sales, lev. 1, "Niveau de Vires", Ramade Fm. (NV3).

PLANCHE 2

1

2

Frau, C., Tendil, A.J.-B., Lanteaume, C., Masse, J.-P., Pictet, A., Bulot, L.G., Luber, T., Redfern, J., Borgomano, J., Léonide, P., Fournier, F., Massonnat, G., 2018. Late Barremian–early Aptian ammonite bio-events from the Urgonian-type series of Provence (Southeast France): regional stratigraphic correlations and implications for the peri-Vocontian carbonate platforms. Cretaceous Research 90, 222-253.

Gauthier, H., Busnardo, R., Combemorel, R., Delanoy, G., Fischer, J.-C., Guérin-Franiatte, S., Joly, B., Kennedy, W. J., Sornay, J., Tintant, H., 2006. Volume IV : Céphalopodes crétacés. *In* : Fischer, J.-C. (Ed.), Révision critique de la Paléontologie française d'Alcide d'Orbigny. Backhuys Publishers, Leiden :1-292 ; 293-662.

Gill, T., 1871. Arrangement of the families of mollusks. Smithsonian Miscellaneous Collections 227 xvi + 1-49.

Gottis, M. (1957). Contribution à la connaissance géologique du Bas-Languedoc. Thèse doctorat ès sciences naturelles, Montpellier. 344 p.

Guibbert, B. & Fauré, Ph. (2019). Fichier bibliographique des fossiles cités dans le Crétacé inférieur du massif de la Clape. Edition ASNAT, Gaillac. https://asnat.fr/fichiersdefossiles/Fichier%20fossiles%20clape%20compresse.pdf

Haeckel, E. (1876). Natürliche Schöpfungsgeschichte: Gemeinverständliche wissenschaftliche Vorträge über die Entwickelungslehre im Allgemeinen und diejenige von Darwin, Goethe und Lamarck im Besonderen über die Anwendungen derselben auf den Ursprung des Menschen und andere damit zusammenhängende Grundfragen der Naturwissenschaft. (8th ed.). Berlin: Georg Reimer.

Haq, B. U. (2014). Cretaceous eustasy revisited. *Global and Planetary Change*, 113: 44-58.

Hardenbol, J., Thierry, J., Farley, M. B., Jacquin, T., De Graciansky, P. C., & Vail, P. R. (1998). Mesozoic and Cenozoic sequence chronostratigraphic framework of European basins. In P. C. De Graciansky, J. Hardenbol, T. Jacquin, & P. R. Vail (Eds.), Mesozoic and Cenozoic Sequence Stratigraphy of European Basins (SEPM Special Publication No. 60, pp. 3-13). Tulsa, OK: Society for Sedimentary Geology (SEPM).

Hébert, M. (1867). Le terrain crétacé des Pyrénées (1er partie). *Bulletin de la Société géologique de France*, 2, XXIII : 323-380.

Hyatt, A. (1883-1884).- Genera of fossil cephalopods. *Proceedings of the Boston Society of Natural History*, 22 (1882-1883): 253-338.

Hyatt, A. (1900). Cephalopoda, in Zittel K. A. von, Text-Book of Palaeontology (translated and edited by C. R. Eastman). McMillan, London: 502-604.

Hyatt, A., (1903). *Pseudoceratites* of the Cretaceous. Monographs of the United States Geological Survey XLIV: 1-250.

Jaffrézo, M. (1971). Stratigraphie de l'Aptien (s.l.) du massif de la Clape (Aude). *Comptes-rendus sommaires de la Société géologique de France* :184-187.

Jaffrézo, M. (1980). Les formations carbonatées des Corbières (France) du Dogger à l'Aptien : micropaléontologie stratigraphique, biozonation, paléoécologie. Extension des résultats à la Mésogée. Thèse de Doctorat d'État ès Sciences naturelles. 615 p.

Klein, J., & Bogdanova, T. (2013). Lower Cretaceous Ammonites VI. Douvilleiceratoidea & Deshayesitoidea. *Fossilium Catalogus I: Animalia*, 151, 299.

Klein, J., Busnardo, R., Company, M., Delanoy, G., Kakabadze, M.V., Reboulet, S., Ropolo, P., Vasícek, Z., Vermeulen, J., (2007). Fossilium catalogus, I: Animaliae Lower Cretaceous Ammonites III: Bochianitoidea, Protancyloceratoidea, Ancyloceratoidea, Ptychoceratoidea, 144. Backhuys Publishers, Leiden: 1-381.

Klug, C., Korn, D., Landman, N. H., Tanabe, K., De Baets, K., & Naglik, C. (2015a). Describing ammonoid conchs. Ammonoid Paleobiology: From anatomy to ecology: 3-24.

Klug, C., Zatoń, M., Parent, H., Hostettler, B., & Tajika, A. (2015b). Mature modifications and sexual

PLANCHE 3

Fig. 1-4: ***Cheloniceras*** **sp.** *Deshayesites forbesi* Zone and/or the lower *Deshayesites deshayesi* Zone, Gruissan, Saint-Martin, "Niveau de Saint-Martin", Estagnol Fm.
Fig. 1-2: NMS1
Fig. 3-4: NMS2

Fig. 5: ***Ammonitoceras*** **sp.** *Deshayesites forbesi* Zone and/or the lower *Deshayesites deshayesi* Zone, Gruissan, Saint-Martin, "Niveau de Saint-Martin", Estagnol Fm. (NSM 3).

Fig. 6: ***Macroscaphites*** **sp.** *Deshayesites forbesi* Zone and/or the lower *Deshayesites deshayesi* Zone, Gruissan, L'Estagnol, "Niveau de Saint-Martin", Estagnol Fm. (NSM4).

Fig. 7-8: ***Deshayesites*** **sp.** *Deshayesites forbesi* Zone and/or the lower *Deshayesites deshayesi* Zone, Narbonne, La Ramade, "Niveau de Saint-Martin", Estagnol Fm. (NSM 5).

PLANCHE 3

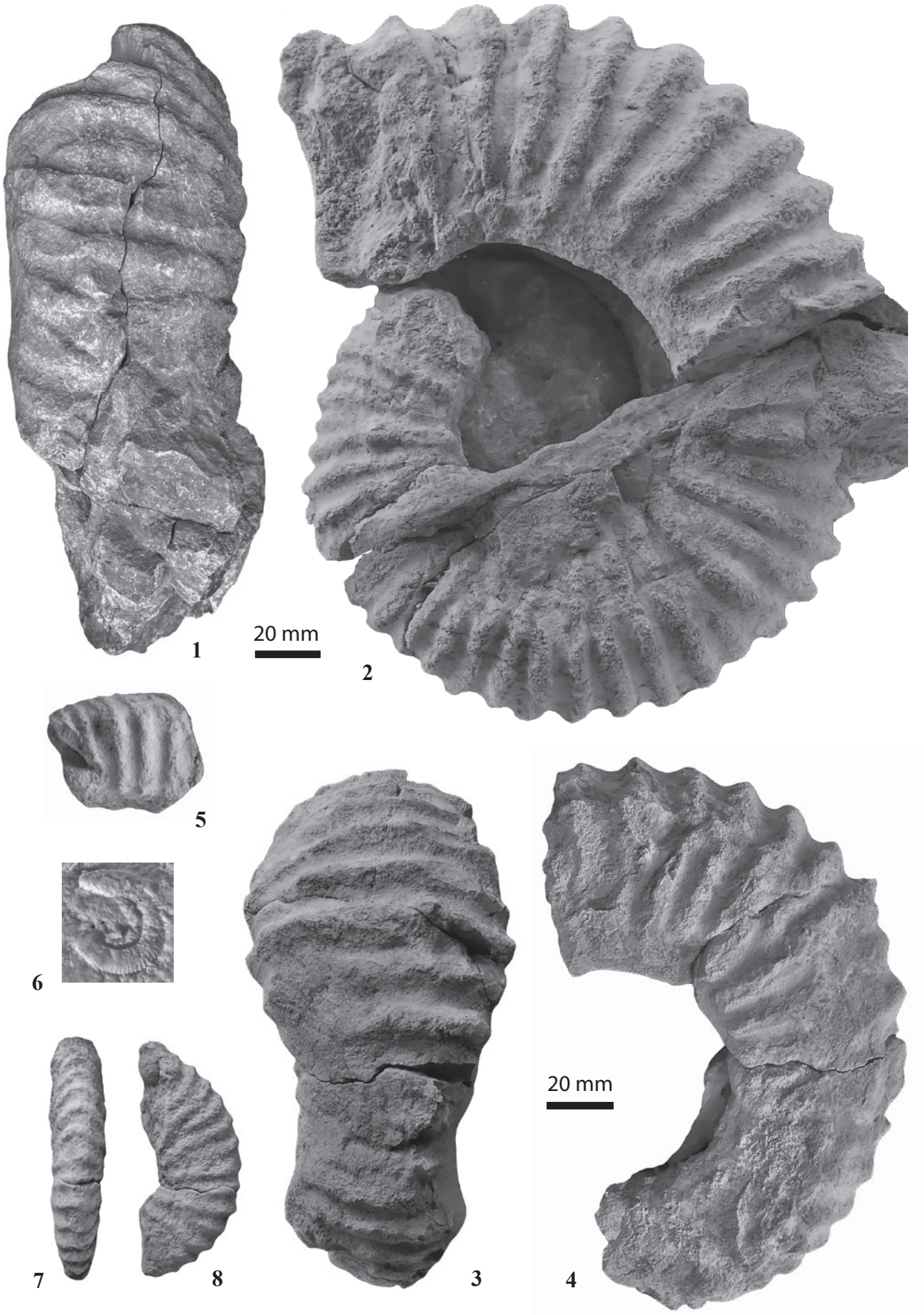

dimorphism. Ammonoid paleobiology: From anatomy to ecology: 253-320.

Léenhardt, F. (1887). Le Crétacé inférieur de la Clape (Aude). *Bulletin de la Société géologique de France*, 3, XV : 742-755.

Lehmann, J., Friedrich, O., Von Bargen, D., & Hemker, T. (2012). Early Aptian Bay deposits at the southern margin of the Lower Saxony Basin: Integrated stratigraphy, palaeoenvironment and OAE 1a. *Acta Geologica Polonica*, 62(1): 1-22.

Lehmann, J., Maisch, M. W., Baudouin, C., & Salfinger-Maisch, A. (2017). Origin and evolutionary history of *Anglonautilus* (Nautilida, Cymatoceratidae) and a new species from the lower Aptian of Spain. *Cretaceous Research*, 72: 66-80.

Lespinasse, P., Aloïsi, J.C., Barruol, J., Durand-Delga, M., Got, H., Monaco, A. & Marchal, J.-P. (1982). Carte géologique de Narbonne au 1 50 000e (1061).

Linder, P., Gigandet, J., Hüsser, J.-L., Gainon, F., & Föllmi, K.B., (2006). The Early Aptian Grünten Member: description of a new lithostratigraphic unit of the helvetic Garschella Formation. *Eclogae Geologicae Helvetiae*. 99: 327-341.

Magnan, H. (1872). Mémoire sur la partie inférieure du terrain de Craie (Néocomien, Aptien, Albien) des Pyrénées françaises et des Corbières. *Mémoire de la Société géologique de France*, 2, 9. 82 p.

Masse, J. P. (1995). Lower Cretaceous rudist biostratigraphy of southern France. A reference for Mesogean correlations. *Revista Mexicana de Ciencias Geológicas*, 12(2), 14.

Masse, J.-P., Frau, C., Tendil, A.J.-B., & Fenerci-Masse, M., 2020. Evidence for three successive late Barremian rudist faunas from the Urgonian-type carbonate platforms of southeast France. Cretaceous Research 115, 104561.

Meek F. B. 1876. A report on the invertebrate Cretaceous and Tertiary fossils of the upper Missouri country. Hayden F. V. (Ed.). Report of the United States Geological Survey of the Territories 9: lxiv +629 p.

Mikhailova, I. A., & Baraboshkin, E. Y. (2001). First finds of *Lithancylus* Casey, 1969 (Ammonoidea, Ancyloceratidae) in the Lower Aptian of Ul'yanovsk Povolzhye. *Paleontologicheskii Zhurnal*, 4: 32-42.

Moreno-Bedmar J.A. (2010). Ammonits de l'Aptià inferior de la Peninsula Iberica. Biostratigrafia i aportacions a l'estudi del Oceanic Anoxic Event 1a. Tesis, Universitat de Barcelona. 67 p.

Moreno-Bedmar, J. A., Bover-Arnal, T., Salas, R., Delanoy, G., Maurrasse, F. M., Grauges, A., & Martínez, R. (2010). Lower Aptian ammonite biostratigraphy in the Maestrat Basin (Eastern Iberian Chain, Eastern Spain). A Tethyan transgressive record enhanced by synrift subsidence. *Geologica Acta*, 8(3): 281-299.

Moreno, J.A., Company, M., Sandoval, J. & Tavera, J.M (2007). Caracterización estratigráfica y paleontológica de un pulso regresivo/transgresivo en el interior del ciclo Ap3 (Aptiense inferior) en la Cordillera Ibérica y en el Dominio Prebético. *Jornadas de la Sociedad Española de Paleontología,* XXIII : 155-156.

Nikolov, T. & Parashkevanov, P. (1995). Some fossil cephalopods from the Lovec Urgonian Group at the Village of Pusevo, Veliko Tarnovo District (Lower Cretaceous, central Fore-Balkan). *Geologica Balcanica* 25(1): 61-70.

Orbigny, d'A., (1840e1842). Paléontologie française, Description zoologique et géologique de tous les animaux mollusques et rayonnes fossiles de France. Terrains Crétacés, vol. 1. Céphalopodes. Masson, Paris. 662 p.

Parona, C.F., & Bonarelli, G., (1897). Fossili Albiani d'Escragnolles, del Nizzardo e della Liguria occidentale. *Paleontologica ltaliana*, 2 (for 1896): 53-112.

Peybernès, B. (1971). Le Crétacé inférieur du massif de la Clape (Aude). *Bulletin de la Société d'Histoire naturelle de Toulouse,* 107 : 408-413.

Peybernès, B. (1973). Biostratigraphie du Néocomien des Corbières et du Pays de Sault (Aude, Pyrénées-Orientales). *Bulletin de la Société d'Histoire naturelle de Toulouse,* 109 : 216-233.

PLANCHE 4

Fig. 1-19: ***Deshayesites grandis*** Spath, 1930. Deshayesi Zone, Grandis Subzone, Narbonne, Parets d'en Sales, lev. 1, "Niveau de Vires", Ramade Fm.
Fig. 1-2: NV22
Fig. 3-4: NV4
Fig. 5-6: NV5
Fig. 7: NV6
Fig. 8-10: NV9
Fig. 11: NV7
Fig. 12: NV8
Fig. 13-14: VN10
Fig. 15-16: NV13
Fig. 17-18: NV11
Fig. 19: NV12

PLANCHE 4

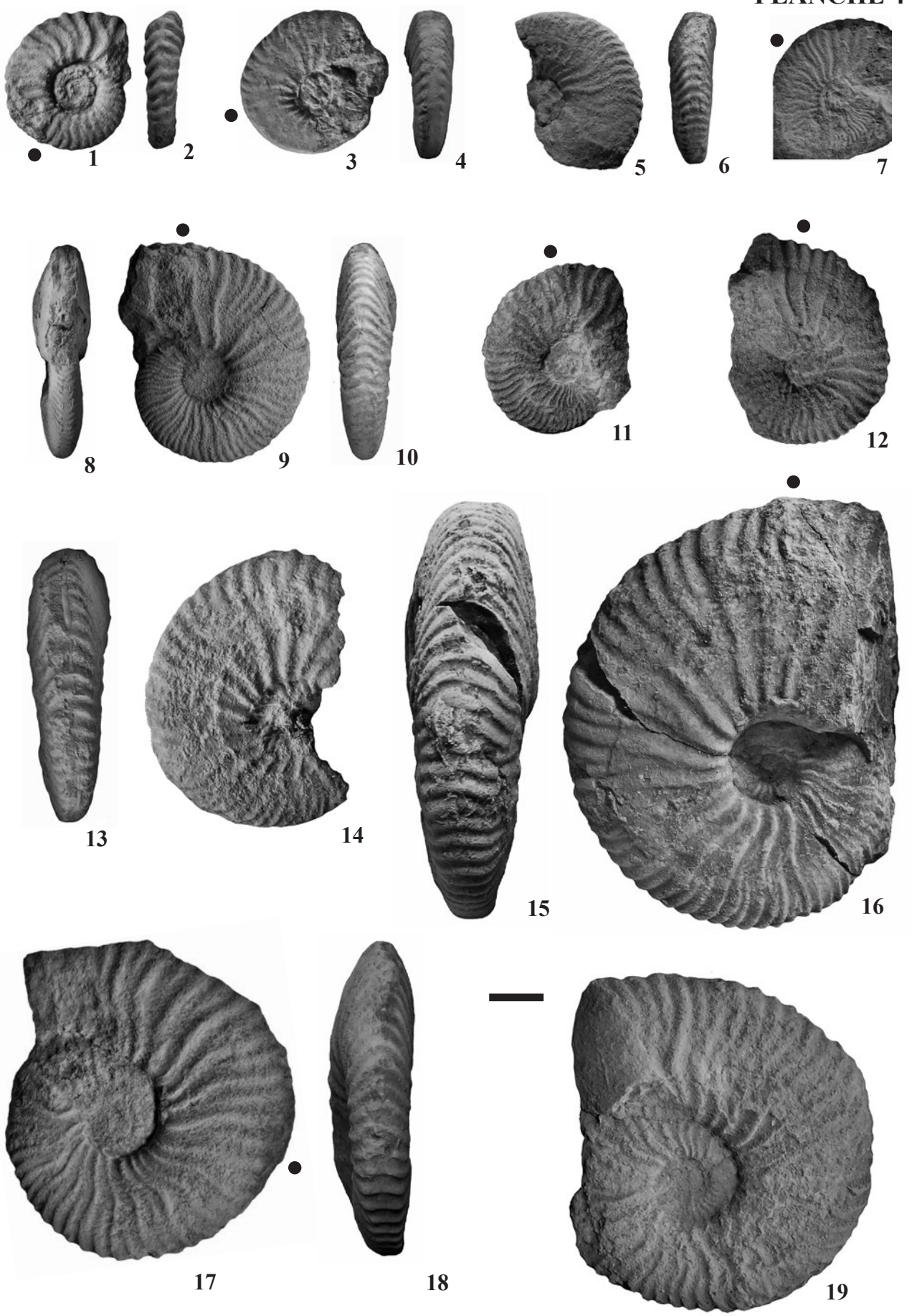

Peybernès, B. (1976). Le Jurassique et le Crétacé inférieur des Pyrénées franco-espagnoles entre la Garonne et la Méditerranée. Thèse de doctorat ès sciences naturelles, Univ. Toulouse 3. Imp. CRDP Toulouse. 695 p.

Peybernès, B. (2012). Berriasien – Albien inférieur. *In* Synthèse géologique et géophysique des Pyrénées, vol. 2 : Cycle alpin, stratigraphie, Crétacé inférieur : 230-293

Pictet, A. (2011). Les marnes à *Exogyra aquila* (Aptien inférieur) sur la plate-forme du Vivarais (Ardèche, France) : sédimentologie, stratigraphie et biostratigraphie. Thèse de licence, Section des Sciences de la Terre, Université de Genève.

Pictet, A., Delamette, M., & Matrion, B. (2016). The Perte-du-Rhône Formation, a new Cretaceous (Aptian-Cenomanian) lithostratigraphic unit in the Jura mountains (France and Switzerland). *Swiss Journal of Geosciences*, 109(2): 221-240.

Pictet, A., Delanoy, G., Adatte, T., Spangenberg, J. E., Baudouin, C., Boselli, P., Boselli, M., Kindler, P., & Föllmi, K. B. (2015). Three successive phases of platform demise during the early Aptian and their association with the oceanic anoxic Selli episode (Ardèche, France). *Palaeogeography, Palaeoclimatology, Palaeoecology*, 418: 101-125.

Pictet, A., Delanoy, G., Baudouin, C., Boselli, P., (2009). Le genre *Lithancylus* CASEY, 1960 (Ammonoidea, Ancyloceratina) dans l'Aptien inférieur du Couloir rhodanien (Drôme, Sud-Est de la France). *Revue de Paléobiologie* : 491-509.

Puzos M. 1832. Sur le Scaphites Yvani. *Bulletin de la Société Géologique de la France*, 2 : 355-356.

Reboulet, S., Ottilia, S., Aguirre-Urreta, B., Barragán, R., Company, M., Frau, C., Kakabadze, M.V., Klein, J., Moreno-Bedmar, J.A., Lukeneder, A., Pictet, A., Ploch, I., Raisossadat, S.N., Vašíček, Z., Baraboshkin, E.J., Mitta, V., 2018. Report on the 6th International Meeting of the IUGS Lower Cretaceous Ammonite Working Group, the Kilian Group (Vienna, Austria, 20th August 2017). Cretaceous Research 91, 100-110.

Roch, E. (1927). Étude stratigraphique et paléontologique de l'Aptien inférieur de La Bédoule (près Cassis) (Bouches-du-Rhône). Thèse de doctorat, Faculté des sciences de Marseille.

Roman, F. (1938). Les ammonites jurassiques et crétacées : essai de genera, Masson et Cie., Paris. 554 p.

Ruffell, A. H., & Wach, G. D. (1991). Sequence stratigraphic analysis of the Aptian-Albian Lower Greensand in southern England. *Marine and Petroleum Geology*, 8(3): 341-353.

Sharikadze, M. Z. (1979). *Procolombiceras*. A new genus of the family Parahoplitidae from the Lower Aptian deposits of Georgia (in Russian). *Soobshcheniya Akademii Nauk Gruzinskoi* SSR, 94(2): 381-384.

Sinzow, J. (1906). Die Beschreibung einiger Douvilleiceras-Arten aus dem Oberen Neocom Russlands. *Mémoire du Comité Géologique*, 22: 1-45.

Sowerby, J. (1812-1813). The Mineral Conchology of Great Britain: or coloured figures and descriptions of those remains of testaceous animals or shells which have been preserved at various times and depths in the earth. Benjamin Meredith, London, vol. 1. p. 1-234.

Sowerby, J. de C., (1828). The Mineral Conchology of Great Britain, part 102, In : Sowerby, J. & Sowerby, J. de C. (1812-1846), The Mineral Conchology of Great Britain, vol. 6. Meredith. London: 185-200

Spath, L. F. (1927). LVI. On the classification of the Tertiary Nautili. *Annals and Magazine of Natural History*, 20(118): 424-428.

Spath, L.F., 1923, On the Ammonite horizons of the Gault and contiguous deposits in Great Britain Geological Survey summary of progress for 1922: *Memoirs of the Geological Survey of Great Britain*: 139-149.

Spath, L.F., (1924). On the ammonites of the Speeton Clay and the subdivisions of the Neocomian. *Geological Magazine*, 61: 73-89.

Spath, L.F., 1930. On some Ammonoidea from the Lower Greensand. *Annals and Magazine of Natural History* 10 (5): 417-464.

Stoyanow, A. (1949). Lower Cretaceous stratigraphy in southeastern Arizona. *Geological Society of America Memoir*, 38: 1-169.

Szives, O., Moreno-Bedmar, J.A., Aguirre-Urreta, B., Company, M., Frau, C., López-Horgue, M., Pictet, A., Ploch, I., Salazar, C., Barragán, R., Latil, J.-L., Lehmann, J., Robert, E., Reboulet, S. (2023). Report on the 7th International Meeting of the IUGS Lower Cretaceous Ammonite Working Group, the Kilian

PLANCHE 5

Fig. 1-17 : ***Deshayesites grandis*** Spath, 1930. Deshayesi Zone, Grandis Subzone, Narbonne, Parets d'en Sales, lev.1, "Niveau de Vires", Ramade Fm.
Fig. 1: NV14
Fig. 2-4: NV15
Fig. 5-7: NV17
Fig. 8-9: NV16
Fig. 10-11: NV20
Fig. 12: NV19
Fig. 13: NV18
Fig. 14-15: NV21
Fig. 16-17: NV50

PLANCHE 5

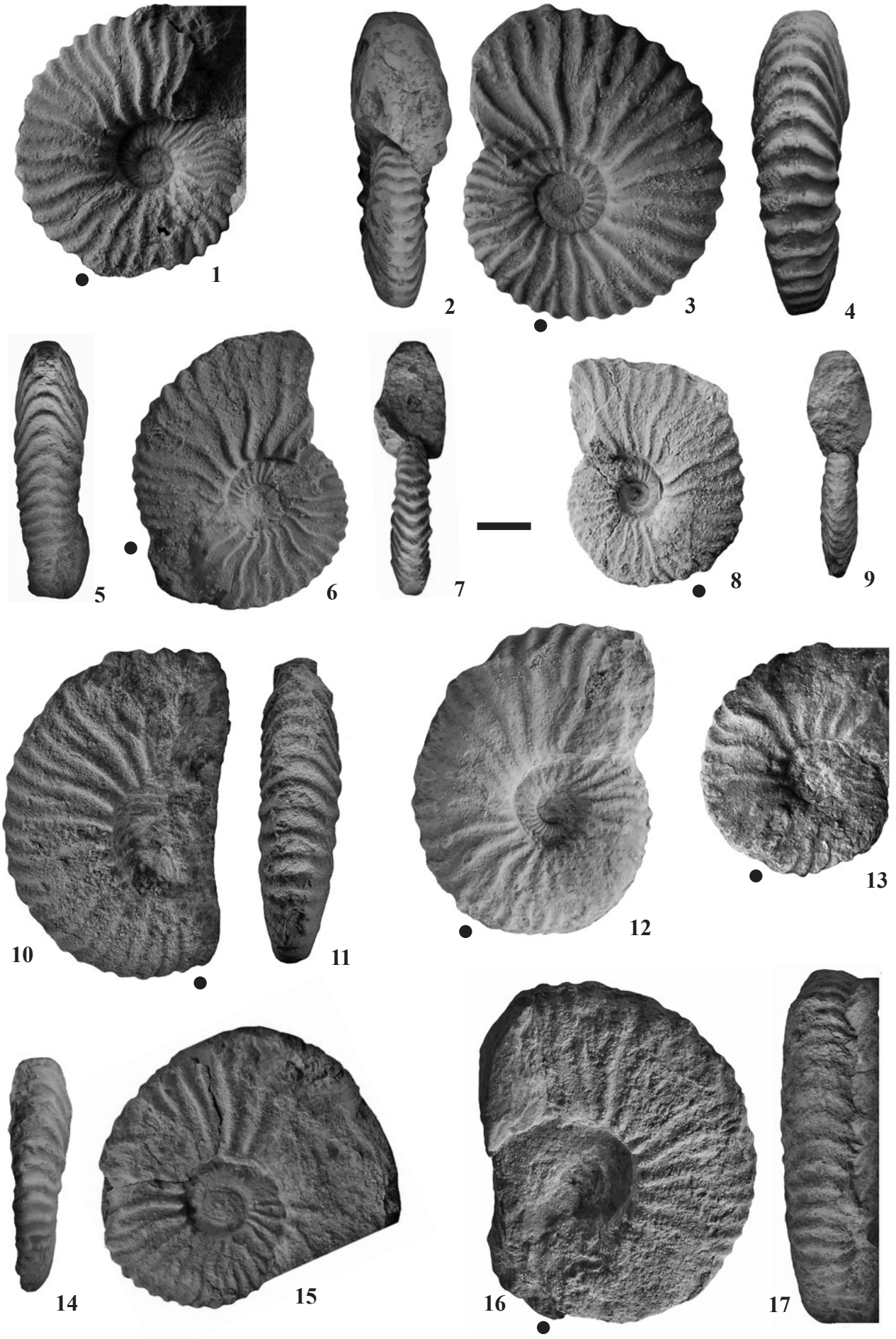

Group (Warsaw, Poland, 21st August 2022): State of the art on the current Standard Ammonite Zonation of the Western Tethyan Mediterranean Province. *Cretaceous Research* 153, 105716.

Thieuloy, J. P. (1990). Un ancyloceratide géant de l'Aptien du Gard (France). *Toxoceratoides* ? sp. inc. « gigantomorphe godeti » nov. *Géologie Alpine*, 66 : 101-106.

Tintant, H., & Kabamba, M. (1983). Le Nautile, fossile vivant ou forme cryptogène ? Essai sur l'évolution et la classification des Nautilacés. *Bulletin de la Société zoologique de France*, 108(4) : 569-579.

Toucas A. (1888). Note sur le Jurassique supérieur et le Crétacé inférieur de la Vallée du Rhône. *Bulletin de la Société géologique de France*, 16 : 903-927.

Vermeulen, J. (2006). Nouvelle classification à fondement phylogénétique des ammonites hétéromorphes du Crétacé inférieur. Annales du Muséum d'Histoire naturelle de Nice, 21 : 137-178.

Vermeulen, J. (2010). Sur les familles des Helicancylidae Hyatt, 1894 et des Acrioceratidae Vermeulen, 2004 ; réponses et précisions apportées au travail de Bert, 2009. *Annales de paléontologie,* 96, 2 : 61-65.

Zeuschner, L. 1856. Über eine alte Längsmoräne im Thale des Biaiy Dunajec beim Hochofen von Zakopane in der Tatra. *Sitzungsberichte der Kaiserlichen Akademie der Wissenschaften, Mathematisch-Naturwissenschaftliche Klasse*, 21, 105-112.

Zittel, C. A. 1895. Desmoceratinae. In: Zittel, C. A., & von Zittel, K. A. (eds.). *Grundzüge der Palaeontologie (Palaeozoologie)*. Oldenbourg.

eISSN 2606-1171. Article available in **Open Access :** Open, free, immediate and permanent access. Authors and their institutions are not charged any fees for the submission or publication of their articles. There is no requirement to register in advance, no subscription fees and no financial contribution required to view or download articles

PLANCHE 6

Fig. 1-16: ***Deshayesites grandis*** Spath, 1930. Deshayesi Zone, Grandis Subzone, Narbonne, Parets d'en Sales, lev. 1, "Niveau de Vires", Ramade Fm.
Fig. 1: NV23
Fig. 2-3: NV24
Fig. 4-5: NV25
Fig. 6-8: NV26
Fig. 9-10: NV27
Fig. 11-12: NV28
Fig. 13-14: NV30
Fig. 15-16: NV29

PLANCHE 6

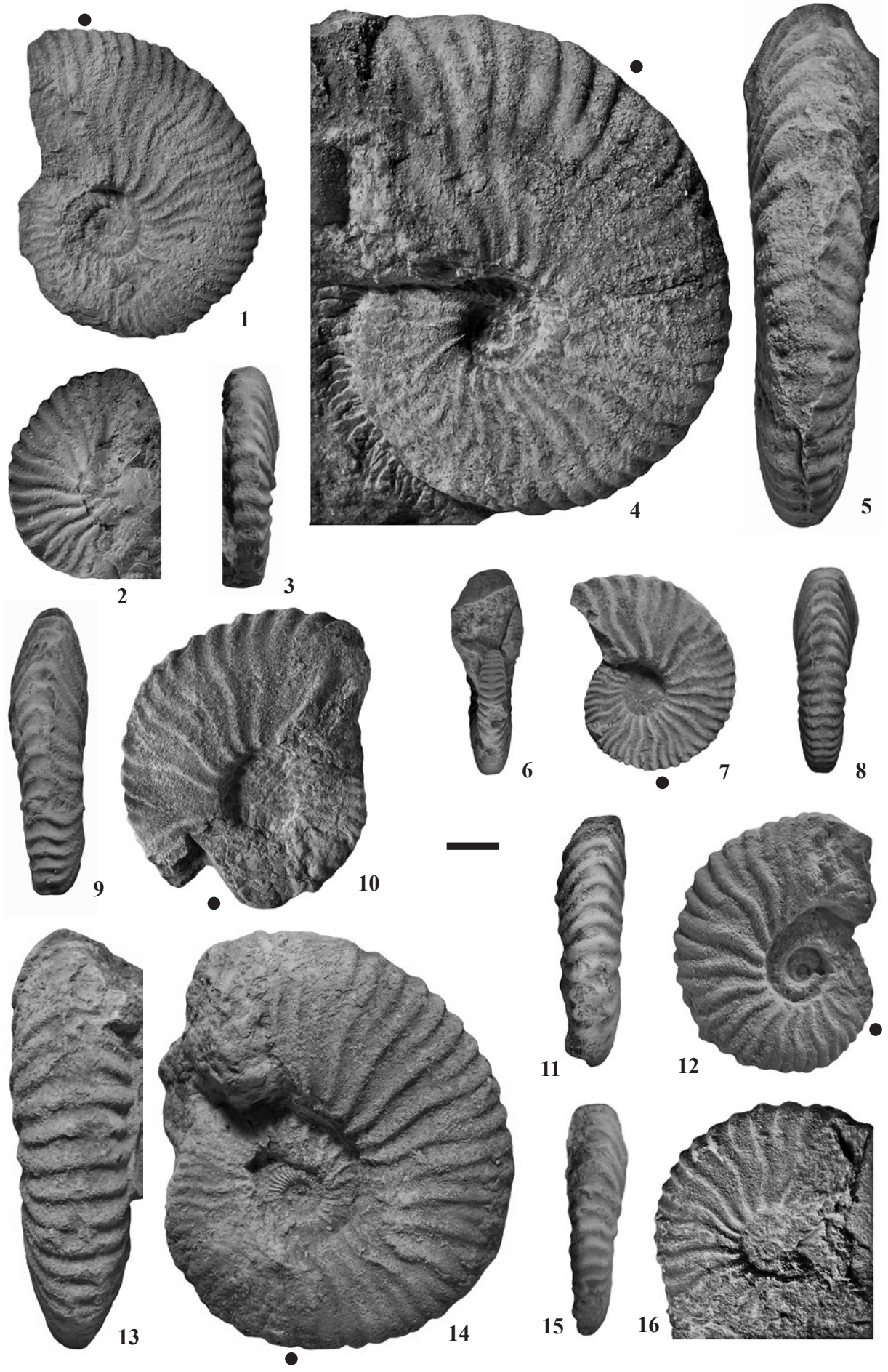

PLANCHE 7

Fig. 1-6: ***Deshayesites grandis*** Spath, 1930. Narbonne, Parets d'en Sales, lev. 1, "Niveau de Vires", Ramade Fm., Deshayesi Zone, Grandis Subzone.
Fig. 1: NV31
Fig. 2: NV32
Fig. 3: NV33
Fig. 4-5: NV34
Fig. 6: NV35

PLANCHE 7

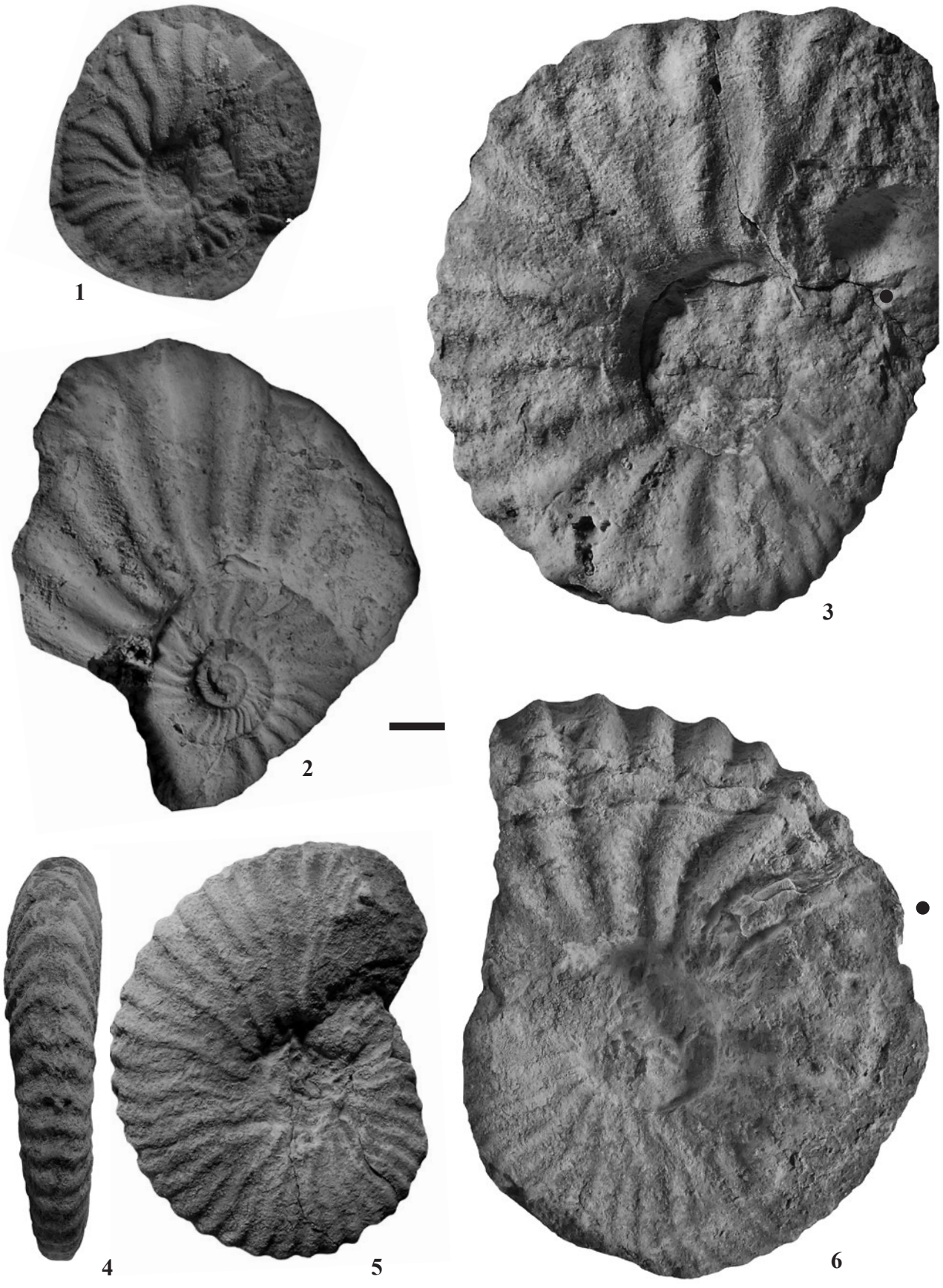

PLANCHE 8

Fig. 1-5: ***Deshayesites grandis*** Spath, 1930. Deshayesi Zone, Grandis Subzone, Narbonne, Parets d'en Sales, lev. 1, "Niveau de Vires", Ramade Fm.
Fig. 1-2: NV36
Fig. 3-4: NV37
Fig. 5: NV38

PLANCHE 8

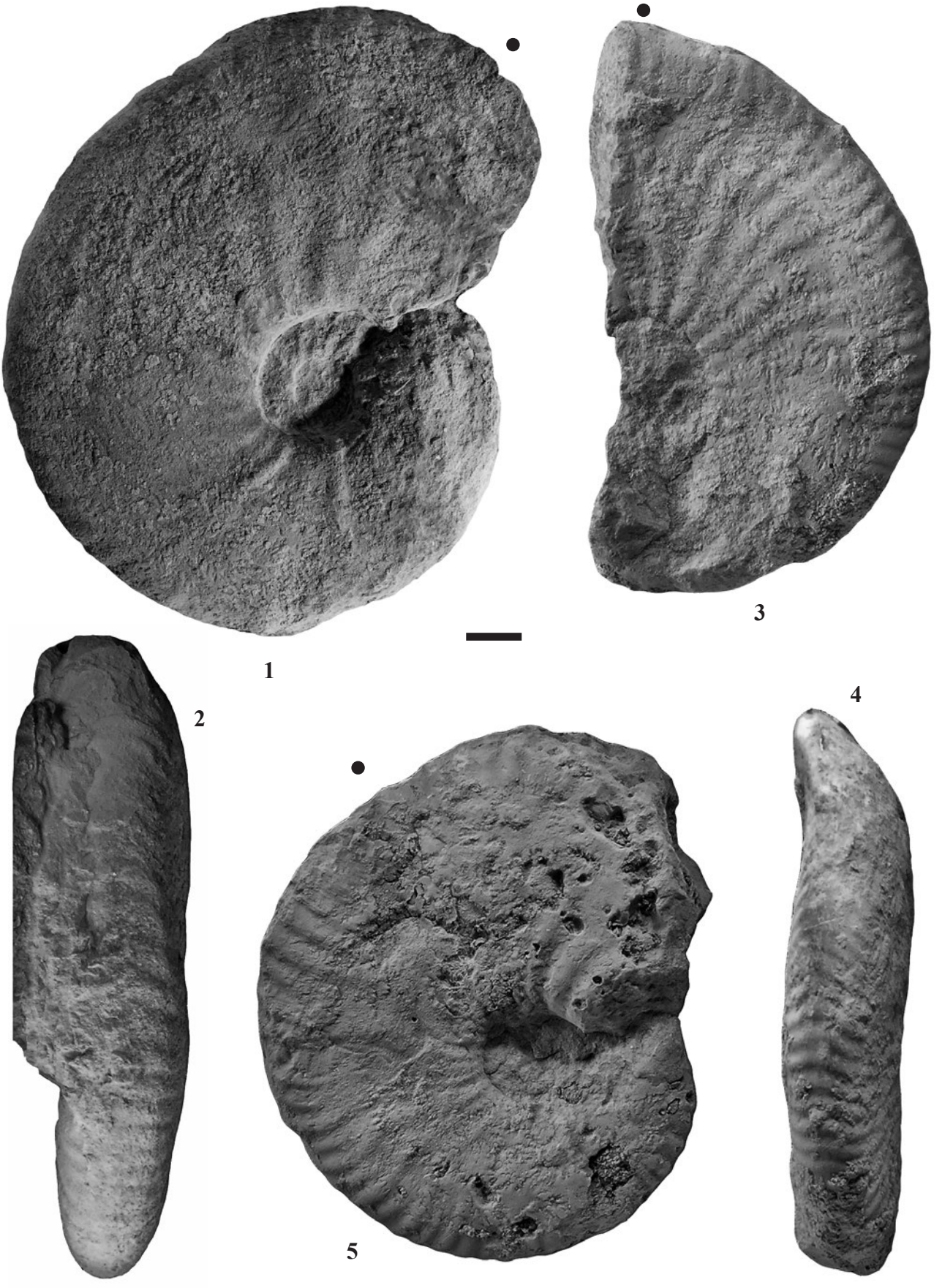

PLANCHE 9

Fig. 1-4: ***Deshayesites grandis*** Spath, 1930. Deshayesi Zone, Grandis Subzone, Narbonne, Parets d'en Sales, lev. 1, "Niveau de Vires", Ramade Fm.
Fig. 1-2: NV39
Fig. 3: NV40
Fig. 4: NV41

PLANCHE 9

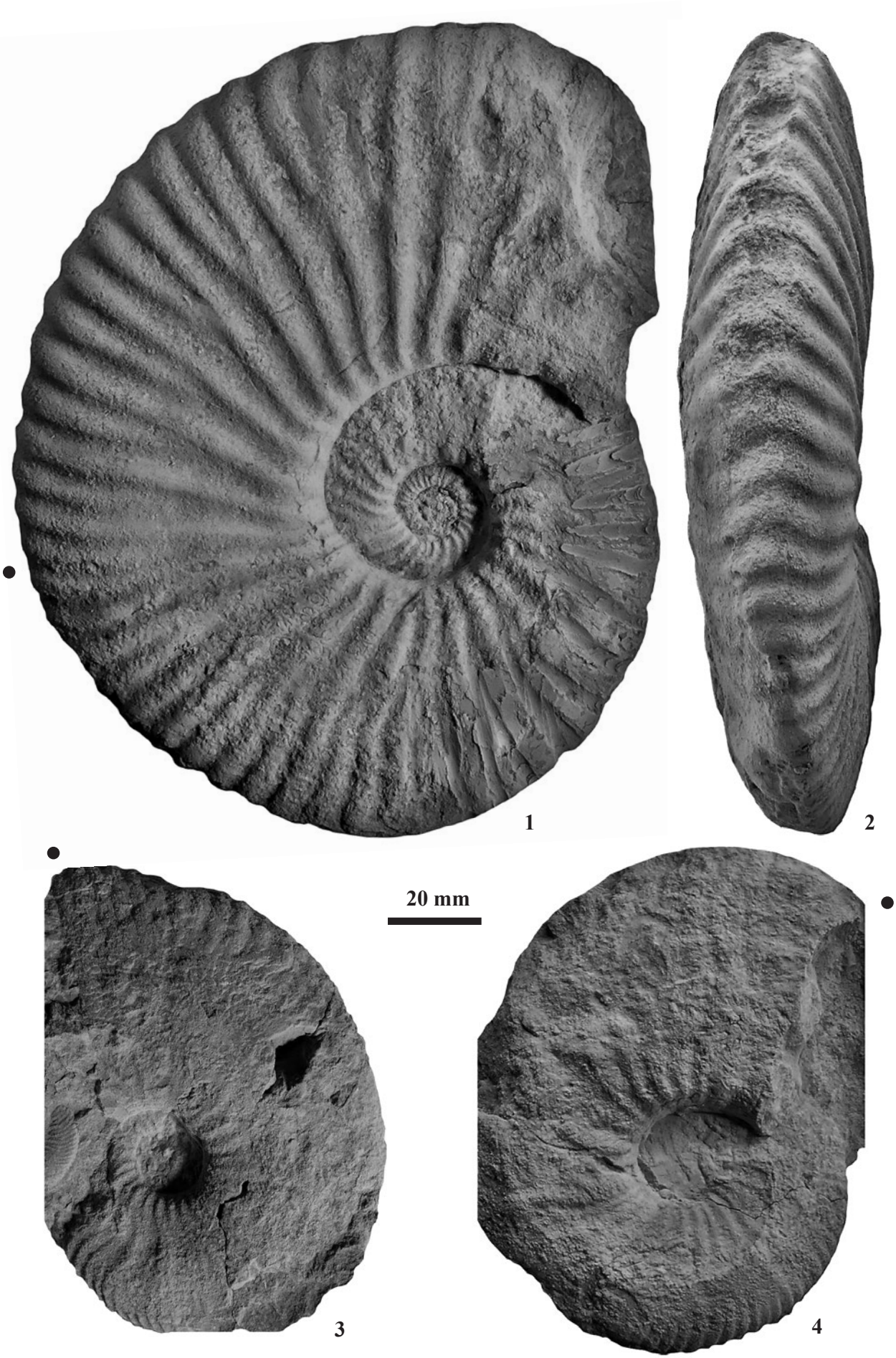

PLANCHE 10

Fig. 1-5: ***Deshayesites grandis*** Spath, 1930. Deshayesi Zone, Grandis Subzone, Narbonne, Parets d'en Sales, lev. 1, "Niveau de Vires", Ramade Fm.
Fig. 1-2: NV42
Fig. 3: NV43
Fig. 4: NV44
Fig. 5: NV45

PLANCHE 10

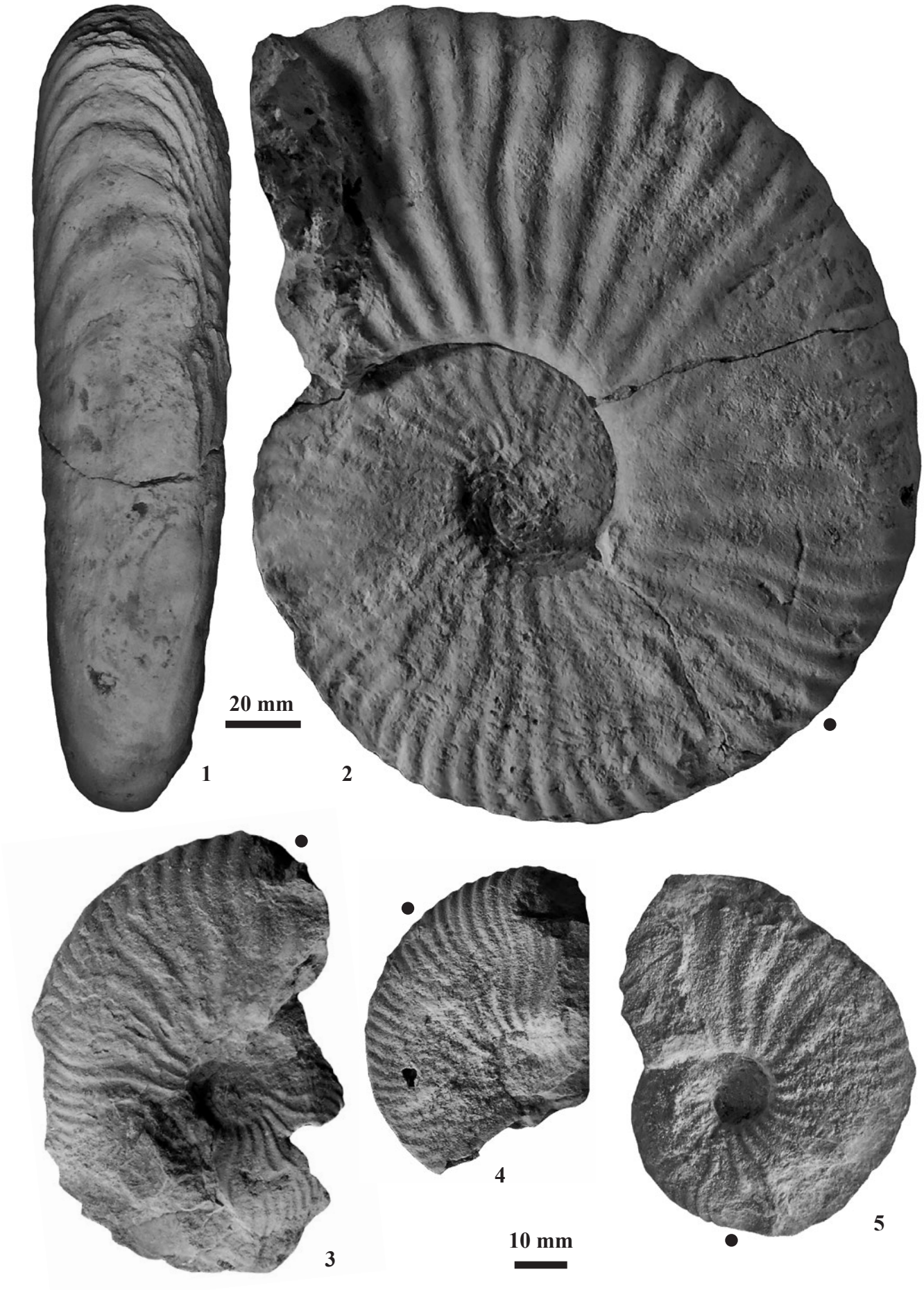

PLANCHE 11

Fig. 1-3: ***Deshayesites grandis*** Spath, 1930. Deshayesi Zone, Grandis Subzone, Narbonne, Parets d'en Sales, lev. 1, "Niveau de Vires", Ramade Fm.
Fig. 1: NV46
Fig. 2: NV47
Fig. 3: NV49

PLANCHE 11

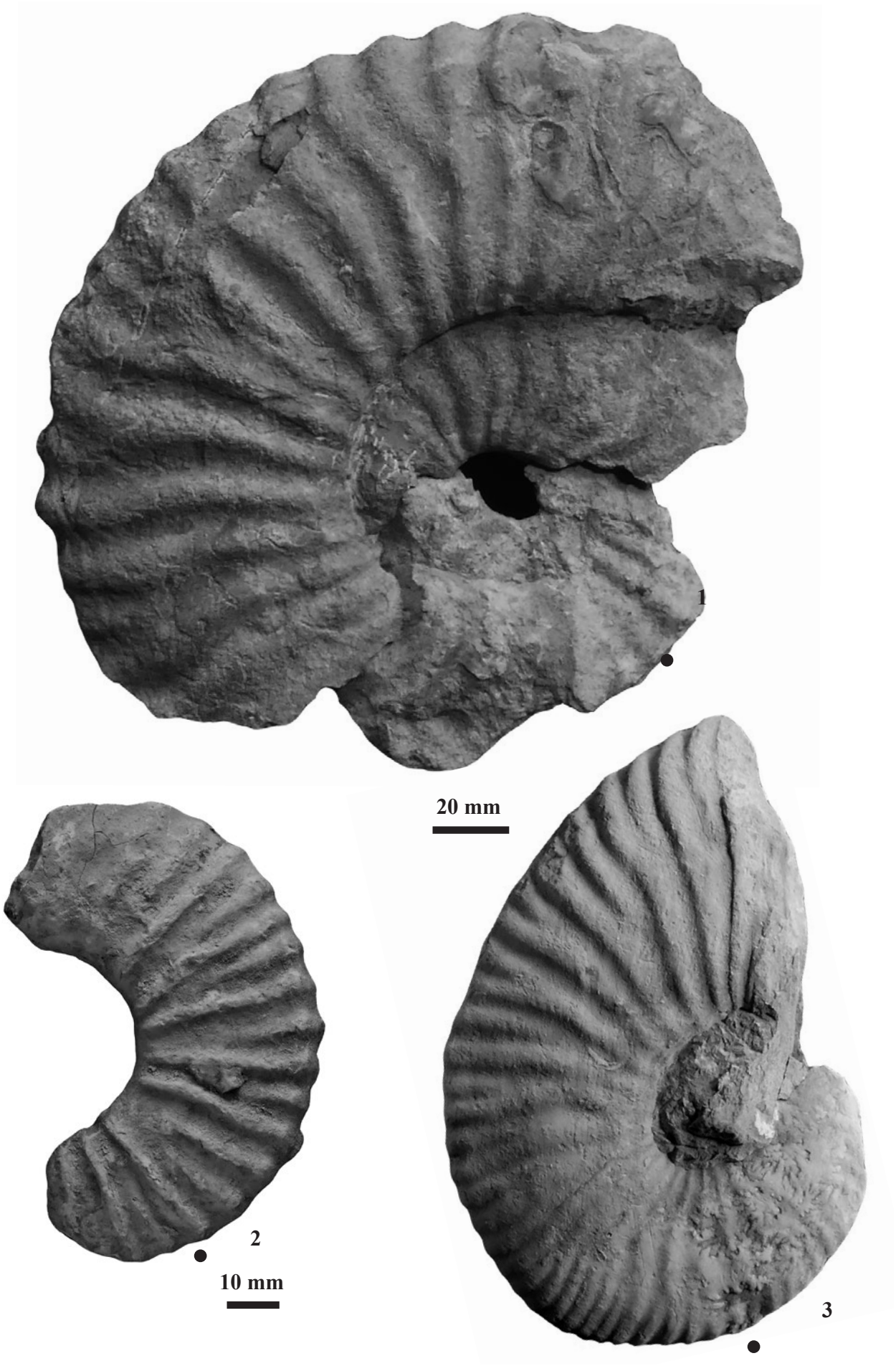

PLANCHE 12

Fig. 1: ***Deshayesites grandis*** Spath, 1930. Deshayesi Zone, Grandis Subzone, Narbonne, Parets d'en Sales, lev. 1, "Niveau de Vires", Ramade Fm, NV48.

PLANCHE 12

1

50 mm

PLANCHE 13

Fig. 1-20: ***Cheloniceras crassum*** Spath, 1930. Deshayesi Zone, Grandis Subzone, Narbonne, Parets d'en Sales, lev. 1, "Niveau de Vires", Ramade Fm.
Fig. 1-2: NV51
Fig. 3-4: NV52 (coll. M. Ricard)
Fig. 5-6: NV53
Fig. 7-8: NV44
Fig. 9-10: NV55
Fig. 11-12: NV56
Fig. 13-14: NV57
Fig. 15-16: NV59
Fig. 17-18: NV58
Fig. 19-20: NV60

PLANCHE 13

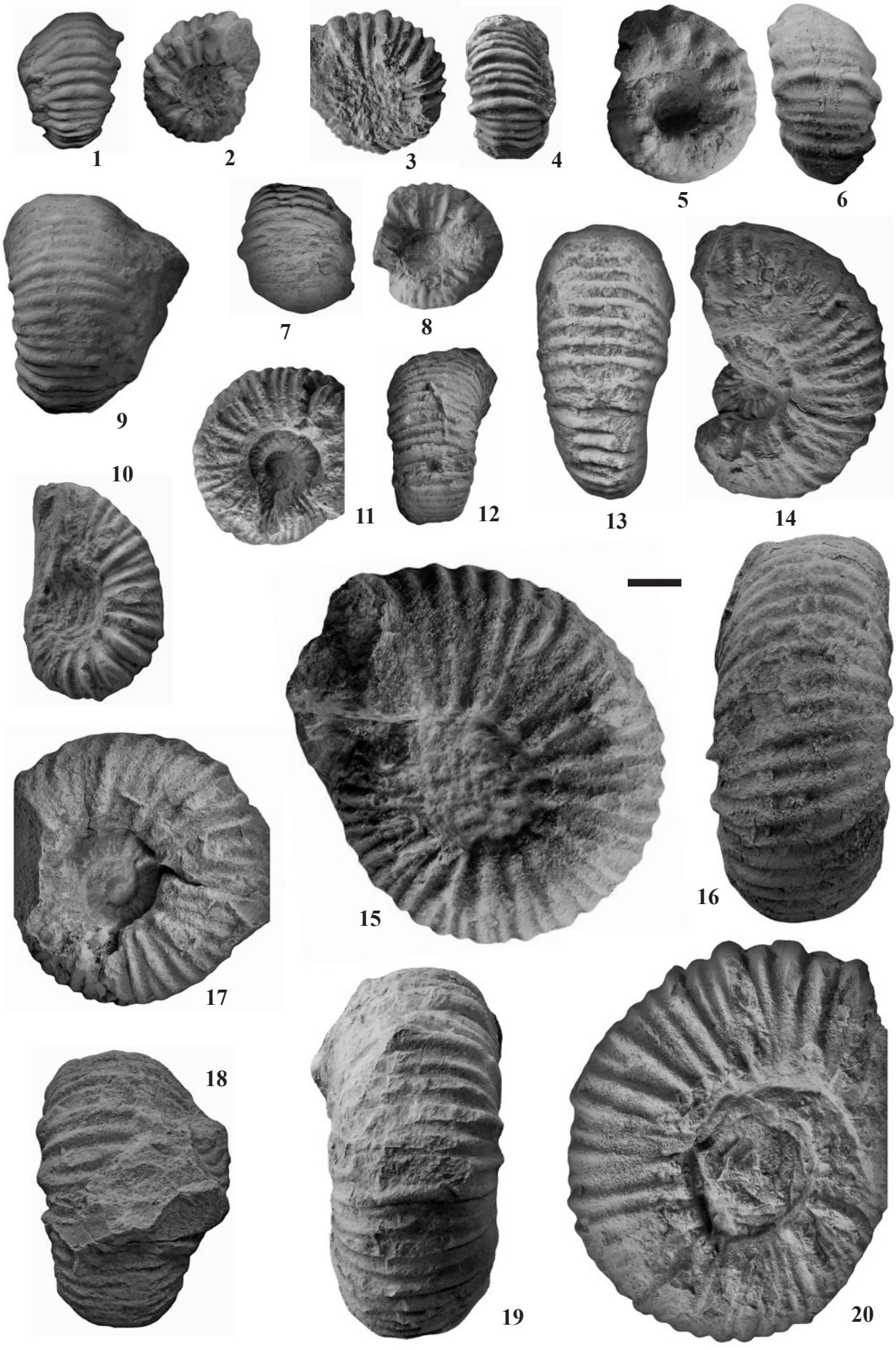

PLANCHE 14

Fig. 1-8 : ***Cheloniceras crassum*** Spath, 1930. Deshayesi Zone, Grandis Subzone, Narbonne, Parets d'en Sales, lev. 1, "Niveau de Vires", Ramade Fm.
Fig. 1-2: NV61
Fig. 3-4: NV62
Fig. 5-6: NV63
Fig. 7-8: NV64

PLANCHE 14

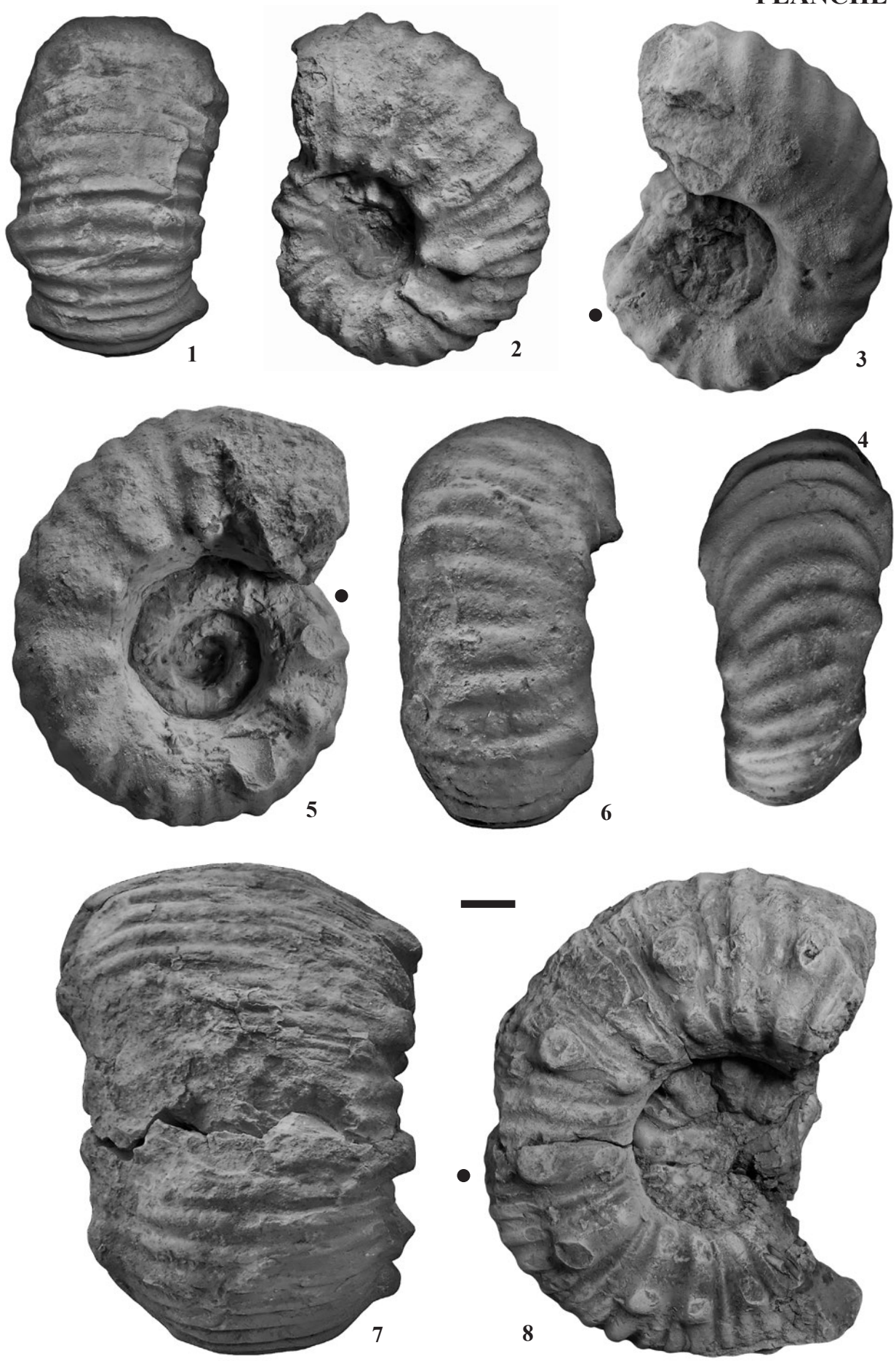

PLANCHE 15

Fig. 1-8: ***Cheloniceras crassum*** Spath, 1930. Deshayesi Zone, Grandis Subzone, Narbonne, Parets d'en Sales, lev. 1, "Niveau de Vires", Ramade Fm.
Fig. 1-2: NV65
Fig. 3-4: NV66
Fig. 5-6: NV67
Fig. 7-8: NV68

PLANCHE 15

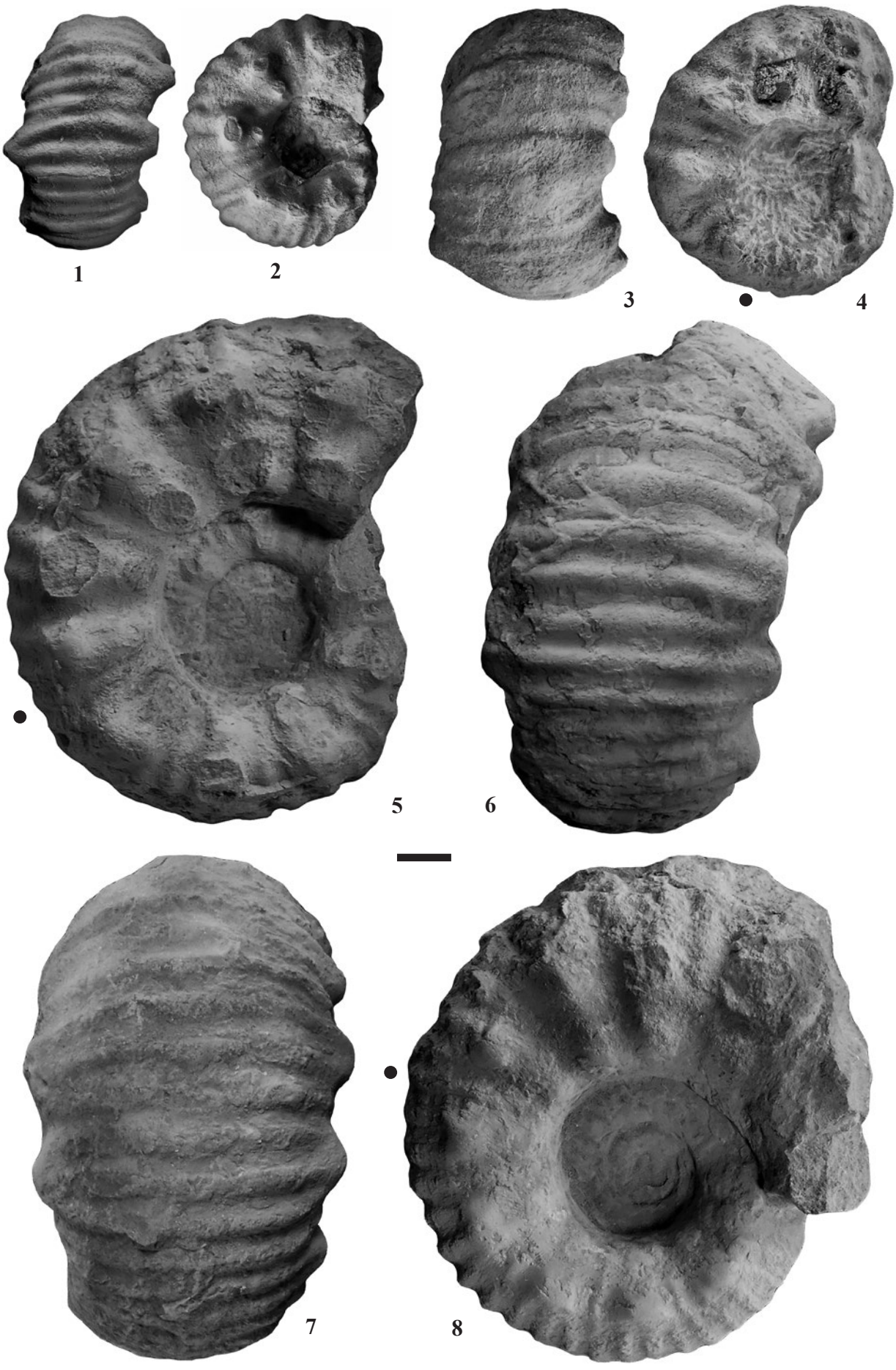

PLANCHE 16

Fig. 1-4: ***Cheloniceras crassum*** Spath, 1930. Deshayesi Zone, Grandis Subzone, Narbonne, Parets d'en Sales, lev. 1, "Niveau de Vires", Ramade Fm.
Fig. 1-2: NV69
Fig. 3-4: NV70

PLANCHE 16

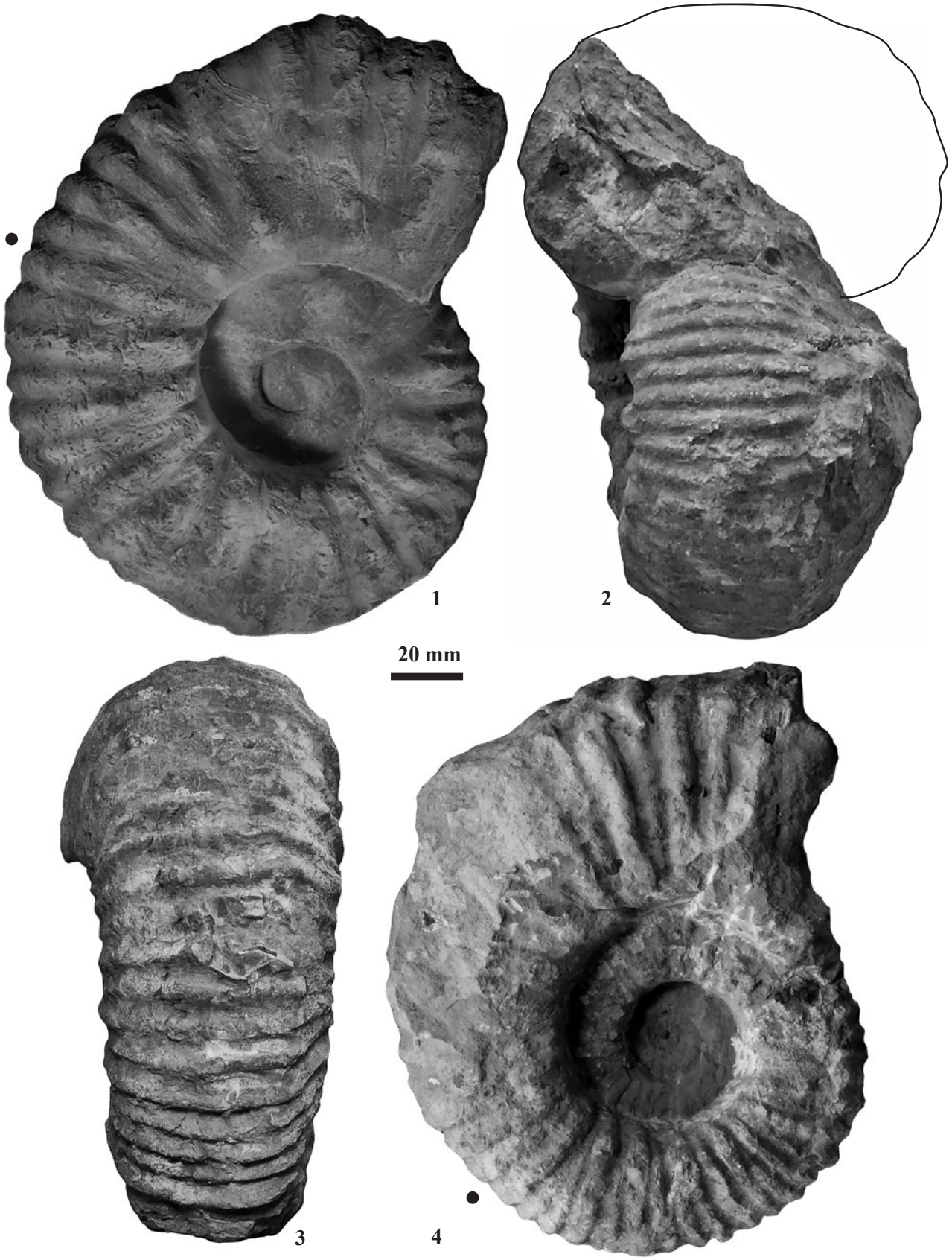

PLANCHE 17

Fig. 1-4: ***Cheloniceras crassum*** Spath, 1930. Deshayesi Zone, Grandis Subzone, Narbonne, Parets d'en Sales, lev. 1, "Niveau de Vires", Ramade Fm.
Fig. 1-2: NV71
Fig. 3-4: NV72

PLANCHE 17

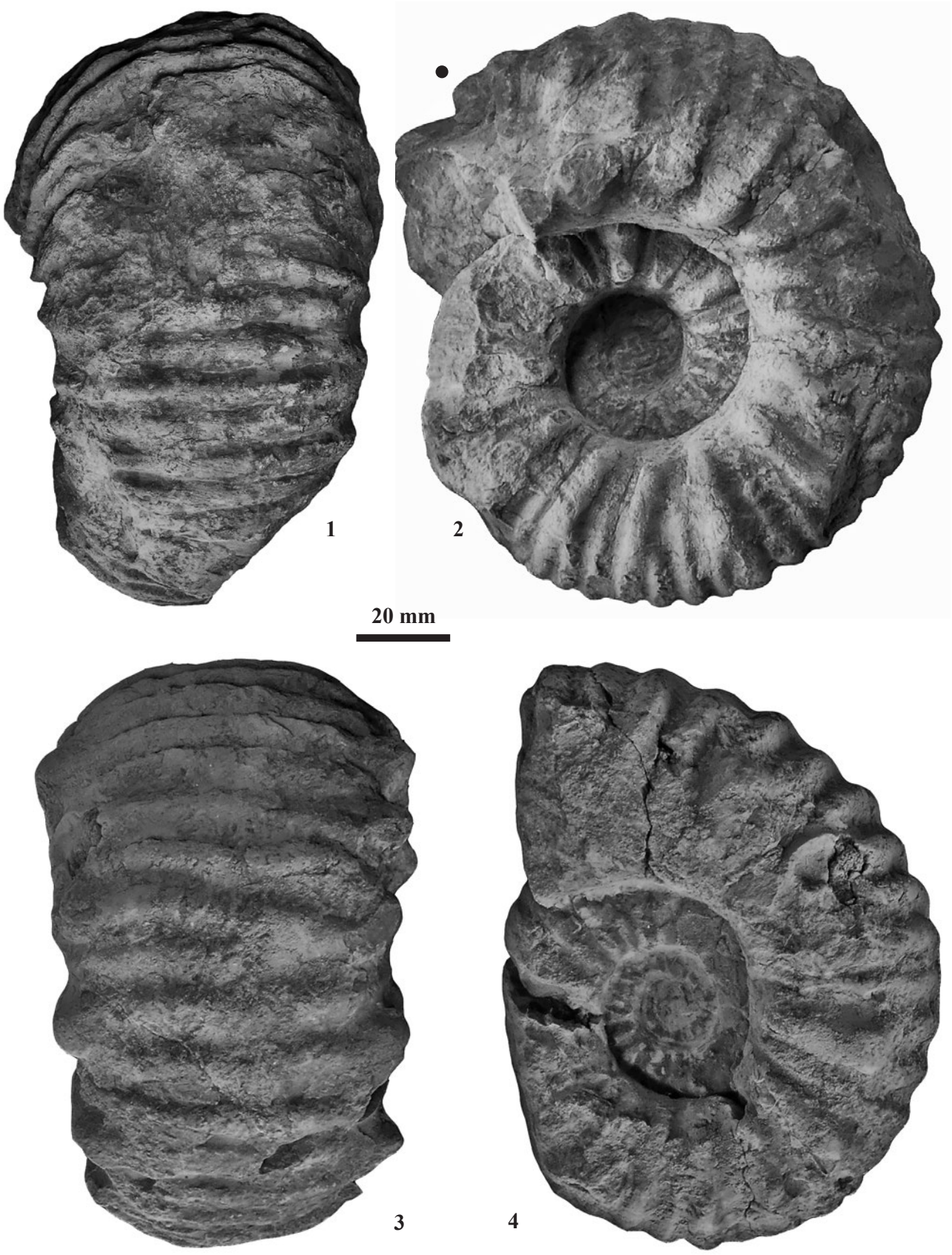

PLANCHE 18

Fig. 1-8: ***Cheloniceras crassum*** Spath, 1930. Deshayesi Zone, Grandis Subzone, Narbonne, Parets d'en Sales, lev. 1, "Niveau de Vires", Ramade Fm.
Fig. 1: NV73
Fig. 2: NV74
Fig. 3-4: NV75
Fig. 5: NV76
Fig. 6-7: NV77
Fig. 8: NV78

PLANCHE 18

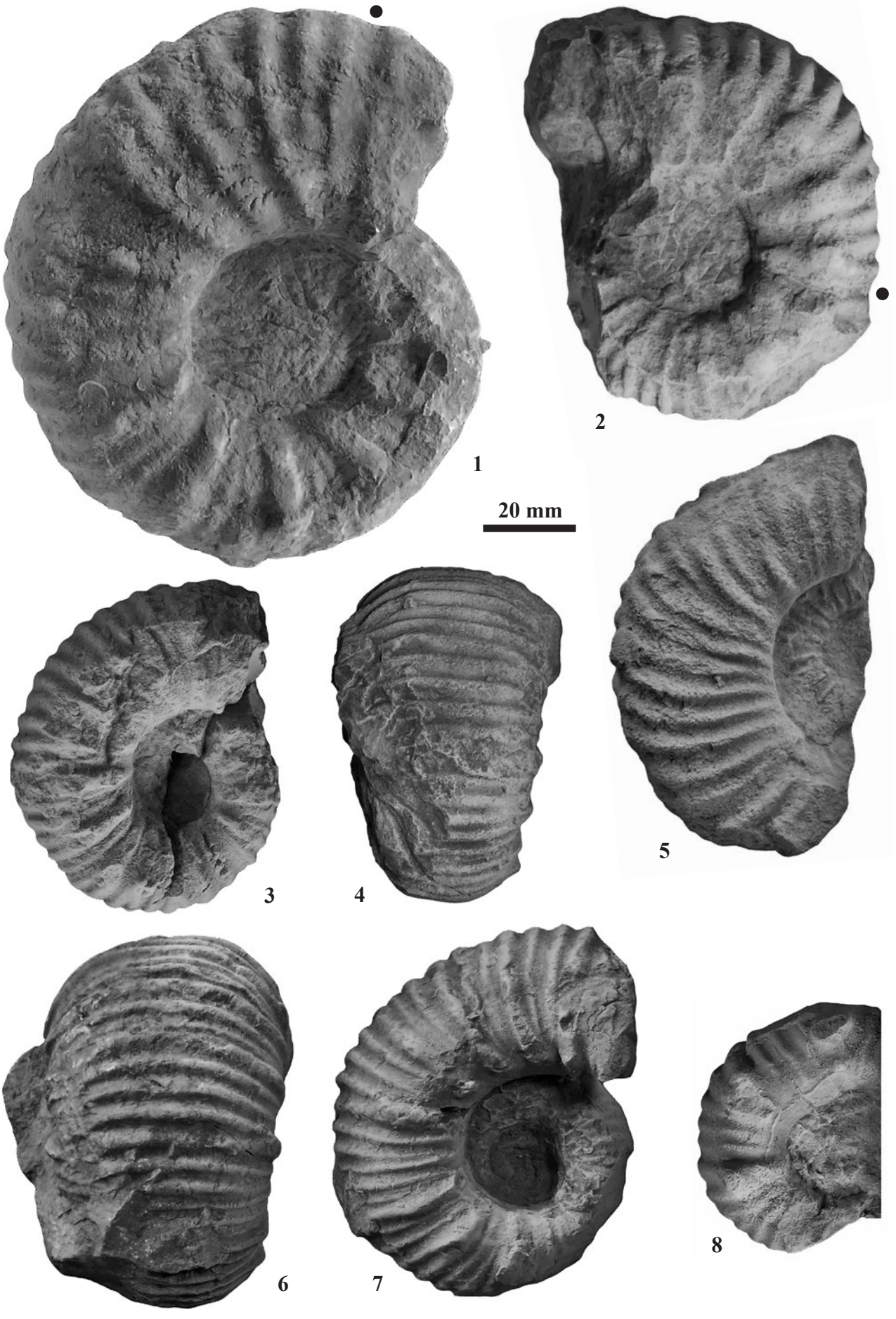

PLANCHE 19

Fig. 1: ***Cheloniceras crassum*** Spath, 1930. Deshayesi Zone, Grandis Subzone, Narbonne, Parets d'en Sales, lev. 1, "Niveau de Vires", Ramade Fm. (NV79).

PLANCHE 19

PLANCHE 20

Fig. 1-3: ***Procolombiceras*** **sp.** Deshayesi Zone, Grandis Subzone, Narbonne, Parets d'en Sales, lev. 1, "Niveau de Vires", Ramade Fm.
Fig. 1-3: NV80

Fig. 4-7: ***Delanoyites*** **gen. nov. sp. A.** Deshayesi Zone, Grandis Subzone, Narbonne, Parets d'en Sales, lev. 1, "Niveau de Vires", Ramade Fm.
Fig. 4-5: NV81
Fig. 6-7: NV82

Fig. 8-13: ***Pseudohaploceras matheroni*** (d'Orbigny, 1841). Deshayesi Zone, Grandis Subzone, Narbonne, Parets d'en Sales, lev. 1, "Niveau de Vires", Ramade Fm.
Fig. 10-11: NV84
Fig. 12-13: NV85

Fig. 14-15: ***Macroscaphites*** **sp. cf.** ***striatisulcatus*** (d'Orbigny, 1841). Deshayesi Zone, Grandis Subzone, Narbonne, Parets d'en Sales, lev. 1, "Niveau de Vires", Ramade Fm.
Fig. 14: NV86
Fig. 15: NV87

Fig. 16: ***Pseudohaploceras*** **sp.** Deshayesi Zone, Grandis Subzone, Narbonne, Parets d'en Sales, lev. 1, "Niveau de Vires", Ramade Fm.
Fig. 16: NV88

PLANCHE 20

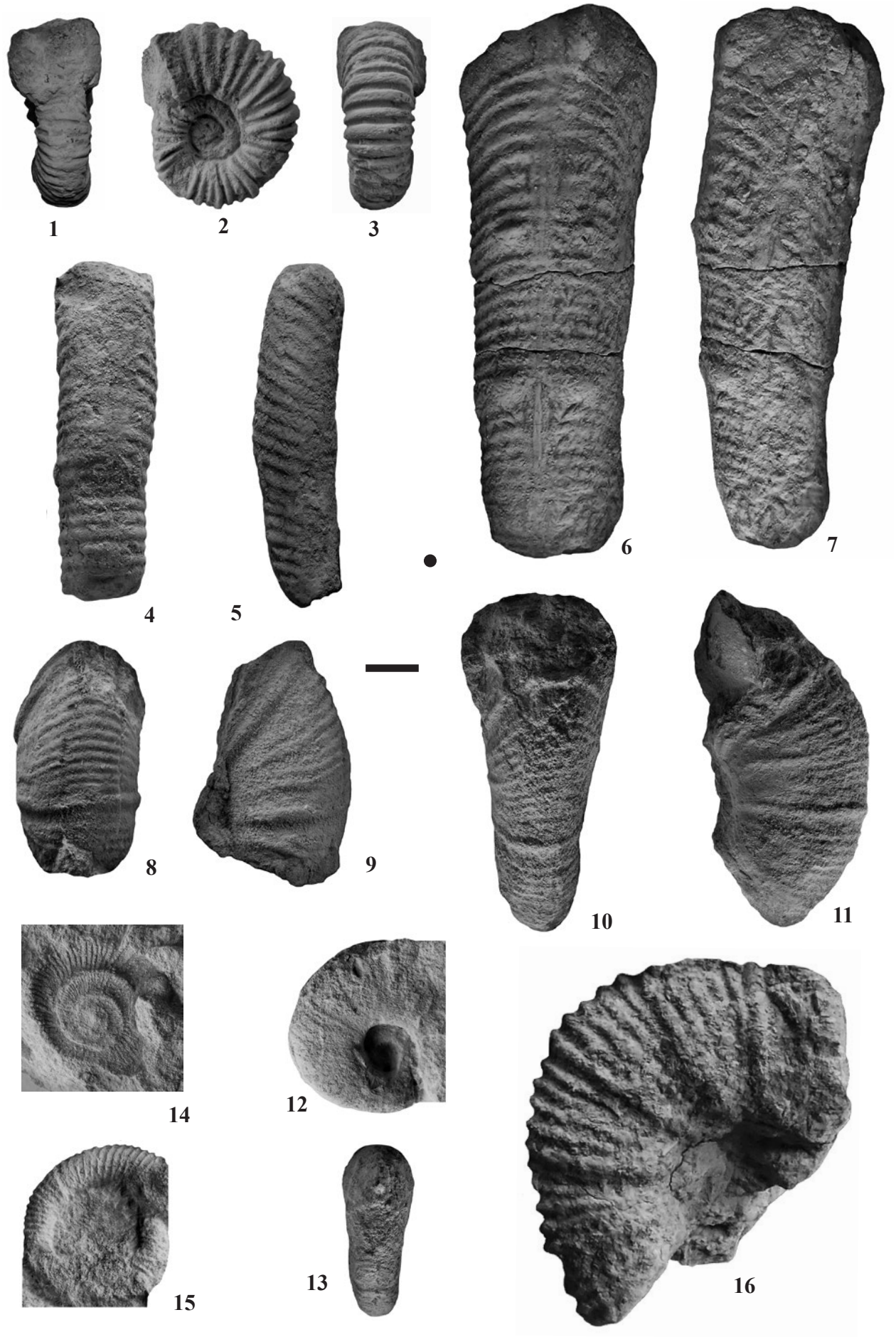

PLANCHE 21

Fig. 1-4: ***Delanoyites* gen. nov. sp. A.** Deshayesi Zone, Grandis Subzone, Narbonne, Parets d'en Sales, lev. 1, "Niveau de Vires", Ramade Fm.
Fig. 1-2: NV89
Fig. 3: NV90
Fig. 4: NV91

PLANCHE 21

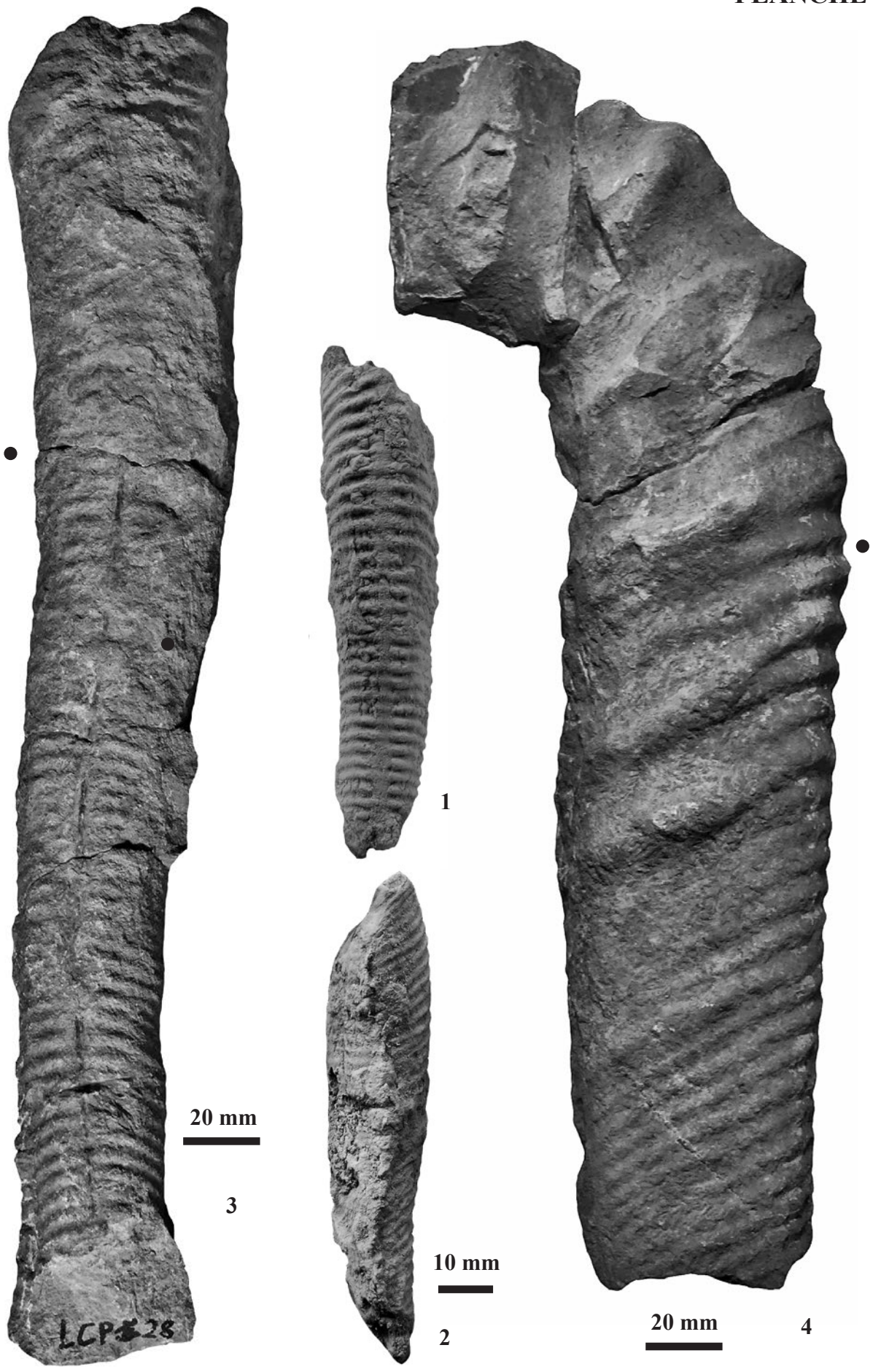

PLANCHE 22

Fig. 1-3: ***Toxoceratoides rochi*** Casey, 1961. Deshayesi Zone, Grandis Subzone, Narbonne, Parets d'en Sales, lev. 1, "Niveau de Vires", Ramade Fm.
Fig. 1: NV92
Fig. 2-3: NV93

Fig. 4-9: ***Delanoyites*** **gen. nov. sp. B.** Narbonne, Parets d'en Sales, lev. 1, "Niveau de Vires", Ramade Fm., Deshayesi Zone, Grandis Subzone.
Fig. 4-5: NV94
Fig. 6-7: NV95
Fig. 8-9: NV96

PLANCHE 22

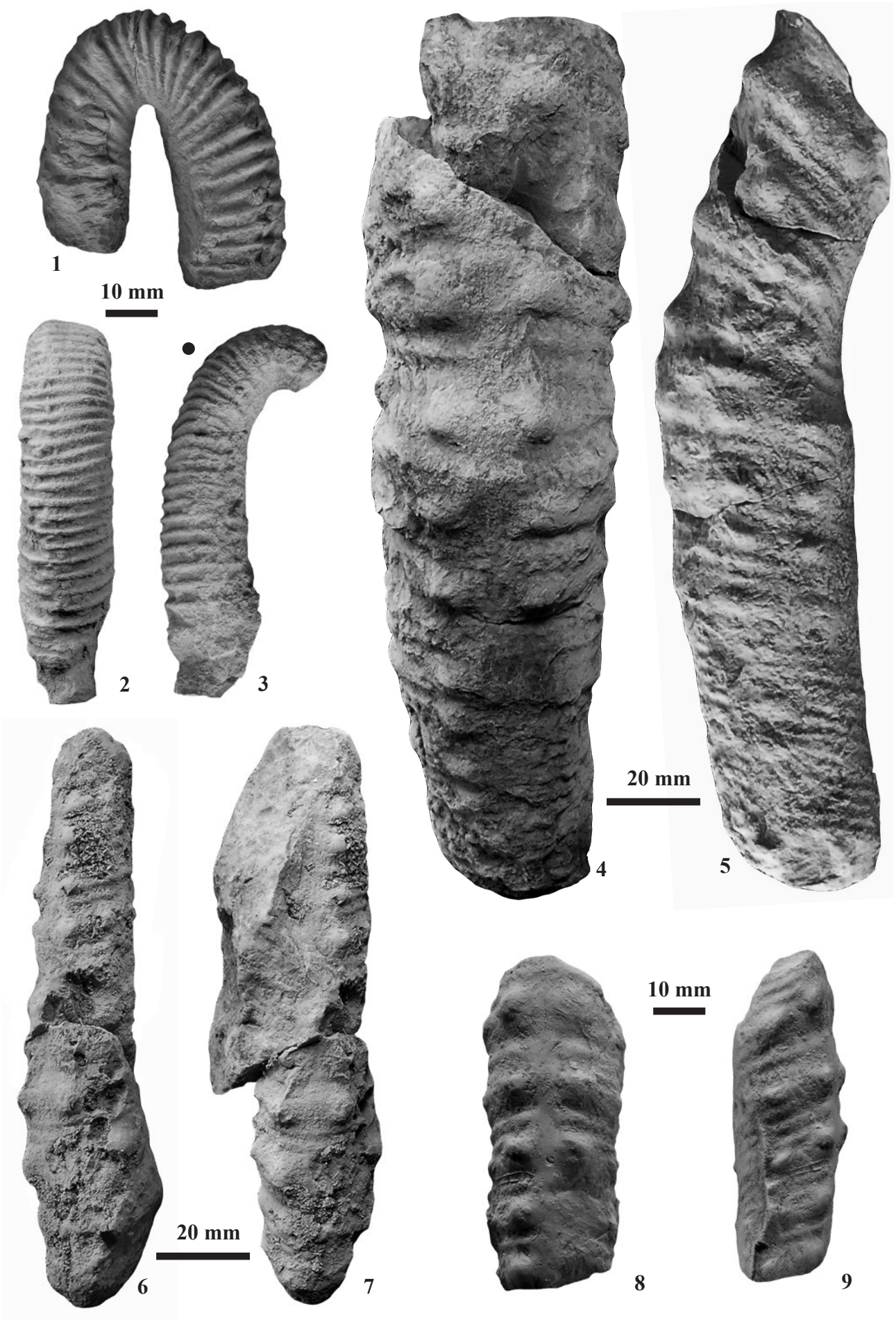

PLANCHE 23

Fig. 1-4: ***Ammonitoceras*** **aff.** ***lahuseni*** (Sinzow, 1906). Deshayesi Zone, Grandis Subzone, Narbonne, Parets d'en Sales, lev. 1, "Niveau de Vires", Ramade Fm.
Fig. 1-2: NV97
Fig. 3-4: NV98

PLANCHE 23

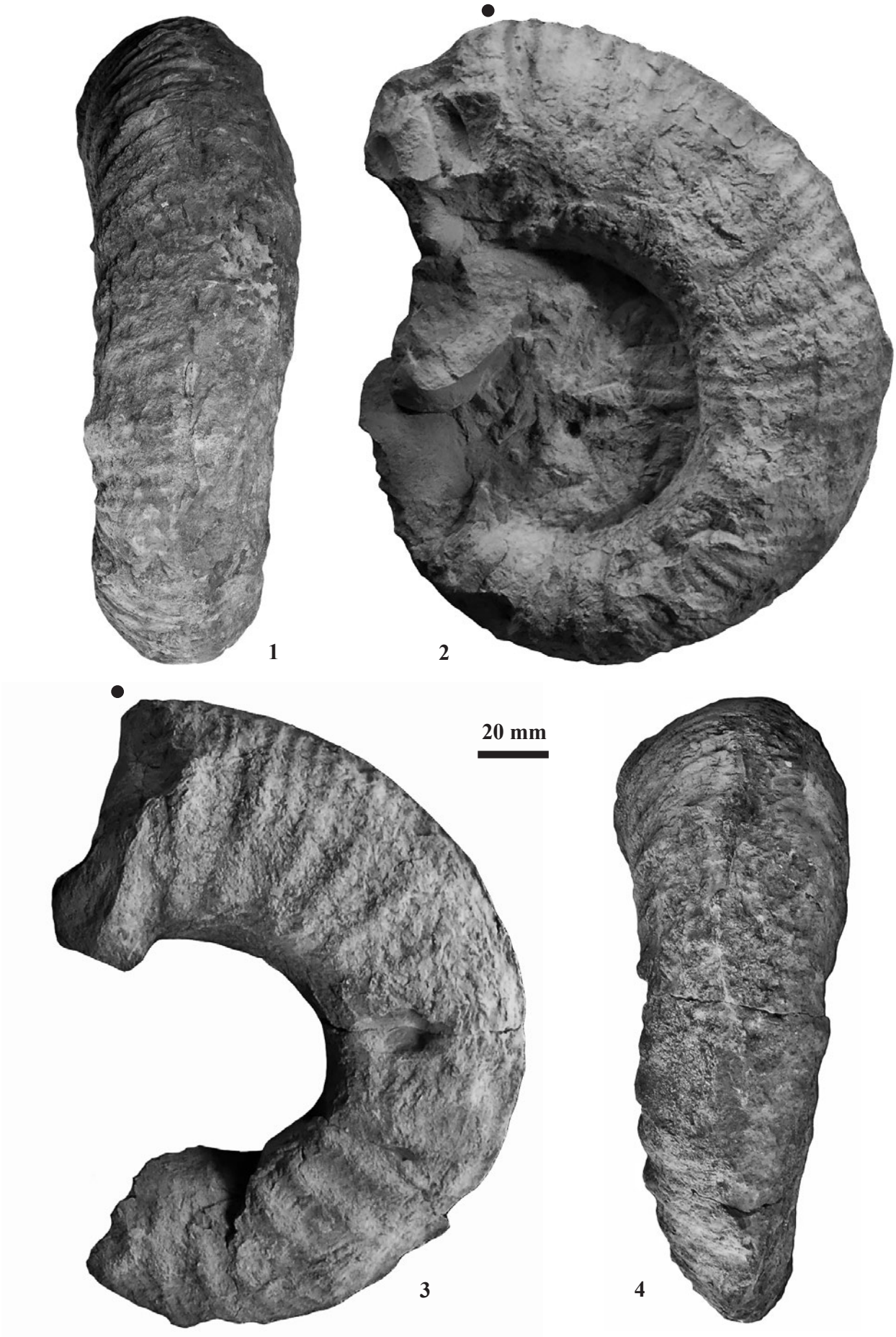

PLANCHE 24

Fig. 1-3: ***Ammonitoceras* aff. *lahuseni*** (Sinzow, 1906). Deshayesi Zone, Grandis Subzone, Narbonne, Parets d'en Sales, lev. 1, "Niveau de Vires", Ramade Fm.
Fig.1: NV99
Fig. 2-3: NV100

PLANCHE 24

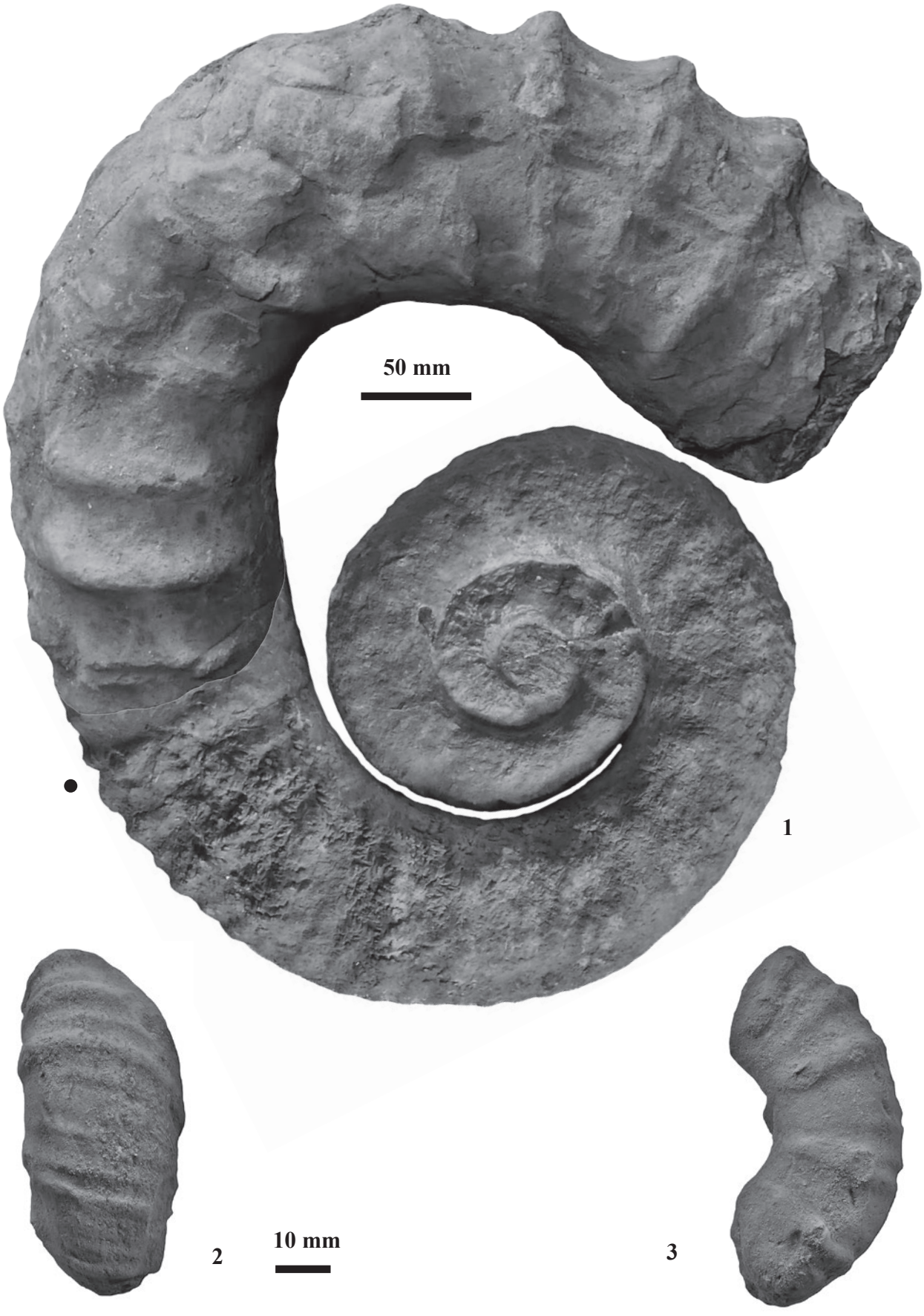

PLANCHE 25

Fig. 1: ***Ammonitoceras*** **aff.** ***lahuseni*** (Sinzow, 1906). Deshayesi Zone, Grandis Subzone, Narbonne, Parets d'en Sales, lev. 1, "Niveau de Vires", Ramade Fm. (NV10).

PLANCHE 25

PLANCHE 26

Fig. 1: ***Ammonitoceras*** **aff.** ***lahuseni*** (Sinzow, 1906). Deshayesi Zone, Grandis Subzone, Narbonne, Parets d'en Sales, lev. 1, "Niveau de Vires", Ramade Fm. (NV102).

PLANCHE 26

1

PLANCHE 27

Fig. 1: ***Ammonitoceras*** **aff.** ***lahuseni*** (Sinzow, 1906). Deshayesi Zone, Grandis Subzone, Narbonne, Parets d'en Sales, lev. 1, "Niveau de Vires", Ramade Fm. (NV103).

PLANCHE 27

ANNEXES

Tabl. 2 - Dimensions of the material assigned to the Deshayesitidae *Deshayesites grandis* Spath, 1930. See text for acronyms. NF: not figured.

Specimen	Figured Pl.	Anti-Dimorphs	D	U	Wh	Ww	R1 (totalNp)	R2 (primaries)	SSB
NV4	4	m	26,45	7	11,15	8,7	21	10	25
NV5	4	m	35	19	15,6	9,13			
NV6	4	m	27,14	6,6	12,87				
NV7	4	m	34,17	9,6	15,3		22	12	
NV8	4	m	40,25			8,6	22	11	
NV9	4	m	41,7	9,7	19,6	11,3	25	11	
NV10	4	m	55,1		26,3	14,5	25	11	
NV11	4	m		18,13	25,7	14,3	24	12	
NV12	4	m	65	19,6	28,1		29	14	
NV13	14	m	78,97	15,56	41,31	24,9	30	12	
NV14	5	m	48	13,17	19,7	12,3	20	10	
NV15	5	m	59,26	17,5	26,7	17,5	19	10	
NV16	5	m	42,4	12	18,58	13	21	11	
NV17	5	m	51,35	13,4	23,3	13,87	26	10	
NV18	5	m	40,4	10,5	16,9		18	10	
NV19	5	m	59,9	15,6	26,6	14,8	21	10	
NV20	5	m			25,2	15,1			
NV21	5	m	57, 7	19,75	18,8		23	12	
NV22	4	m	24,4	9,15	8,67	7	16	10	15
NV23	6	m	62	12,78	30,5		33	12	
NV24	6	m	44		19	10	17	8	
NV25	6	m	96,15	17,5	49,5			13	
NV26	6	m	38,6	10,39	17,95	12,2	22	10	16
NV27	6	m	55,56	15,1	26,9	14,12	24	10	
NV28	6	m	48,7	14,88	19,35	10	19	10	
NV29	6	m	45,6	11,1	20			10	
NV30	6	m	80,13	24,5	35,2		26	13	
NV31	7	m			19,5	1,1	28	18	
NV32	7	m		24,4					
NV33	7	m	114,46	33,15	50,43		20	10	
NV34	7	m	73,18	19,1	30,13	17,23	20	10	
NV35	7	m	111,95	31,15	49,37	30,5	23	10	
NV36	8	m	113	20,53	56		28	11	
NV37	8	m	99	19	52	19	38	16	
NV38	8	m	94,66	16	50,5	26	12	30	
NV39	9	[M]	165,3	44	70	36,6	31	15	
NV40	9	m	85	14,63	45,5	22,95		14	
NV41	9	m	105	18,65	54,2			13	
NV42	10	[M]	214,6	65	84,2	51,3	30	15	
NV43	10	m		22,6	45	21,5		12	
NV44	10	m	69,1		34,4	17,95			

NV45	10	m		15,09		17,4		12	
NV46	11	m		73	75,1				
NV47	11	m			40,5				
NV48	12	[M]	258,3	79	97	56	26	17	
NV49	11	m	140,1	30	62	39	30	15	
NV50	5	m	66,7	18,6	28				
NV104	NF	m			44,8		30	12	
NV105	NF	m	38	8,1	21,5				
NV106	NF	m		13,8	25,5				
NV107	NF	m		16,5	35,5	19,3			
NV108	NF	m		15,14				14	
NV109	NF	m			19,8				
NV110	NF	m		24,78	50,2			12	
NV111	NF	m	60,44						
NV117	NF	[M]	187	40,8	84	42,6		15	
NV118	NF	[M]	204	56	80	38	30		
NV119	NF	[M]	206,2		78	47,5	30	15	
NV120	NF	[M]	273,9	87,2	102,4			20	

Tabl. 3 - Dimensions of the material assigned to the Douvilleiceratidae *Cheloniceras crassum* Spath, 1930. NF: not figured; D: Deformed; P: Pathological. See text for other acronyms.

Spec.	fig. Pl.	D	U	Wh	Ww	R	HT	IT	MTU	IN	STR	STC	STP	STA
NV51	13	23,7	8	9,2	14,15	16	5			4	9			
NV52	13	24	6,7	11	10,5	19	5			4				
NV53	13	33	11,16	11,3	18,7									
NV54	13	D			17									
NV51	13	23,7	8	9,2	14,15	16	5			4	9			
NV55	13	D												
NV56	13	33,4	12	14,4	18,08	23		7				25		
NV57	13	49,4	16	19,3	25,3	21		4	4		15	30		
NV58	13	49,8	19,06	17,4	24,5	19	4	2		10		49,6	50,2	49,8
NV59	13	80,9	27	37,3	33,16	23	5	3		9		65,7		
NV60	13	75,13	30	26,8	36	22	1		6	15		60		
NV61	14	63,15	19,4	26,5		17	7			7				
NV62	14	68,75	22,5	26,1	31,8	17	5			8				
NV63	14	78,95	30,8	31,8		19	6							
NV64	14	90,5	31,36	34,1	48	23	8			10				
NV65	15	40,5	14,5	15	22	19	5			4				
NV66	15	58,4	20,4	22,5	34,75	16	5			6				
NV67	15	96,1	36,4	34,14		21	6			6				
NV68	15	94,6	29,4	40,4		19	6			6				
NV69	16	127,3	48,8	45,2	78	23	1	0	6	7		95		
NV70	16	157	59,2	60,1	59,9	26	9			7				
NV71	17	125	44,5	46,1	74,2	23	9	2		7				
NV72	17	115,2	46,8	41,6	68,6	16	6					105,8		
NV73	18	128,6	44,3	50,7		22	2	5				104,4		
NV74	18	84,4	26,4	33,35		19	7							
NV75	18	68	24,4	26,08	45,3	23	8							
NV76	18	P												
NV77	18	D				25	1	4	1					
NV78	18				17	22	5			11				
NV79	19	222,1	80	77		20	10	2	9				155	
NV112	NF	96,7	34,5	30,5		21	0	9		11		60		
NV113	NF	88,9	33,4	36,7			1	7						
NV114	NF	70		27,3	38	19	5					65		
NV115	NF	153,6	60,8	62,2	57								148	
NV116	NF	134	50	50		20	2	5				104		